CREEP RECOVERY OF CONCRETE SUBJECTED TO MULTIAXIAL COMPRESSIVE STRESSES AND ELEVATED TEMPERATURES

By Amin Hijazi
and Thomas W. Kennedy

RESEARCH REPORT 3661-1

to
OAK RIDGE NATIONAL LABORATORY
operated by
UNION CARBIDE CORPORATION
for
U.S. ATOMIC ENERGY COMMISSION

DEPARTMENT OF CIVIL ENGINEERING
THE UNIVERSITY OF TEXAS AT AUSTIN

MARCH 1972

CREEP RECOVERY OF CONCRETE SUBJECTED TO MULTIAXIAL COMPRESSIVE STRESSES AND ELEVATED TEMPERATURES

by

Amin Hijazi
Thomas W. Kennedy

Research Report Number 3661-1

An Evaluation of the Creep Behavior of Concrete

conducted for

Oak Ridge National Laboratory

operated by
Union Carbide Corporation
for the
United States Atomic Energy Commission

by the

DEPARTMENT OF CIVIL ENGINEERING

THE UNIVERSITY OF TEXAS AT AUSTIN

March 1972

PREFACE

This is the fourth in a series of reports dealing with the findings of a research project concerned with the evaluation of the creep behavior of concrete subjected to triaxial compressive stresses and elevated temperature. This report evaluates the recovery data obtained after the compressive stresses were removed. The effects of curing history, temperature during the loading and unloading periods, and stress conditions were evaluated for instantaneous and creep recovery strains. In addition, the accuracy of superposition as a method of estimating creep recovery was evaluated.

The experimental investigation was conducted and financed under Union Carbide Subcontract 2864. The analysis of the recovery data and the preparation of the report were conducted and financed under Union Carbide Subcontract 3661. Both studies were for the Oak Ridge National Laboratory, which is operated by the Union Carbide Corporation for the United States Atomic Energy Commission.

The planning, conducting, and analyzing of data for this investigation required the assistance and cooperation of many individuals and organizations; the authors would like to acknowledge the cooperation and assistance obtained from the Concrete Division of the Waterways Experiment Station, Jackson, Mississippi, and the Department of Civil Engineering of the University of California at Berkeley. In addition, special thanks are extended to Mr. G. D. Whitman, Coordinator Pressure Vessel Technology Program of the Oak Ridge National Laboratory, whose active participation and support enabled this investigation to be successfully conducted, and to Dr. J. P. Callahan, Mr. J. G. Stradley, and Dr. J. M. Corum of the Oak Ridge National Laboratory. Appreciation is also extended to Professor Clyde E. Kesler, Department of Civil Engineering, University of Illinois, who served as a consultant to the project. Special appreciation is due Mr. Victor N. Toth, Dr. Ervin S. Perry, Dr. Nabil Jundi, Dr. Guy P. York, and Dr. John W. Chuang for their aid in the planning of the experiment, the preparation of the specimens, and the collection of the

data. And finally, the aid extended by personnel of the Center for Highway Research, The University of Texas at Austin, is acknowledged.

Future reports will be concerned with a detailed inspection and evaluation of the specimens used in this investigation and an evaluation of the effect of curing time on creep behavior.

Amin Hijazi
Thomas W. Kennedy

March 1972

ABSTRACT

This report presents the findings of an experimental investigation to evaluate the effects of three different factors on the instantaneous and creep recovery strain of plain concrete after being subjected to sustained loads for a period of one year. The factors investigated were (1) temperature during the loading and unloading periods (75^{o} F and 150^{o} F); (2) curing history (as-cast and air-dried); and (3) state of stress, which varied from 0 psi to 3600 psi in both the axial and radial directions.

This experiment consisted of applying compressive loads along the three principal axes of cylindrical concrete specimens for a period of one year, after which the loads were removed and creep recovery strains were observed for an additional five months. The loads were applied by means of a hydraulic loading system that permits independent variations of loads along the axial and radial axes allowing triaxial, biaxial, and uniaxial states of stress. The strains were measured using vibrating wire strain gages that were cast in the concrete specimens along the axial and radial axes.

The effect of each of the above factors on the creep recovery strain was evaluated separately, after which a comparison of the different relations between strains during the loading period and strains during the unloading period was made. In addition, Poisson's ratio during the recovery period and the applicability of the principle of superposition of strains were evaluated and are discussed briefly.

TABLE OF CONTENTS

LIST OF TABLES

LIST OF FIGURES

CHAPTER 1. INTRODUCTION

An important consideration in the design and safety evaluation of prestressed concrete nuclear reactor vessels is the time-dependent behavior of the concrete subjected to different temperatures, curing times, curing histories or moisture conditions, and loading conditions. The three basic forms of time-dependent deformation that can occur are shrinkage, creep, and creep recovery. Any one of these three types of deformation can have serious effects on the behavior of a reactor vessel unless carefully considered during the design of the reactor. Because of the long-term nature and complexity of some of the tests required to evaluate the creep and creep recovery behavior of concrete, there is limited information on creep and essentially no detailed information on creep recovery.

At the request of the United States Atomic Energy Commission, the Oak Ridge National Laboratory formulated and coordinated a basic research and development program to develop the technology of prestressed concrete reactor vessels. As a part of this program, an experimental investigation was initiated at The University of Texas at Austin to study the behavior of creep and creep recovery of concrete subjected to multiaxial compressive stresses and elevated temperatures. The investigation consisted of measuring strains in cylindrical specimens subjected to 54 test conditions involving a variety of multiaxial loading conditions (compressive stresses ranging from zero to 3600 psi), three curing times (90, 183, and 365 days), two curing histories (air-dried and as-cast), and two temperatures (75° F and 150° F). After curing, the specimens were subjected to a prescribed load and temperature for 12 months, followed by a five-month unloading period. During the curing, loading, and unloading periods, strain measurements were made in order to evaluate the creep and creep recovery behavior of the concrete.

The purpose of this report is to summarize and discuss the findings from the evaluation of the data obtained during the recovery period after the removal of loads. The report consists of six chapters and appendices. Chapter 2 summarizes the current status of knowledge concerning the creep and creep

recovery phenomena of concrete, factors affecting creep recovery, and methods of estimating creep recovery behavior. Chapter 3 describes the experimental program, including the preparation of specimens, equipment and instrumentation, experimental procedures, and experimental designs. A summary of the test findings before and after the removal of loads is presented in Chapter 4, and the recovery results are discussed and evaluated in detail in Chapter 5. Conclusions and recommendations are contained in Chapter 6. The appendices include data complementary to those of Ref 35 and recovery strain-time relationships for the recovery period for the different test conditions.

CHAPTER 2. CURRENT STATUS OF KNOWLEDGE

This chapter summarizes the current status of knowledge concerning the phenomena of creep and creep recovery of concrete and the relationships of one to the other.

CREEP AND CREEP RECOVERY

When a sustained load is initially applied to a concrete specimen, the specimen exhibits an instantaneous elastic strain ϵ_i which is proportional to the magnitude of the load applied. This is followed by a time-dependent strain which consists of a shrinkage strain ϵ_s, due to environmental effects, and a creep strain ϵ_c, due to the sustained load (Fig 1a). The creep strain is usually considered to be the algebraic difference between the total strain and the sum of the instantaneous elastic strain and the shrinkage strain (Fig 1b).

Similarly, when the load is removed, an instantaneous recovery strain ϵ_{ir} occurs in the direction opposite to the instantaneous elastic strain. This instantaneous recovery is followed by a gradual time-dependent recovery of strain, known as creep recovery ϵ_r. The creep recovery strain eventually reaches a limiting value, and a permanent deformation or strain $\epsilon_{\infty r}$ is left in the concrete. The creep recovery is also termed reversible creep, and the permanent deformation caused by the load is known as irreversible creep.

MECHANISM OF CREEP AND CREEP RECOVERY

To fully understand the nature of creep and creep recovery, it is necessary to consider the creep mechanism and the relation between creep and creep recovery. Several mechanisms, which have been reviewed by Neville (Ref 25), have been proposed to explain the behavior of concrete under sustained load. Some investigators (Refs 3, 9, and 34) suggested that the creep of concrete is the result of plastic deformation, including intracrystalline slips and local rupture of the cement paste. Other investigators (Refs 2, 6, and 32) considered

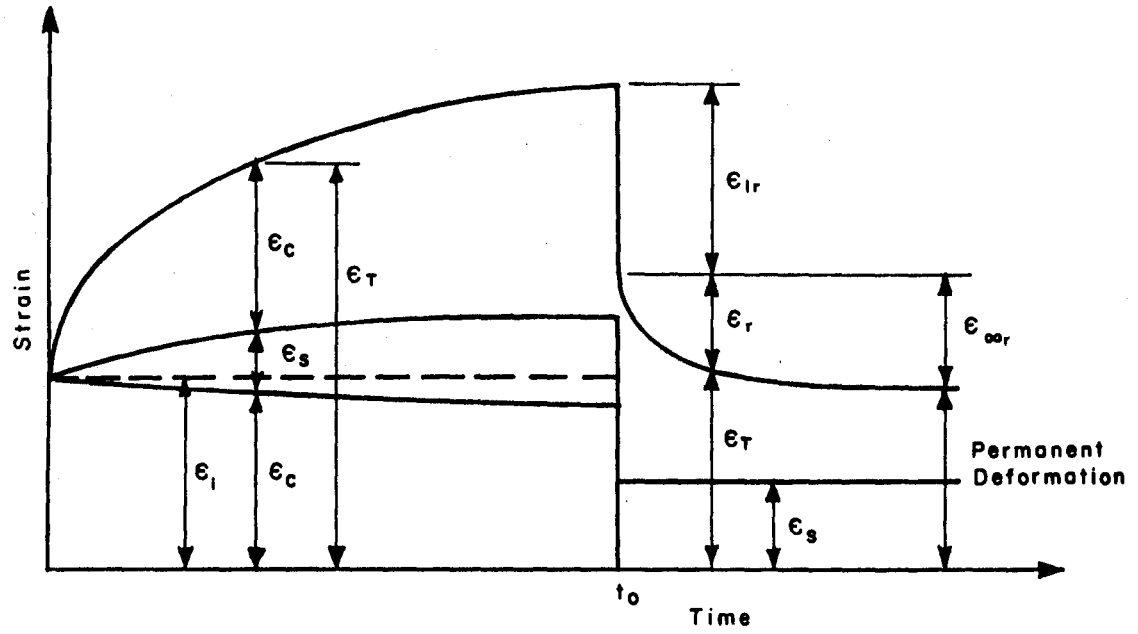

(a) Total strain components.

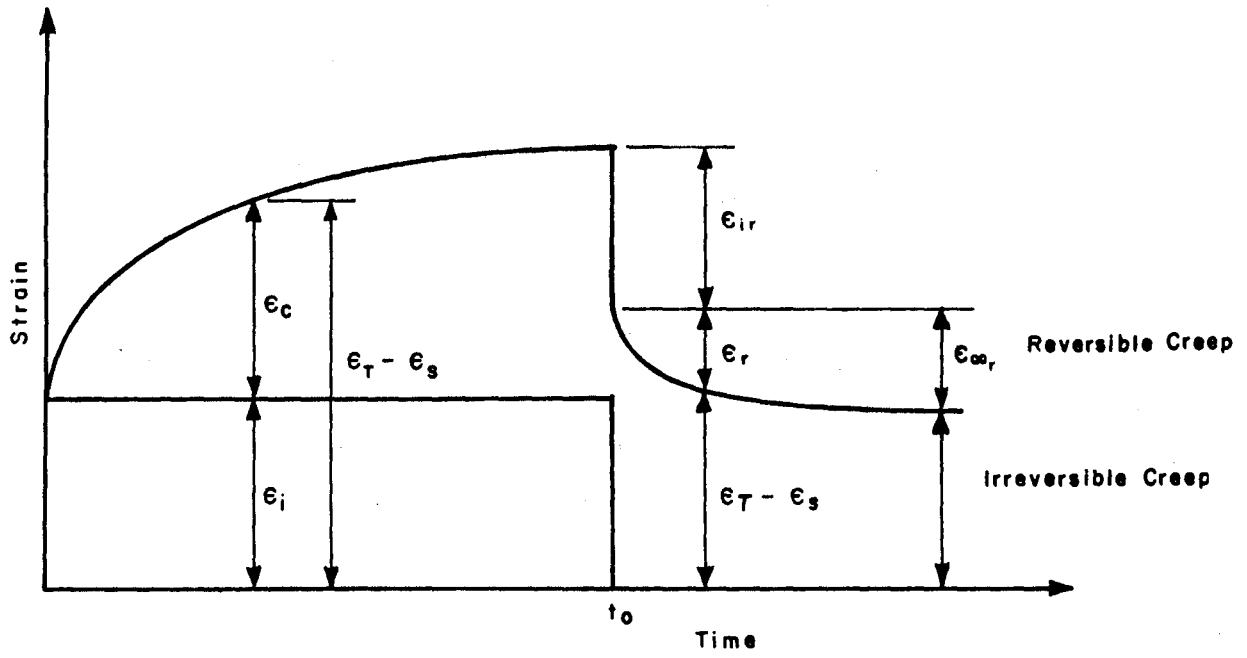

(b) Total strain less shrinkage.

Fig 1. Typical strain-time relationship for concrete under load which is sustained and then removed at t_o .

the creep of concrete to be a form of viscous flow of the cement paste. According to Lynam (Ref 21) and many others (Refs 19, 20, 30, and 31), the creep of concrete is due to the loss of moisture from the cement paste to the surrounding environment under the pressure of the applied load. Freyssinet (Ref 8) explained that creep deformations of concrete are the result of change in the arrangement of the capillary structure of the cement paste under load. However, even though some of these theories offer a reasonable explanation of the behavior of concrete under sustained load, none of them provides a full explanation of all the aspects of the creep phenomenon.

Adsorbed water was emphasized as one of the main causes of creep of concrete by many investigators. Freudenthal and Roll (Ref 7) found that when a concrete specimen is subjected to an external load, the adsorbed gel water is expelled toward the surface by the hydrostatic pressure gradient that builds up internally, thus causing creep strain to occur. This indicates that creep should be completely reversible when the expelled water is restored, but it has been shown that creep is not completely reversible.

Ali and Kesler (Ref 1) considered creep to be the summation of two components. One component, basic creep, occurs under conditions of hygrometric equilibrium and is essentially a process of molecular diffusion and shear deformation of the gel and the adsorbed water, while the other component is characterized by delayed elastic action of the gel.

Powers (Ref 27) concluded that water molecules, which occupy the narrow interstitial spaces between the quasi-crystalline solid bodies of the paste, are able to resist forces tending to expel them from their positions by maintaining static pressure. The free energy resulting from this pressure produces a movement of the load-bearing adsorbed water molecules in the direction of the non-loaded regions of the system in an attempt to achieve thermodynamic equilibrium. This change of state in the adsorbed water after the specimen has been stabilized by previous loading (Ref 10) accounts for the reversible component of creep, and the irrecoverable component is considered to be due to nonelastic deformation, perhaps plastic yielding which results in a permanent deformation.

The physical structure of the hydrated cement paste was considered by many investigators (Ref 26) to be a main cause of creep of concrete. Freyssinet (Ref 8) stated that loading increases the probability of rearrangement of the

colloidal size particles in the gel, thus causing a reduction of the volume of the concrete. Other investigators (Refs 9, 22, and 34) suggested that crystalline flow, slipping within the crystal lattice, or localized fracture of hydrated cement paste contributes to the creep of concrete.

Gopalakrishnan et al (Ref 11) considered that the deformation of a hydrated cement gel subjected to an external load consists of two parts: (1) deformation of the individual gel particles due to a change in intermolecular spacing and (2) relative movement of the gel particles due to deformation of the load-bearing adsorbed water between the particles. With further deformation in the elastic skeleton of the paste, a strain energy buildup will develop within the system due to the high contact stresses of the solid surfaces. The release of this strain energy when the load is removed causes a part of the creep recovery of the concrete. The other part is due to the change of the free energy distribution in the adsorbed water which develops from the change in spacing of the solid particles when the load is removed. The recovery is gradual because of the restraint imposed by the viscous properties of the adsorbed water.

EVALUATION OF CREEP RECOVERY

A useful method for evaluating creep recovery employs the principle of superposition of strains (Ref 22). This principle states that strains produced in concrete at any time t by a stress increment applied at any time t_o are independent of the effects of any stress applied either earlier or later than t_o. The stress increment could be either an addition of stress or a relief of stress. Thus, if a compressive load on a concrete specimen is removed, the magnitude of the creep recovery strain* would be equal in magnitude to the creep strain which would have occurred if the concrete had been subjected to stress equal to the stress which was removed at the same time t_1 (Fig 2).

The accuracy of this method of estimating creep recovery has been questioned by many investigators and Neville (Ref 24) summarized the conclusions from

---

* Defined as the difference between the actual strain at any time and the strain that would occur at the same time if the specimen had continued to be loaded by the original stress.

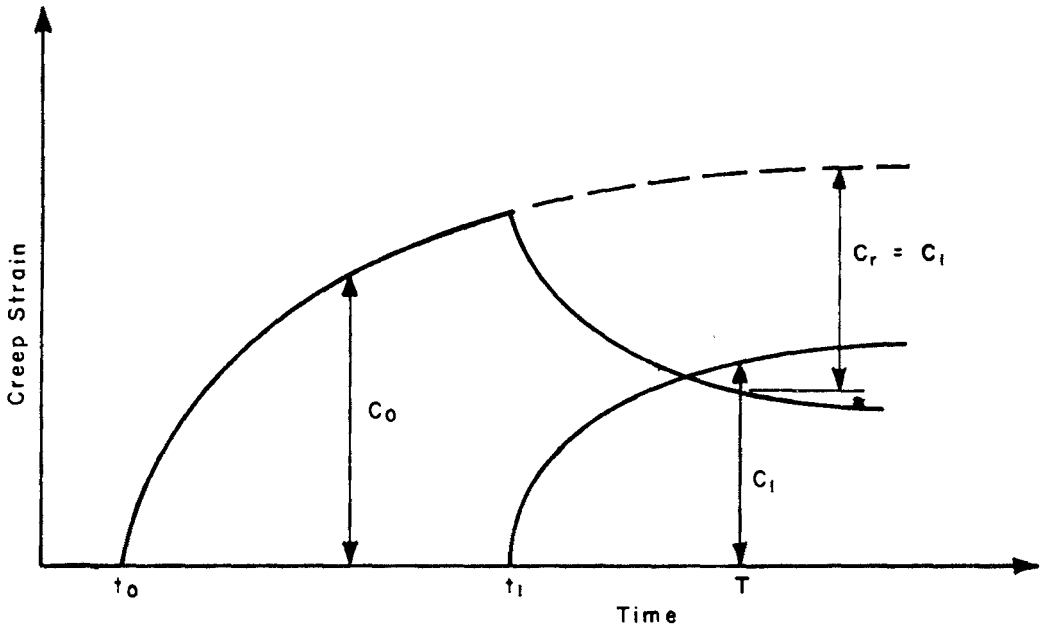

Fig 2. McHenry's principle of superposition (Ref 22).

some of the results of tests of various evaluations of the accuracy of superposition (Refs 5, 29, and 33) and reported that the principle of superposition overestimates the creep recovery strain.

It has been suggested (Ref 14), however, that in some instances overestimation of creep recovery was due to the effect of drying shrinkage, which is greater in a virgin specimen, and in other instances it was due to the use of the principle of superposition on total strain rather than on creep strain only. Jessop et al (Ref 14) stated that the main reason for the overestimation of creep recovery was that the principle of superposition was being considered for the usual basic creep, which represents creep under conditions of no moisture exchange with the ambient humidity. This basic creep includes a part, denoted as stress-induced shrinkage, which is partially irrecoverable and is due to the movement of some moisture from the adsorbed water layers on the gel surfaces to the nearby capillary void regions. According to these investigators an improvement in the applicability of the principle of superposition to the evaluation of creep recovery would result if the principle of superposition were used on a new parameter which included only the reversible part of the basic creep, since its full reversibility is possible only when the original moisture content at the time of loading is restored. The new parameter represents deformation under constant hygrometric conditions, exclusive of stress-induced shrinkage, and is termed new basic creep. In the recovery state, the new basic recovery response, which is the strain under constant hygrometric conditions obtained from the continuation of the creep curve less the amount of stress relief swelling and the continuation of stress induced shrinkage, is used with the new basic creep parameter.

Jessop et al (Ref 14) conducted an experimental program to verify the accuracy of the principle of superposition on these new parameters. The results obtained showed that the accuracy in some cases was not much better than the accuracy of the principle of superposition generally used.

Other investigators, such as Illston (Ref 13) and Roll (Ref 28), suggested the use of rheological models to obtain an equation suitable for the prediction of creep recovery strains. However, it would be desirable to use superposition as a tool for design and evaluation, and additional work should be conducted to evaluate the accuracy of the method.

FACTORS AFFECTING CREEP RECOVERY

The effect of different factors on creep has been discussed thoroughly in the literature, but little has been published about factors affecting creep recovery. In this section, several observations on the effect of some factors on the creep recovery are reviewed briefly. A broader summary of the effect of these factors on creep strain was included in an earlier report (Ref 35) on the experimental program at The University of Texas at Austin.

As far as the effect of cement on creep recovery is concerned, Neville (Ref 24) found that creep recovery could not be related to the type of cement in the mortar or to its chemical composition. He also concluded that there was no correlation between creep recovery and the strength of concrete, either at the time the load was applied or the time the load was removed. On the other hand, he found that instantaneous recovery is a function of the modulus of elasticity of concrete at the time of unloading, which in turn is related to the strength. Thus the ratio of creep recovery to instantaneous recovery depends on the strength of the cement paste.

The level of the previously sustained stress also affects creep recovery. Freudenthal and Roll (Ref 7) reported that creep recovery varies linearly with the magnitude of sustained stress. At a later time, Roll (Ref 28) found that generally both instantaneous recovery and total time dependent recovery were linear functions of stress up to 65 percent of the ultimate strength of the concrete. On the other hand, Nasser and Neville (Ref 23) reported that creep recovery is independent of the magnitude of the stress that is removed and that creep recovery is independent of temperature and storage conditions.

In a paper on the mechanism of creep, Gopalakrishnan et al (Ref 11) pointed out that the magnitude of creep recovery is a function of both creep at the time of unloading and elastic recovery strain. On the other hand, from the results of a multiaxial compression test on concrete, Hannant (Ref 12) concluded that creep recovery is proportional to neither elastic recovery strain nor the magnitude of measured creep but rather is dependent on the magnitude of stress removed parallel to the direction of the strain measurement.

Creep recovery can take place in a given direction under multiaxial compression even if the applied stress in that direction is zero or if the creep due to Poisson's effect is negligible. Hence the magnitude of creep recovery

in a given direction for the same stress applied in the same direction may vary when the other principal stresses are not the same.

Based on 84 days of creep recovery and a preliminary evaluation of the data , York concluded in a previous report (Ref 35) that

(1) The modulus of elasticity and Poisson's ratio for elastic recovery were essentially equal to the modulus of elasticity and Poisson's ratio at the time of loading.

(2) The elastic recovery strains were generally slightly higher than the initial elastic strains, except for air-dried specimens loaded at 150° F and most hydrostatically loaded specimens.

(3) Curing history appeared to be the only factor studied that significantly affected the percentage of creep recovered. A larger percentage of the creep strain, which occured during one year under load, was recovered from the as-cast concrete than from the air-dried concrete.

(4) Factors that caused larger creep strains generally caused larger total recovery strains although they did not necessarily cause a larger percentage of the creep strains to be recovered.

CHAPTER 3. EXPERIMENTAL PROGRAM

This chapter contains a brief description and discussion of the factors investigated, the design of the experiment, the techniques used to prepare the specimens, the equipment used, and the test procedure. A more detailed discussion and description are contained in Refs 18 and 35.

The tests consisted of applying compressive loads along the three principal axes of cylindrical concrete specimens and measuring the strains in the axial and radial directions throughout the testing period. The axial and radial loads were applied by means of a hydraulic loading system and were varied independently, permitting triaxial, biaxial, and uniaxial states of stress to be developed. Strains were measured by two vibrating wire strain gages embedded in the concrete along the axial and radial axes of the cylindrical specimen.

TEST CONDITIONS

Although numerous factors affect the creep and creep recovery behavior of concrete, this study included only temperature during loaded and unloaded recovery periods, curing time, curing history, and state of stress.

Temperature During Test Period

During the loaded and unloaded periods, the concrete was subjected to the two temperature levels which are the limits of the range of temperatures that would be expected to occur in the concrete of a nuclear reactor vessel. The low level was 75° F, which approximates the temperature at the outer surface of a reactor, and the high level was 150° F, which approximates the temperature at the inner surface of a vessel. The temperature was controlled within $\pm 2^{\circ}$ F of the desired levels and was recorded continuously.

Curing Time

In this investigation, the major portion of the study involved specimens cured for a period of 90 days prior to being loaded. In addition, a limited number of specimens were cured for a period of 183 and 365 days prior to loading.

Curing History

Two curing histories were selected for study and were designated as "as-cast" and "air-dried." These two histories simulated the range of curing conditions to which concrete in a prestressed concrete reactor would be subjected during curing. The as-cast condition is representative of the curing history of concrete at the inner face of a reactor or of concrete in any massive structure except that near a free-air surface. This condition involved sealing the specimens shortly after casting to maintain their initial water content by preventing evaporation losses.

The air-dried condition is representative of the curing history of the concrete at the outer surface of a reactor or other mass-concrete structure, or of concrete in relatively thin members. In this case, the concrete was moist cured for approximately seven days and then allowed to air-dry for the remainder of the curing period. Thus, curing history was closely related to moisture condition in the concrete during the curing and loading periods. However, since it was difficult to determine the actual moisture conditions which resulted from the two types of curing, and because it was impossible to assign the cause of an observed effect to anything but the curing procedure, this variable was designated as curing history. The procedures associated with the various curing histories are described in detail in this chapter under TEST SPECIMENS, Curing and Sealing.

All specimens were removed from the molds 24 hours after casting and were placed in a moisture curing room for 24 hours. Subsequent to this initial 48-hour curing period, the as-cast specimens were sealed in copper and allowed to cure at 75° F for an additional 81, 174, or 365 days, depending on the designated curing period for each specimen, and then they were placed in the test temperature environment. After the initial 48-hour curing period, the air-dried specimens were placed in lime-saturated water for five days (a total of seven days of moist curing), after which they were removed and allowed to air-dry in the laboratory at 75° F and 60 percent relative humidity long enough to give a total curing period of 83, 176, or 385 days after casting, when they were sealed and placed in the test temperature environment.

State of Stress

Specimens were loaded triaxially at five stress levels, ranging from 0 to 3600 psi for both axial stress σ_a and radial confining stress σ_r. Since

the combination of stresses involved some zero stress levels, the loading conditions were classified as uniaxial, $\sigma_r = 0$; biaxial, $\sigma_a = 0$; and triaxial. The five stress levels involved were 0, 600, 1200, 2400, and 3600 psi nominal pressures. A schematic of the basic test unit and photographs of the units used to achieve these loading conditions are shown in Figs 3 and 4.

Prior to the actual testing, it was determined that the actual stress in the axial direction was somewhat less than the indicated stress due to friction in the hydro-mechanical system which was used to load the specimens axially. Therefore, each loading unit was calibrated using a standard load cell, and it was established that the average initial axial stresses delivered to the specimens were 0, 545, 1080, 2185, and 3460 psi, respectively. The variation of the axial stresses with time was monitored with mechanical dial gages and found to be negligible.

TEST SPECIMENS

Description of Specimens

A total of 430 specimens were cast in nine batches, which were designated A through I.

Three basic types of specimens were utilized in this investigation: creep, shrinkage, and strength. All creep and shrinkage specimens were 6 inches in diameter by 16 inches in length and were attached to 3-inch-thick steel end slugs, through which the axial load was applied (Fig 5). The specimens were cast horizontally in specially designed molds. The tensile and compressive strength specimens were 6 inches in diameter by 12 inches in length and were cast vertically in standard 6 × 12-inch molds.

The experiment design contained 66 creep specimens and 36 shrinkage specimens which were used to measure the total strains experienced by the concrete under the various combinations of the four factors. For each batch of concrete and for each environmental test condition, an unloaded shrinkage specimen was placed in the same test environment as its companion loaded specimens. These shrinkage specimens were used to evaluate shrinkage strains in order to estimate the time-dependent strains due to the load and in order to check batch-to-batch variations.

In addition, a total of 328 concrete strength specimens were cast. These were distributed among the nine batches and consisted of as-cast, air-dried,

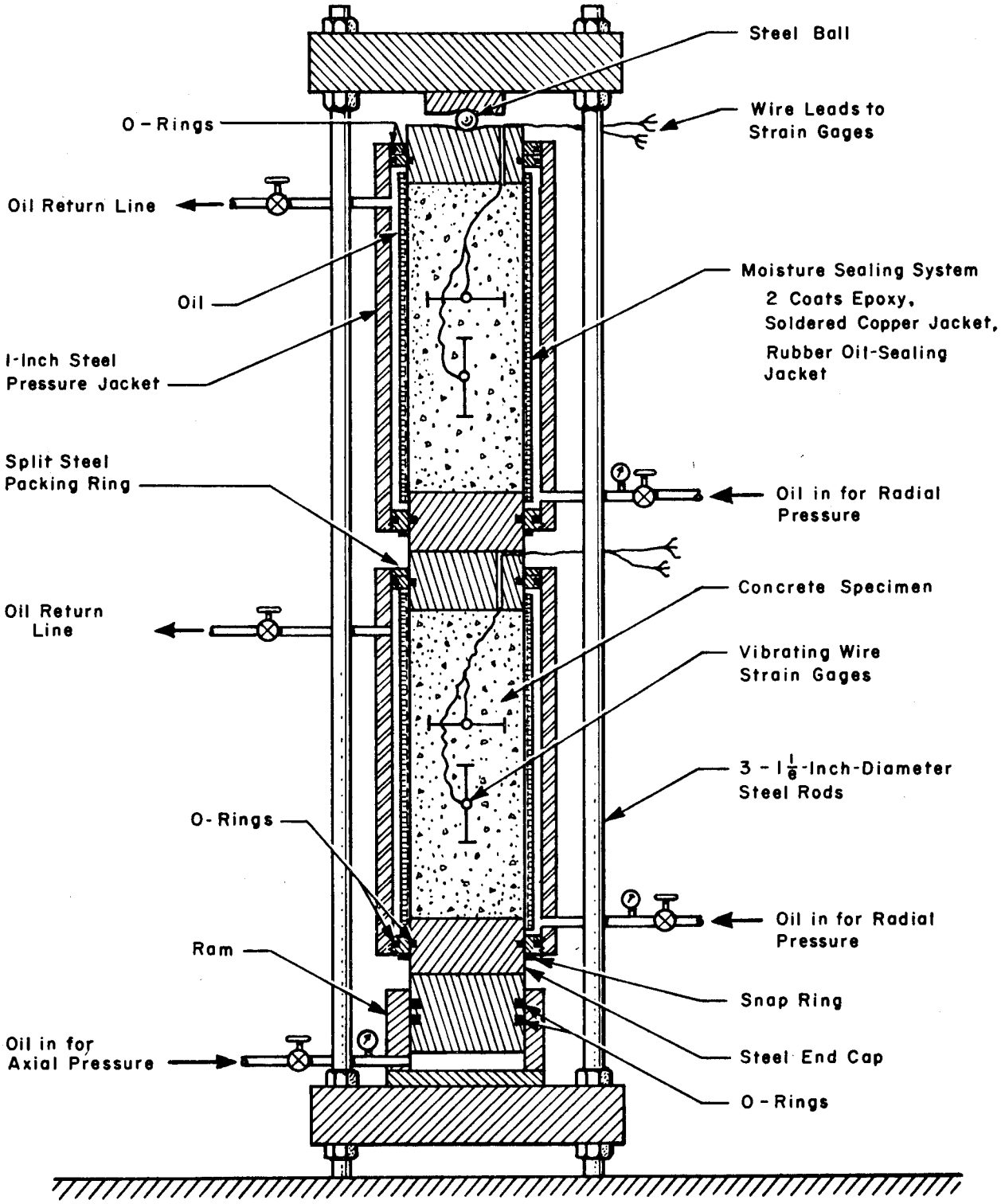

Fig 3. Schematic of triaxial test unit (Ref 18).

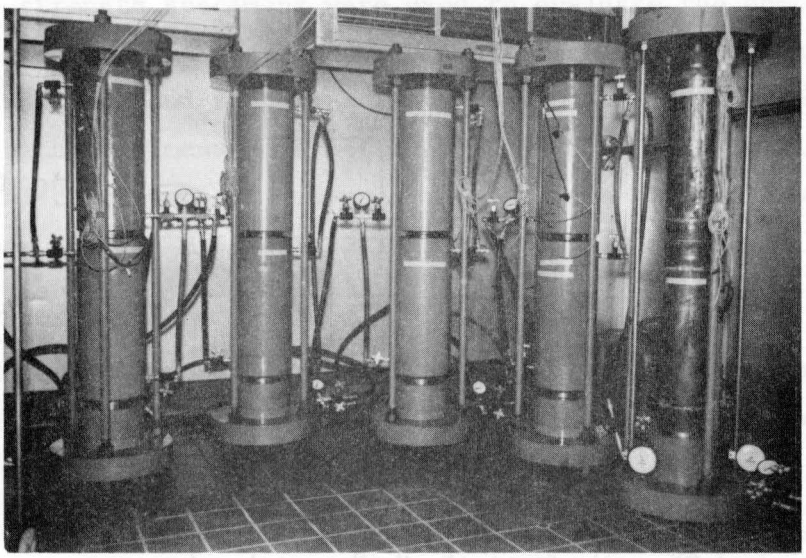

(a) Uniaxial and triaxial loading conditions.

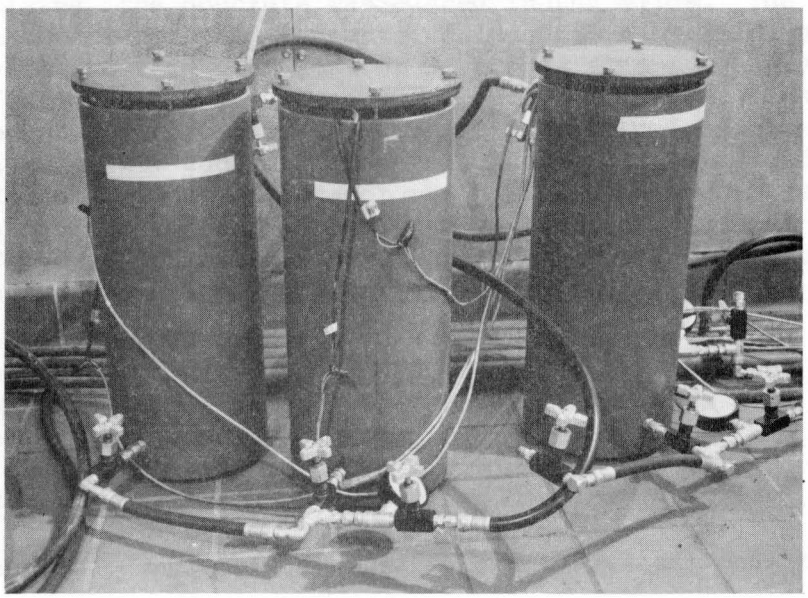

(b) Biaxial loading condition.

Fig 4. Test units.

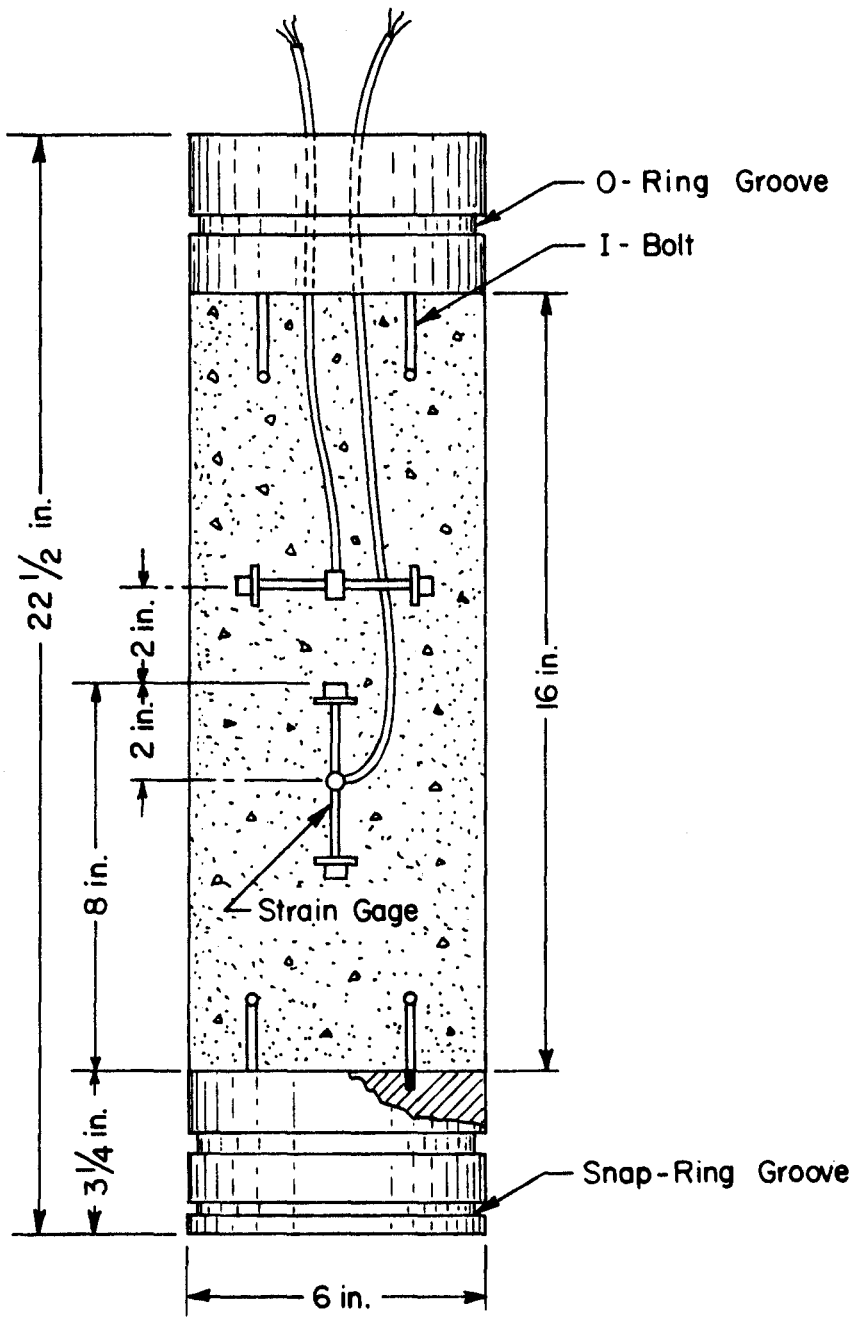

Fig 5. Test specimen and gage locations.

and standard cured specimens. The as-cast and air-dried specimens were subjected to the same curing and temperature conditions as the creep and shrinkage specimens. These strength specimens were used to evaluate the compressive and tensile strengths of the concrete for the various test conditions at various times throughout the test and to compare any existing batch-to-batch variations. The standard strength specimens were cured by being submerged in lime-saturated water and were used to compare the as-cast and air-dried concrete with concrete cured in accordance with ASTM Specifications C-192.

Casting and Compaction

A detailed description of the preparation of the test specimens for various test conditions was presented in Ref 18. A brief summary of the casting and compaction operations follows:

(1) The various molds were assembled in numerical order for casting, and the strain gages were positioned in the 6 × 16-inch molds by use of a wooden template and held in place with steel wire and nylon strings. The 6 × 12-inch specimens were cast in standard molds, except that those for the as-cast specimens contained 0.008-inch thick copper inserts which were used for sealing the specimens.

(2) After mixing, the concrete was placed in the molds. The 6 × 12-inch specimens were cast and compacted as described by ASTM Specification C-192 and then vibrated for 3 seconds at a frequency of 3600 cycles per minute. The 6 × 16-inch specimens were cast horizontally and compacted by approximately 200 strokes of a 1/4-inch diameter rod. A specially constructed curved trowel was used to finish the exposed longitudinal surface of the 6 × 16-inch specimens, which were then vibrated for 5 seconds on a vibrating table at a frequency of 3600 cycles per minute. The entire casting and compaction operation to this point took approximately 45 minutes.

(3) Four hours after casting, the 6 × 12-inch specimens were capped with neat cement and a glass plate was used to smooth the end surfaces. The exposed sides of the 6 × 16-inch specimens were also finished, with neat cement applied with the curved trowel.

Curing and Sealing

All specimens were completely covered with wet burlap immediately after casting and cured in the laboratory for 24 hours. Forms were removed after 24 hours and the specimens stored in the curing room at 100 percent relative humidity for an additional 24 hours. Immediately after the forms were removed, the surfaces of the 6 × 16-inch specimens were scrubbed with a wire brush and

a pumice stone to remove surface irregularities. All surface voids were filled with a neat cement paste. Subsequent curing and sealing procedures depended on the type of the specimen and are summarized in Table 1.

The sealing procedure (Ref 18) included the application of two coats of epoxy to the surface of the specimens, applied 24 hours apart. While the second coat was still wet, a 0.008-inch-thick copper jacket was wrapped around the specimen and soldered to the steel end slugs and to itself along the longitudinal seam. Just prior to assembling of the specimens in the test units, a 6-inch diameter, 0.12-inch-thick neoprene sleeve was slipped over the copper jacket for added protection against oil penetrating the specimen. The ends of the neoprene jacket were sealed with liquid neoprene and clamped to the specimen with a 1/4-inch stainless steel clamp.

MIXTURE DESIGN

The mixture design and all materials utilized in this investigation except water were furnished by the Concrete Division, Waterways Experiment Station, Jackson, Mississippi. Prior to shipping, the materials were proportioned into thirteen 12-cubic-foot batch quantities and placed in sealed containers.

The materials consisted of Type II cement and crushed fine and coarse limestone aggregates with a maximum size of 3/4 inches. The concrete was designed for a 28-day compressive strength of 6000 $\pm$ 600 psi for specimens cured while submerged in lime-saturated water (ASTM C-192). Mix proportions and a summary of the results of engineering tests on the materials are presented in Refs 18 and 35. A brief summary of the concrete design proportions is shown in Table 2.

EQUIPMENT AND INSTRUMENTATION

A detailed description and a discussion of the test equipment used in this experimental program are contained in Refs 18 and 35, and, therefore, the loading unit, hydraulic system, environmental control system, instrumentation, and recording system are discussed only briefly in this section.

Loading Unit

The schematic of the loading unit (Fig 3) shows all components of the loading systems. The radial load was applied directly to the sealed specimen

TABLE 1. CURING AND LOADING HISTORY OF SPECIMENS AFTER INITIAL 24 HOURS OF CURING

Specimen Type	Age	Curing/Sealing Operation
6 × 16-inch As-Cast	24 hours	First coat of epoxy applied
		Specimens placed in curing room
	48 hours	Second coat of epoxy applied
		Specimens sealed in copper
		Specimens placed in laboratory at 73.4 ± 3° F
	83 days	90-day specimens sealed in neoprene and placed in test unit at designated testing temperature
	90 days	90-day creep specimens loaded
		Shrinkage specimens remained unloaded in test environment
	176 days	183-day specimens sealed in neoprene and placed in test unit at 75° F
	183 days	183-day creep specimens loaded
	358 days	365-day specimens sealed in neoprene and placed in test unit at 75° F
	365 days	365-day specimens loaded
	454 days	90-day specimens unloaded
6 × 16-inch Air-Dried	24 hours	Specimens placed in curing room
	48 hours	Specimens submerged in lime-saturated water at 73.4 ± 3° F
	7 days	Specimens removed from lime-saturated water and placed in laboratory at 73.4 ± 3° F and 60 percent relative humidity
	81 days	First coat of epoxy applied to 90-day specimens

(Continued)

TABLE 1. (Continued)

Specimen Type	Age	Curing/Sealing Operation
	82 days	Second coat of epoxy applied to 90-day specimens, which were then sealed in copper
	83 days	90-day specimens sealed in neoprene and placed in test unit at designated testing temperature
	90 days	90-day creep specimens loaded
		Shrinkage specimens remained unloaded in test environment
	174 days	First coat of epoxy applied to 183-day specimens
	175 days	Second coat of epoxy applied to 183-day specimens, which were then sealed in copper
	176 days	183-day specimens sealed in neoprene and placed in test unit at 75° F
	183 days	183-day creep specimens loaded
	356 days	First coat of epoxy applied to 365-day specimens
	357 days	Second coat of epoxy applied to 365-day specimens, which were then sealed in copper
	358 days	365-day specimens sealed in neoprene and placed in test unit at 75° F
	365 days	365-day specimens loaded
	454 days	90-day specimens unloaded
6 × 12-inch As-Cast	24 hours	Specimens placed in curing room
	48 hours	Specimens sealed in copper

(Continued)

TABLE 1. (Continued)

Specimen Type	Age	Curing/Sealing Operation
		Specimens placed in laboratory at 73.4 ± 3° F
	83 days	Specimens to be tested at 183 days or beyond stored at designated temperature
	28, 90, 183 365, 538 days	Compressive or tensile strengths determined; 24 hours prior to strength test, copper seal removed and specimen stored at 73.4 ± 3° F
6 × 12-inch Air-Dried	24 hours	Specimens placed in curing room
	48 hours	Specimens submerged in lime-saturated water at 73.4 ± 3° F
	7 days	Specimens removed from lime-saturated water and placed in laboratory at 73.4 ± 3° F and 60 percent relative humidity
	83 days	Specimens to be tested at 183 days or beyond sealed in copper and stored at designated temperature
	28, 90, 183, 365, 538 days	Compressive or tensile strengths determined; 24 hours prior to strength test, copper seal removed and specimen stored at 73.4 ± 3° F
6 × 12-inch Standard	24 hours	Specimens placed in curing room
	48 hours	Specimens submerged in lime-saturated water at 73.4 ± 3° F
	28, 90 days	Specimens removed from lime-saturated water, compressive strength determined

TABLE 2. MIX DESIGN SUMMARY

Water-cement ratio, by weight	0.425
Cement content, sacks/cu yd	7.25
Maximum size of coarse aggregate, inches	3/4
Slump, inches	2

Material	Size Range	Mix Proportion, Percent	
		By Volume	By Weight
Cement	----	15.5	17.8
Fine aggregate	Sand	37.1	35.9
Coarse aggregate (A)	No. 4	14.2	13.9
Coarse aggregate (B)	3/8 inch	16.6	16.2
Coarse aggregate (C)	1/2 inch	16.6	16.2

by hydraulic oil pressure contained within a 1-inch-thick steel pressure jacket; the axial load was applied by a hydraulic ram. Thus, the triaxial loading unit consisted of both an axial and a radial loading system, which permitted each to be varied independently. The axial loading frame without the pressure jackets was used for the uniaxial case. The radial pressure jacket without the axial loading frame was used for the biaxial case (Fig 4b).

Each loading unit contained two specimens from the same batch, one as-cast and one air-dried, which were simultaneously subjected to the same temperature and stress conditions. The relative positions of the as-cast and air-dried specimens within the frame were determined randomly in order to minimize bias in the results due to specimen location. The biaxial specimens were also simultaneously loaded in pairs under identical conditions.

The loading system developed for this investigation was generally satisfactory; however, preliminary tests (Refs 15, 16, and 17) revealed that the axial stresses were less than those indicated by the pressure gage, due to frictional losses in the hydraulic-mechanical pressure system. Therefore, each of the loading units was calibrated with a load cell. The axial stress for the various units ranged from 90 to 97 percent of the desired stress. The average axial stresses for the units with the desired levels of 0, 600, 1200, 2400, and 3600 psi were 0, 545, 1080, 2185, and 3460 psi, respectively.

Hydraulic System

Hydraulic pressure was supplied to the loading units by using the 100-psi air pressure, available in the laboratory, to drive oil pressure intensifiers since only a small quantity of oil had to circulate once the system was pressurized.

The hydraulic system consisted of a pressure control console, eight pressure manifolds to the loading units and the necessary return lines. The pressure control console housed the pressure control valves, pressure intensifiers, air reservoir, auxiliary air compressor, and pressure gages for the four different pressures.

The pressure system was designed for 5000-psi pressure and consisted of hydraulic pressure pipes with flexible pressure hoses to the test units. A dual system was employed for each of the four pressures (600, 1200, 2400, and 3600 psi). One manifold system supplied pressure to the 75° F laboratory and

the other to the 150° F temperature control room. Each manifold system contained a return line with connections to each test unit to allow oil to be circulated in order to remove air from the system and prevent the control valves from sticking.

The hydraulic system was designed with two back-up subsystems. An auxiliary pressure intensifier was installed to be ready to replace any of the four intensifiers which might fail or require maintenance. Also included was an auxiliary air compressor which operated automatically if the laboratory air pressure dropped significantly.

The control system automatically regulated the pressure to within ± 5 percent of the assigned gage pressure. Any of the eight pressure lines could be independently controlled, and each test unit had separate controls.

Environmental Control

To make valid creep comparisons, a constant temperature and relative humidity had to be maintained over a long period of time. The tests performed under the nominal 75° F test condition were conducted in an air-conditioned laboratory, while the tests performed under the nominal 150° F test condition were conducted in a temperature chamber which was designed to maintain a constant temperature anywhere in the range of -20° F to 150° F. The relative humidity was maintained by the air-conditioning system at an average value of about 60 percent, although it fluctuated from about 50 to 65 percent.

Vibrating Wire Strain Gage

A vibrating wire strain gage, PC 641, manufactured in England by Perivale Control Company, was used. This gage, approximately 4 inches long, had a gage length of approximately 3.5 inches, was stable over a relatively long period of time, and was relatively inexpensive.

A cross section of the Perivale gage is shown in Fig 6. The gage basically consisted of a hollow brass tube with a steel cap at each end and a steel wire tensioned between them. The gage measured strain, or change in strain, by detecting changes in frequency of vibration of the wire. The frequency of the wire was measured by an electronic comparator which, when activated, plucked the wire by use of an electromagnet in the gage. The magnetic coil was used to measure the vibration of the wire and the frequency was compared with a standard frequency generated in the comparator. From this comparison, the frequency of the gage wire could be measured and used to calculate

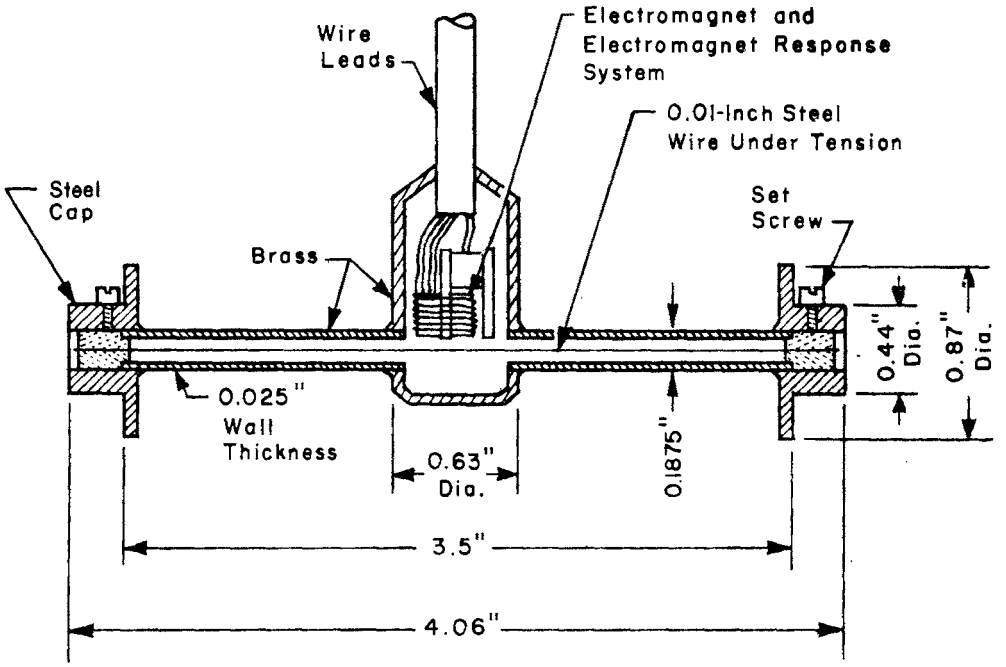

Fig 6. Cross section of Perivale vibrating wire strain gage (Ref 18).

the change in strain (Eq 1), providing the initial and final frequency readings were made at the same temperature and there was temperature equilibrium.

Actual strains were calculated using Mersonnes' and Hooke's Laws, which in combination yielded the following equation:

$$\Delta\epsilon = \epsilon_i - \epsilon_f = K\left(F_i^2 - F_f^2\right) \tag{1}$$

where

K = gage factor,

F_i = the initial (or reference) frequency,

F_f = the frequency at the strain point desired,

ϵ_i = the initial (or reference) strain,

ϵ_f = the strain point desired.

The Perivale gage when cast in concrete had a gage factor of 1.24×10^{-3}, which was determined experimentally by the manufacturer. The range of the gage was approximately 1000 micro-units of strain and it could be read to an accuracy of one micro-unit of strain. The gage was supplied with an initial frequency or wire tension which allowed strain measurements ranging from 285 micro-units in tension to 1050 micro-units in compression.

Temperatures in the creep and shrinkage specimens were measured throughout the test period by a wheatstone bridge circuit in the comparator which measured the change in resistance of the electromagnetic coil in each gage. Thus, two internal temperature readings were recorded for each specimen. An equation relating coil resistance to temperature change was provided by the manufacturer.

For recording strain and temperature data, the comparator was connected to a switchboard. Each gage was connected by an individual cable to the switchboard, and the strain or temperature in any one of the 204 gages (102 specimens) was measured from a central location.

The vibrating wire strain gage was considered generally satisfactory and appeared to remain stable throughout the test period. However, 39 of the 204 gages became inoperative before the end of the test: 11 stopped functioning

because the range of the gage was exceeded, 5 exceeded the range of the comparator, and 23 simply failed, probably due to oil or water leakage. The number of gage failures was much higher for the test conditions at 150° F than at 75° F.

OUTLINE OF EXPERIMENTAL PROCEDURE

The actual test program began with the casting of Batch A on October 29, 1968. Thereafter a new batch was cast each week in alphabetical order through Batch G. Batches H and I were cast in June 1969. Batches A through G provided concrete for specimens of the 90-day loading condition, while Batches H and I provided concrete for specimens of the 183 and 365-day loading conditions and for replacements of specimens which failed in Batches A through G. The casting and testing procedures were identical for all batches. All specimens cured for 90 days were loaded for a period of 12 months, after which the load was removed and observations of creep recovery continued for five months. Specimens cured for 183 or 365 days were loaded for an indefinite period of time.

The loading and unloading operation for each batch followed the same procedure. Each as-cast specimen was loaded or unloaded simultaneously with its companion air-dried specimen. Both axial and radial loads were applied or removed at the same time with maximum stress applied or removed at a rate of 35 psi per second. The ratio of the axial to radial loads during loading or unloading was maintained constant and equal to the ratio of the final axial and radial loads. The gages in each test unit were read in the following order: as-cast axial gage, as-cast radial gage, air-dried axial gage, air-dried radial gage.

In addition, the unconfined compressive and tensile strengths were determined for various environmental conditions during the test period. The compressive strength was determined at 28, 90, 183, 365, and 538 days after casting (ASTM C-39). Tensile strengths at 28, 90, and 538 days were determined for Batches B through F using the indirect tensile test (ASTM C-496).

EXPERIMENTAL DESIGN

The various specimens of the 90-day loading condition investigated in this experimental program were randomly assigned to the first seven batches,

with the restrictions that each batch contain specimens at both test temperatures and an equal number of specimens for each curing history. The only restrictions on Batches H and I were to provide specimens for the 183 and 365-day loading conditions and replacements for specimens of the 90-day loading condition that failed before or during the test. The specimens in each batch were prepared and tested in a random numerical sequence in order to eliminate bias resulting from the casting and testing operations. The various combinations of test variables for the creep and shrinkage specimens are shown in Table 3.

TABLE 3. EXPERIMENTAL DESIGN FOR CREEP AND SHRINKAGE SPECIMENS

Age of Loading*	Temperature, °F	Axial Load, psi	Radial Load, psi	Creep Specimens**		Companion Shrinkage Specimens**	
				As-Cast	Air-Dried	As-Cast	Air-Dried
90	75	0	600	F-13	F-42	F-23	F-17
		0	3600	H-22r	H-14r	H-24	H-1
		600	0	E-39	E-40	E-28	E-23
		600	600	E-5	E-13	E-28	E-23
		600	3600	G-35	G-30	G-18	G-10
		1200	1200	C-16x	C-17	C-39	C-6
		1200	2400	B-41	B-42	B-29	B-23
		2400	0	B-7	B-19	B-29	B-23
		2400	600	C-23	C-11	C-39	C-6
		2400	2400	F-9	F-30	F-23	F-17
		3600	1200	D-26	D-44	D-20	D-33
		3600	3600	D-31	D-40	D-20	D-33
	150	0	600	A-35	I-13rf	A-22	I-1
		0	1200	I-27r	D-3	I-21	D-23
		0	2400	E-43	E-1	E-10	E-42
		0	3600	I-16r	I-30rf	I-21	I-1
		600	0	B-4	B-1	B-13	B-26
		1200	0	D-15	D-22	D-12	D-23
		1200	1200	C-12	C-46x	C-41	C-36
		1200	2400	D-2x	D-41	D-12	D-23
		2400	0	F-33	F-34	F-15	F-21
		2400	600	E-18	E-4	E-10	E-42
		2400	2400	G-9	G-19	G-1	G-21
		3600	0	B-16	B-5	B-13	B-26
		3600	3600	F-20	F-6	F-15	F-21
183	75	600	0	H-45	I-39	H-28	I-17
		2400	0	H-34	I-20	H-28	I-17
365	75	600	0	H-5	H-31	H-28	H-35
		2400	0	H-24	H-17	H-28	H-35

* age of loading for creep specimens

** specimen designation: the letter indicates the batch and the numeral indicates the specimen within the batch

r replacement specimens

x radial pressure zero ($\sigma_r = 0$) due to oil leak in specimen

f specimen failed shortly after loading

CHAPTER 4. EXPERIMENTAL RESULTS

This chapter contains a summary of the data obtained in this investigation. With the exception of the information on creep recovery, most of these results have been presented and discussed in previous project reports (Refs 1 and 35). Nevertheless, it was felt that these results should be briefly summarized in this report in order to completely describe the overall experiment, incorporate information for the evaluation of the observed creep recovery behavior, and to document data obtained subsequent to the completion of the previous reports. Thus, this chapter contains summaries of compressive and tensile strengths, shrinkage strains prior to and subsequent to loading of the creep specimens, instantaneous strains at the time of loading, creep strains, and recovery data, including the instantaneous and creep recovery strains.

STRENGTH OF CONCRETE

The compressive strengths of all the 252 specimens were determined in accordance with ASTM C39-66 testing procedures, and the tensile strengths of 76 specimens were obtained in accordance with ASTM C496-69.

The average compressive and tensile strengths for the nine batches of concrete are shown in Table 4. These strength values usually represent the average of at least three tests although in some cases only two specimens were tested. The individual compressive strengths of the specimens tested at ages of 183 days or less are presented in Appendix B of Ref 1, while the individual strengths at 365 and 538 days are contained in Appendix A of this report.

The average strength of standard cured specimens at 28 days was 6420 psi, which was within the design strength of 6000 ± 600 psi, and the standard deviation was 208 psi. The average strength of standard cured specimens at 90 days was 8220 psi with a standard deviation of 343 psi.

The air-dried specimens had a higher average compressive strength than the as-cast specimens up to a period of 90 days after casting. Subsequent to this time the as-cast specimens were stronger. The probable cause of this phenomenon is associated with the curing procedure for the two types of

TABLE 4. AVERAGE COMPRESSIVE AND TENSILE STRENGTHS

	Age at Testing	Curing Conditions	Temperature, °F	Average Compressive Strengths of Batches, psi									Average of all Batches, psi
				A	B	C	D	E	F	G	H	I	
Compressive	28	Standard		6760	6650	6140	6200	6520	6510	6440	6340	6260	6420
		As-Cast		6580	4710	5700	5980	5410	5650	5940	5650	5790	5710
		Air-Dried		7060	6200	6520	6640	6540	6680	6570	6320	6440	6550
	90	Standard		8550	8690	8290*	8540	8200	8090	7730	8110	7870	8220
		As-Cast		6880	6110	6430*	6500	7290	7410	7460	6330	6160	6640
		Air-Dried		6960	7790	7370*	7790	7420	7870	7460	7280	7060	7450
	183	As-Cast	75	8260	-	-	-	-	-	7620	7660	6960	7630
			150	8120	-	-	-	-	-	8280	-	7730	8040
		Air-Dried	75	7030	-	-	-	-	-	7310	7470	7200	7250
			150	7760	-	-	-	-	-	7100	-	6960	7270
	365	As-Cast	75	8840	-	-	-	-	-	8190	6930	7340	7830
			150	7600	-	-	-	-	-	8310	-	7660	7860
		Air-Dried	75	7480	-	-	-	-	-	7810	6860	7590	7440
			150	7010	-	-	-	-	-	7860	-	7170	7350
	538	As-Cast	75	8430	-	-	-	-	-	9010	7530	7170	8040
			150	9130	-	-	-	-	-	8270	-	7470	8290
		Air-Dried	75	8570	-	-	-	-	-	8070	7550	7470	7920
			150	7940	-	-	-	-	-	7550	-	7860	7780
Tensile	28	Standard		-	630**	580	620	570	550	-	-	-	590
		As-Cast		-	-	-	520	-	-	-	-	-	-
		Air-Dried		-	560**	-	530	-	-	-	-	-	-
	90	Standard		-	540	680	510	710	690	-	-	-	630
		As-Cast		-	550	610	530	590	590	-	-	-	570
		Air-Dried		-	540	580	550	550	580	-	-	-	560
	538	As-Cast	75	-	600	590	-	550	490	-	-	-	560
			150	-	600	550	-	620	610	-	-	-	600
		Air-Dried	75	-	760	740	-	650	690	-	-	-	710
			150	-	660	580	-	610	660	-	-	-	630

* Batch C tested at 83 days.

** Only one sample used.

specimens. The air-dried specimens were moist cured for two days and then submerged in lime-saturated water for five more days before being air-dried at 75° F for the remainder of the 90-day curing period. The as-cast specimens were sealed directly after the first two days of moist curing. The more efficient wet curing experienced by the air-dried specimens during the first seven days produced strength gains in excess of those experienced by the as-cast specimens. However, over an extended period of time continuous curing at a higher moisture content resulted in a greater rate of strength gain for the as-cast specimens than for the air-dried specimens. The average strengths of the specimens subjected to a temperature of 150° F were slightly higher than the average strengths of specimens subjected to 75° F.

The average tensile strength of specimens in all batches increased slightly with age. The individual strengths for the specimens tested at 28 and 90 days are given in Appendix C of Ref 35 and the strengths for specimens tested at 538 days appear in Appendix A of this report.

INSTANTANEOUS STRAINS AND ELASTIC PROPERTIES

The instantaneous or elastic strain due to the applied load was determined by taking readings just prior to loading and immediately after the maximum load had been applied. Since there were four gages to be read, there was a delay in obtaining all of the readings; therefore, the instantaneous strains were estimated by extrapolating the strain-time relationship to obtain the strain at time zero. In general, it was found that these estimated strains were approximately 1 to 5 microunits less than the measured values.

The elastic properties of concrete, i.e., modulus of elasticity and Poisson's ratio, were calculated from theory of elasticity. Calculated values for modulus of elasticity and Poisson's ratio are shown in Table 5. The modulus of elasticity and Poisson's ratio of uniaxially and biaxially loaded specimens were very consistent, while values for the triaxially loaded specimens were inconsistent, probably because the relationships used to calculate the values are very sensitive for a hydrostatic loading condition. In addition, the radial and axial loads were applied at different rates, which may have caused additional errors. For these reasons specimens subjected to a stress condition approaching a hydrostatic state of stress were eliminated.

TABLE 3a. INSTANTANEOUS STRAINS AND CREEP STRAINS AFTER ONE YEAR OF LOADING FOR AS-CAST SPECIMENS AT 75° F

Age at Loading, days	Specimen	Stress, psi		Instantaneous Strain ε_i^*, Micro-Units		Creep Strain After 1 Year ε_c^*, Micro-Units		$\varepsilon_c/\varepsilon_i$		$E \times 10^6$, psi	Elastic Poisson's Ratio	Creep Poisson's Ratio
		Axial	Radial	Axial	Radial	Axial	Radial	Axial	Radial			
90	E-39	527	0	87	-26	75	10	.862	-.385	6.04	.293	-.133
	B-7	2179	0	385	-94	322	-42	.836	.447	5.66	.243	.130
	F-13	0	600	-52	72	-37	57	.712	.792	6.13	.264	.378
	H-22	0	3600	-333	631	-308	739	.925	1.171	4.51	.209	.414
	E-5	562	600	38	57	24	37	.632	.649	2.78	.381	.387
	C-23	2139	600	283	-10	242	-15	.855	1.500	6.54	.244	.260
	C-16x	1100	1200	58	127	216	-207	-	-	2.04	.409	.958
	D-26	3449	1200	473	-12	373	26	.789	-2.167	5.91	.273	.219
	B-41	1092	2400	-8	214	340	154	-42.500	.703	7.14	.239	1.446
	F-9	2147	2400	178	197	191	238	1.073	1.208	12.55	-.017	.192
	G-35	536	3600	-255	524	-176	614	.690	1.172	4.91	.248	.187
	D-31	3472	3600	286	342	300	348	1.049	1.018	3.11	.358	.334
183	H-45	600	0	91	-23	121	42	1.330	-1.828	6.59	.253	-.347
	H-34	2400	0	385	-84	274	-34	.712	.405	6.23	.224	.124
365	H-5	600	0	74	-20	35	2	.473	-.100	8.11	.270	-.057
	H-24	2400	0	328	-90	232	-22	.708	.245	7.32	.274	.095

TABLE 5b. INSTANTANEOUS STRAINS AND CREEP STRAINS AFTER ONE YEAR OF LOADING FOR AIR-DRIED SPECIMENS AT 75°

Age at Loading, days	Specimen	Stress, psi		Instantaneous Strain ϵ_i*, Micro-Units		Creep Strain After 1 Year ϵ_c*, Micro-Units		ϵ_c/ϵ_i		E x 10^6, psi	Elastic Poisson's Ratio	Creep Poisson's Ratio
		Axial	Radial	Axial	Radial	Axial	Radial	Axial	Radial			
90	E-40	527	0	93	-26	69	-17	.742	.655	5.64	.279	.247
	B-19	2179	0	379	-104	398	-43	1.050	.414	5.76	.274	.108
	F-42	0	600	-52	74	-33	81	.635	1.095	5.98	.258	.169
	H-14	0	3600	-340	572	-353	**	1.038	-	4.85	.229	-
	E-13	562	600	32	51	45	77	1.406	1.510	2.84	.329	.406
	C-11	2139	600	331	-21	397	-8	1.199	.381	5.51	.261	.233
	C-17	1100	1200	75	101	35	45	.467	.446	4.92	.306	.273
	D-44	3449	1200	533	-16	**	114	-	-7.125	5.23	.276	-
	B-42	1092	2400	-4	262	233	129	-58.250	.492	6.05	.233	2.152
	F-30	2147	2400	171	220	271	423	1.585	1.923	6.30	.223	.323
	G-30	536	3600	-240	522	-134	**	.558	-	4.99	.241	-
	D-40	3472	3600	298	357	532	705	1.785	1.975	2.97	.359	.602
183	I-39	600	0	77	-23	-9	-39	-.117	1.696	7.79	.299	-4.333
	I-20	2400	0	386	-94	330	-3	.855	.032	6.22	.244	.091
365	H-31	600	0	100	-20	36	5	.360	-.250	6.00	.200	-.139
	H-17	2400	0	442	-85	291	-15	.659	.176	5.43	.193	.052

TABLE 5c. INSTANTANEOUS STRAINS AND CREEP STRAINS AFTER ONE YEAR OF LOADING FOR AS-CAST SPECIMENS AT 150° F

Age at Loading, days	Specimen	Stress, psi		Instantaneous Strain, ϵ_i^*, Micro-Units		Creep Strain After 1 Year ϵ_c^*, Micro-Units		ϵ_c/ϵ_i		E x 10^6, psi	Elastic Poisson's Ratio	Creep Poisson's Ratio
		Axial	Radial	Axial	Radial	Axial	Radial	Axial	Radial			
90	B-4	561	0	94	-22	**	80	-	-3.636	5.94	.235	-
	D-15	1102	0	203	-53	195	**	.961	-	5.44	.259	-
	F-33	2123	0	412	-109	**	**	-	-	5.15	.265	-
	B-16	3450	0	538	-150	**	**	-	-	6.42	.280	-
	A-35	0	600	-48	71	**	70	-	.986	6.35	.253	-
	I-27	0	1200	-101	147	**	**	-	-	6.08	.256	-
	E-43	0	2400	-221	321	**	**	-	-	5.56	.256	-
	I-16	0	3600	-351	350	**	**	-	-	4.97	.242	-
	E-18	2259	600	322	-4	**	**	-	-	6.19	.219	-
	C-12	1032	1200	77	95	147	**	1.909	-	10.36	.096	-
	D-2x	1086	2400	-54	266	391	-402	-	-	5.28	.284	-
	G-9	2268	2400	181	239	273	353	1.508	1.477	3.12	.355	.346
	F-20	3474	3600	423	423	**	**	-	-	1.56	.416	-

TABLE 5d. INSTANTANEOUS STRAINS AND CREEP STRAINS AFTER ONE YEAR OF LOADING FOR AIR-DRIED SPECIMENS AT 150° F

Age at Loading, days	Specimen	Stress, psi		Instantaneous Strain ϵ_i^*, Micro-Units		Creep Strain After 1 Year ϵ_c^*, Micro-Units		ϵ_c/ϵ_i		$E \times 10^6$, psi	Elastic Poisson's Ratio	Creep Poisson's Ratio
		Axial	Radial	Axial	Radial	Axial	Radial	Axial	Radial			
90	B-1	561	0	102	-25	114	0	1.118	-	5.49	.249	-
	D-22	1102	0	255	-54	202	2	.792	-.037	4.32	.210	-.010
	F-34	2123	0	469	-123	623	**	1.328	-	4.53	.262	-
	B-5	3450	0	759	-174	**	**	-	-	4.58	.229	-
	I-13f	0	600	-53	87	-	-	-	-	5.29	.235	-
	D-3	0	1200	-86	160	-36	**	.419	-	5.91	.211	-
	E-1	0	2400	-233	369	**	**	-	-	4.93	.240	-
	I-30f	0	3600	-377	629	-	-	-	-	4.40	.230	-
	E-4	2259	600	378	-15	416	**	1.101	-	5.23	.237	-
	C-46x	1032	1200	101	117	359	-226	-	-	10.28	-.003	-
	D-41	1086	2400	-23	382	131	500	-5.696	1.309	4.04	.246	.118
	G-19	2268	2400	190	253	295	391	1.553	1.546	2.82	.361	.359
	F-6	3474	3600	387	429	700	**	1.809	-	3.80	.278	-

* Compression is positive and tension is negative.
** Gage failed or gage range was exceeded.
f Specimen failed shortly after loading.
x Radial pressure reduced to zero shortly after initial loading due to oil leak.

Excluding hydrostatically loaded specimens, the averages of moduli of elasticity for the as-cast and air-dried specimens loaded at 75° F were 5.86×10^6 and 5.50×10^6 psi, respectively. Specimens loaded at 150° F had lower modulus values, with the average values for the as-cast and air-dried specimens being 5.74×10^6 psi and 4.87×10^6 psi, respectively.

SHRINKAGE STRAINS

In order to estimate creep strains it was necessary to measure shrinkage strains during the creep and the recovery periods. In order to interpret these shrinkage strains it was necessary to evaluate shrinkage strains during the curing period.

During the Curing Period

Estimates of the relationships between shrinkage strain and time for the as-cast and air-dried specimens during the curing period were obtained by averaging the strains measured in both the shrinkage and creep specimens from batches A through I, which provided concrete for the specimens loaded at 90 days (Fig 7). In these relationships the seven-day reading was considered as the initial reference point, since the curing and handling procedures during the first seven days were different.

The average axial and radial strains of the as-cast specimens were essentially zero throughout the curing period (Fig 7a) and these specimens did not show any significant loss of water during the curing period. On the other hand, the average strains of the air-dried specimens showed continuous increase (Fig 7b) accompanied by continuous loss of water during the first 82 days, at the end of which the specimens were sealed in copper. The average axial and radial shrinkage strains for the air-dried specimens were approximately 240 and 190 micro-units respectively, and the loss of water was between 8 and 11 ounces. The apparent increase in strains between 83 and 90 days for as-cast and air-dried specimens subjected to 150° F was due to a difference in thermal characteristics of the gage and concrete and is discussed in Ref 1.

During the Testing Period

Shrinkage strains were measured during the loading period in order to estimate creep strain by separating the total time-dependent strain into that due to moisture loss and that due to load. Throughout the 12-month loading

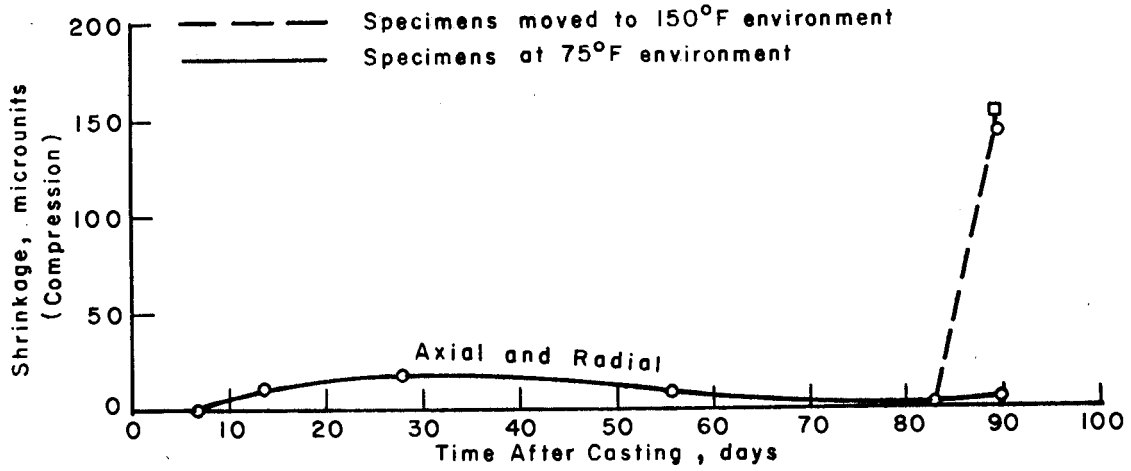

(a) As-cast specimens.

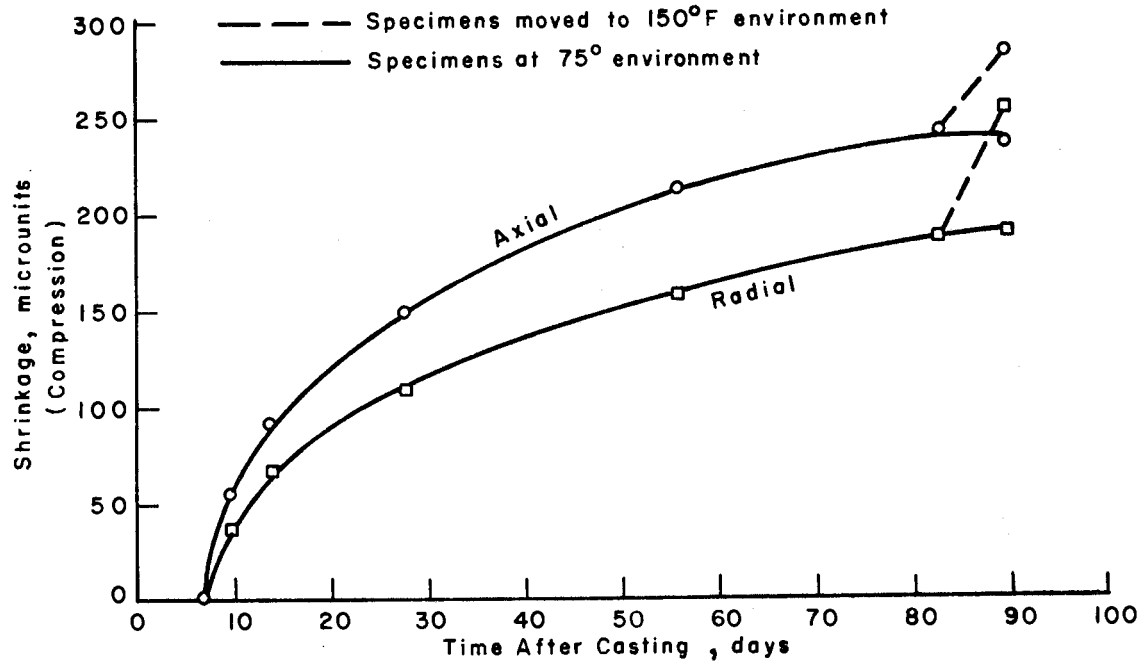

(b) Air-dried specimens.

Fig 7. Average shrinkage strains for as-cast and air-dried specimens during the 90-day curing period.

period shrinkage specimens were subjected to the same environmental condition as the creep specimens. Average shrinkage curves for the as-cast and air-dried shrinkage specimens from batches A through G are shown in Fig 8.

Essentially no shrinkage occurred in the as-cast specimens (Fig 8a) at 75° F; however, at 150° F the specimens exhibited expansion rather than shrinkage. Most of this expansion occurred during the first 84 days of the loading period, at the end of which the axial and radial gages indicated tensile strains of 33 and 37 microunits, respectively. During the remainder of the loading period very little additional strain was detected.

The shrinkage behavior associated with specimens subjected to the 150° F temperature can probably be attributed to an interaction effect involving temperature change, the concrete, and the gage. This effect is believed to be due primarily to the fact that the gage and the concrete are not compatible when subjected to temperature change. When the temperature was raised from 75° F to 150° F the gage tended to expand more than the concrete but was prevented from expanding by the concrete. Nevertheless, localized stresses were produced in the concrete, and as these stresses were relieved by localized creep of the concrete, the gage was allowed to expand, producing increased tension in the gage wire. This increasing tension during the first 84 days after loading accounts for the apparent expansion of the concrete. This effect is discussed in detail in Ref 35.

The axial and radial shrinkage strains in the air-dried specimens at 75° F (Fig 8b) increased at a decreasing rate throughout the entire loading period. However, the radial strains were comperssive (shrinkage) while the axial strains were tensile (expansion). Nevertheless, the magnitudes of the strains after 12 months were relatively small, with the axial gage indicating 34 microunits (tension) and the radial gage 18 microunits (compression).

The shrinkage strain relationships for the air-dried specimens at 150° F were similar to those of the as-cast specimens at the same temperature, although the strains were larger. These specimens expanded continuously at a decreasing rate. At the end of the 12-month loading period the axial and radial strains were 67 and 53 microunits (expansion), respectively.

No special shrinkage specimens were cast for the as-cast specimens which were loaded at 183 and 365 days after casting since all as-cast specimens, regardless of the curing period, were sealed two days after casting. Thus,

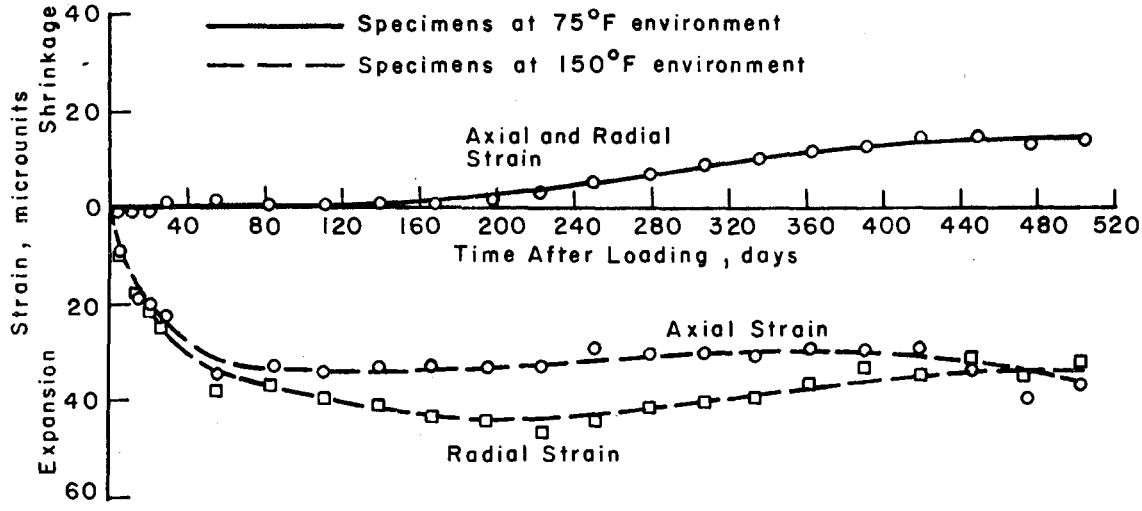

(a) As-cast specimens.

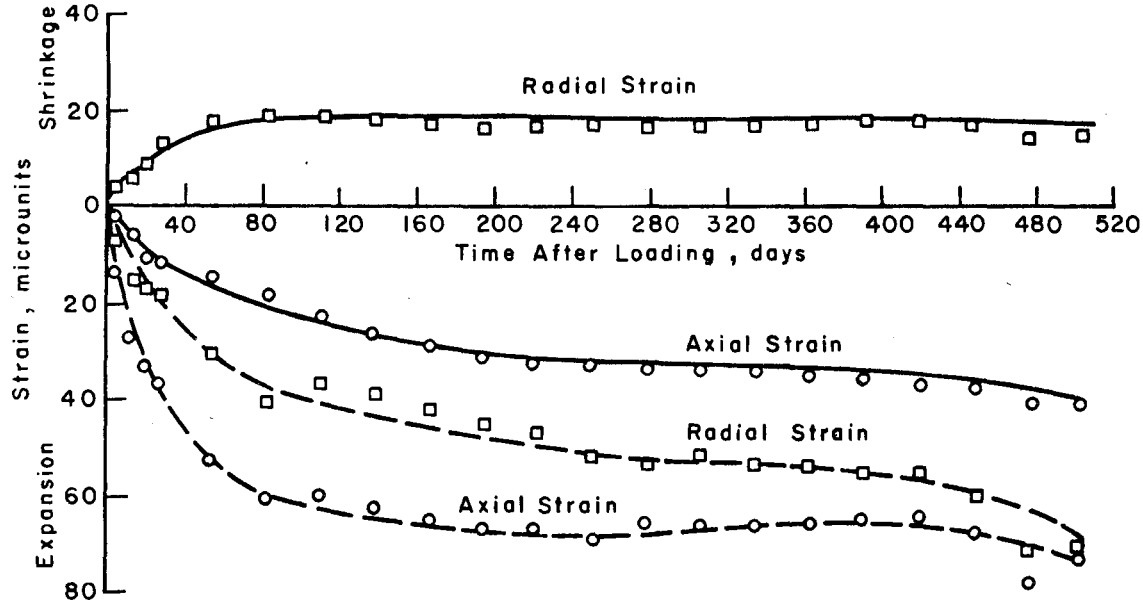

(b) Air-dried specimens.

Fig 8. Average shrinkage strains during the loading and unloading periods for specimens loaded at 90 days.

the shrinkage strains for the as-cast specimens were estimated from the average shrinkage time relationships obtained from the shrinkage specimens associated with the 90-day creep specimens. The average shrinkage strains resulting from these considerations are shown in Table 6. For the air-dried condition, the 183 and 365-day specimens were cured longer than the 90-day specimens before being sealed, thus requiring special shrinkage specimens to obtain satisfactory results. The values obtained from a single shrinkage specimen for each of the air-dried 183 and 365-day specimens are also shown in Table 6.

CREEP STRAINS

Creep strain estimates were obtained by subtracting the instantaneous strains and the shrinkage strains from the total strains. Thus it was assumed that the instantaneous (elastic) strain for each specimen was constant and did not vary with time and that the time-dependent strains, i.e., shrinkage and creep, were not interrelated. The creep strain-time relationships for the various specimens are shown in Figs A.1 through A.19 in Appendix A of Ref 4 and the data are summarized in Appendix G of Ref 35.

The creep rate was much larger during the early portion of the loading period, but about three months after loading the creep strain became relatively constant and no significant change occurred during the remaining nine months of the loading period. The creep strains after one year under load and their ratios to the instantaneous strains at the time of loading are summarized in Table 5. These ratios were larger for the air-dried specimens and for the specimens loaded at 150° F.

A more comprehensive evaluation of the effects of moisture condition and testing temperature is contained in Ref 35. The results discussed above can, however, generally be summarized as follows:

(1) At a constant temperature, air-dried specimens had higher creep strains than as-cast specimens.

(2) Both as-cast and air-dried specimens tested at 150° F exhibited higher creep strains than those tested at 75° F.

(3) In uniaxially and biaxially loaded specimens at both temperatures, creep strains occurred in the direction perpendicular to the direction of the applied stress, indicating a creep Poisson's effect.

TABLE 6. AVERAGE SHRINKAGE STRAINS FOR THE 183 AND 365-DAY LOADING CONDITIONS, TEMPERATURE AT 75° F

Days After Loading	183-Day Loading Condition				365-Day Loading Condition			
	As-Cast		Air-Dried		As-Cast		Air-Dried	
	Axial	Radial	Axial	Radial	Axial	Radial	Axial	Radial
2			-3.9	-1.2			-2.5	0.0
5			-6.2	-.6			-6.3	1.3
7			-7.3	-1.2			-5.0	2.5
14			-11.8	1.8			12.6	0.0
21			-15.7	1.8			-15.2	0.0
28	-0.4	-0.1	-19.1	.6	1.1	2.3	-19.0	1.3
56	0.3	0.8	-31.6	-3.0	4.2	4.4	-27.9	-6.4
84	0.3	1.4	-43.6	-7.8	5.8	5.6	-36.8	-12.8
112	1.9	1.8	-45.3	-9.7	6.3	6.2	-	-
140	3.3	4.0	-	-	9.3	8.9	-43.2	-16.6
168	5.2	5.3	-55.6	-17.5	9.7	8.8	-56.1	-28.1
196	5.9	6.1	-62.0	-23.0			-54.8	-25.6
224	7.7	8.4	-62.5	-23.0			-58.6	-29.4
252	10.1	10.5	-67.7	-27.2			-56.1	-26.9
280	11.7	11.7	-	-			-56.1	-26.9
308	12.2	12.3	-70.1	-29.7			-	-
336	15.2	15.0	-72.4	-32.1			-62.5	-33.3
364	15.6	10.9	-74.1	-34.0			-65.1	-34.6

CREEP POISSON'S RATIO

The results from this investigation definitely indicate a creep Poisson's effect.

The following expression was used to calculate the creep Poisson's ratio for cylindrical specimens subjected to the various states of stress:

$$\nu_c = \frac{\sigma_a(\epsilon_c)_r - \sigma_r(\epsilon_c)_a}{2\sigma_r(\epsilon_c)_r - (\epsilon_c)_a(\sigma_r + \sigma_a)} \qquad (4.1)$$

where

ν_c = creep Poisson's ratio;

σ_a = axial stress, psi;

σ_r = radial stress, psi;

$(\epsilon_c)_a$ = creep strain in axial direction;

$(\epsilon_c)_r$ = creep strain in radial direction.

Creep Poisson's ratios calculated for the as-cast and air-dried specimens tested at 75° F are shown in Fig 9. The ratios for both as-cast and air-dried specimens increased slightly with time. The overall average creep Poisson's ratio for the as-cast specimens was 0.150 and for air-dried specimens was 0.108.

Creep Poisson's ratios calculated for the as-cast and air-dried specimens tested at 150° F are shown in Fig 10. Creep Poisson's ratio decreased rapidly during the first week under load. For the as-cast specimens, the average creep Poisson's ratio decreased from 0.30 at three hours after loading to 0.142 at the end of the first week, and then fluctuated around 0.165. For air-dried specimens, the average creep Poisson's ratio decreased from 0.27 at three hours after loading to 0.17 at the end of the first week, and then fluctuated around 0.14. The overall average of creep Poisson's ratio during the first month was 0.149 for as-cast specimens and 0.140 for air-dried specimens.

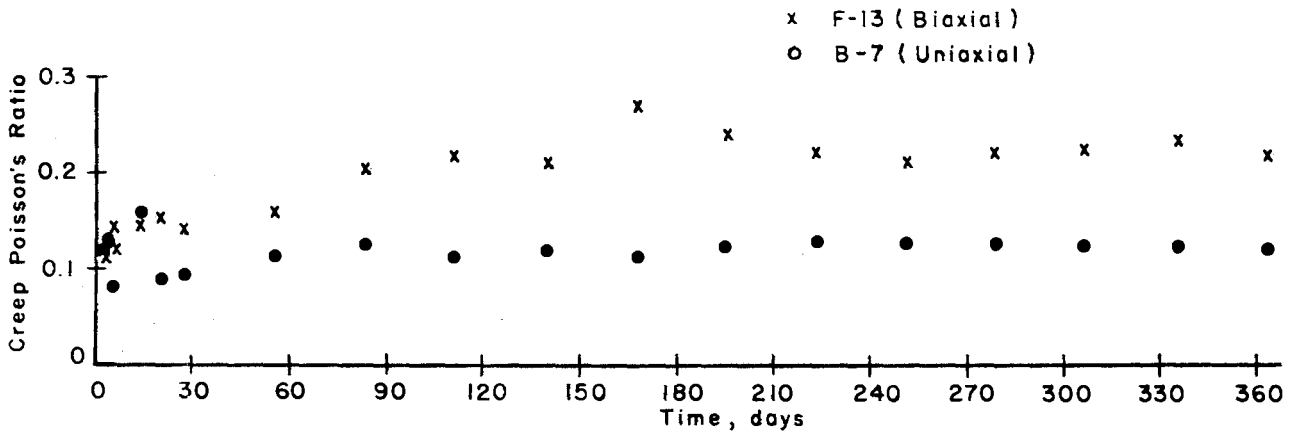

(a) As-cast specimens.

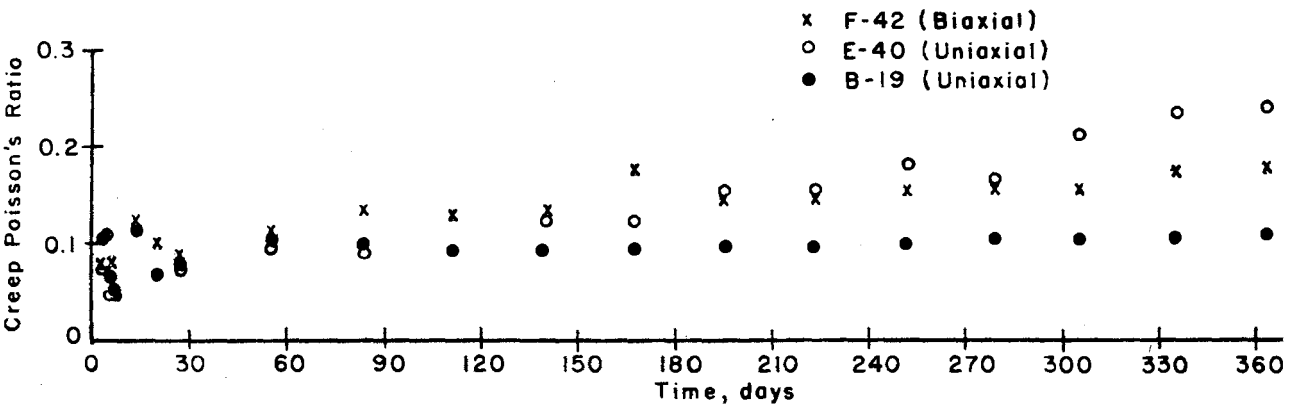

(b) Air-dried specimens.

Fig 9. Creep Poisson's ratio for as-cast and air-dried specimens at 75° F (Ref 4).

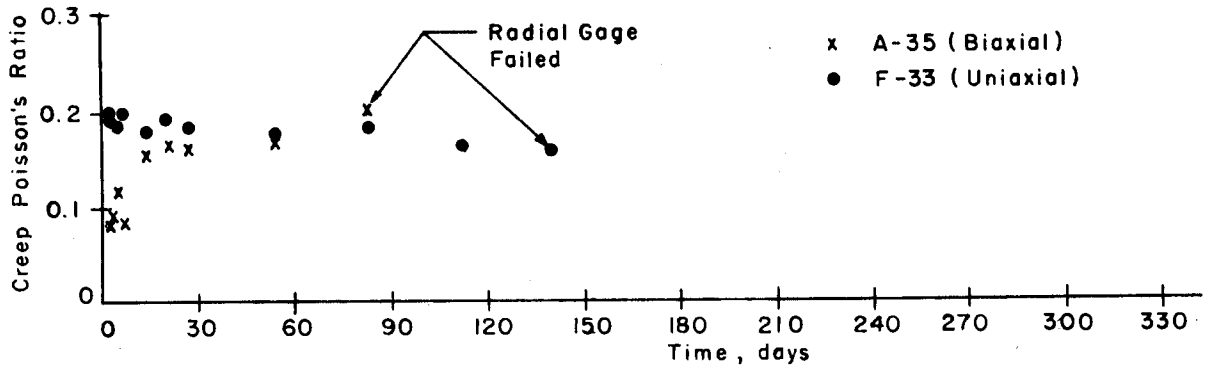

(a) As-cast specimens.

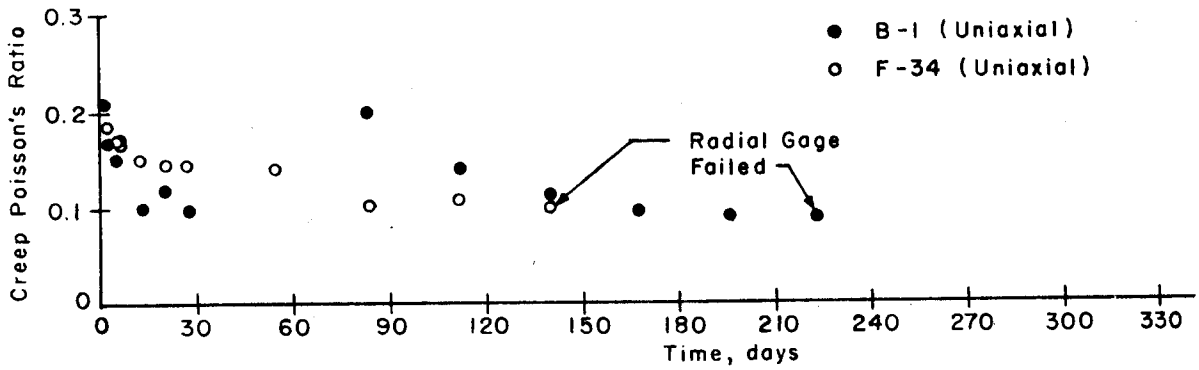

(b) Air-dried specimens.

Fig 10. Creep Poisson's ratio for as-cast and air-dried specimens at 150° F (Ref 4).

The creep Poisson's ratios after one year under load are shown for each specimen in Table 5. Exluding the hydrostatically loaded specimens and specimens that were penetrated by oil, the values of the creep Poisson's ratios after one year of loading ranged from 0.108 to 0.414, and averaged 0.234 for specimens under the 90-day loading condition. This value was somewhat, but not significantly, smaller than the average value of the elastic Poisson's ratio.

RECOVERY AFTER THE REMOVAL OF LOADS

The specimens were subjected to loads for a period of 12 months, after which strain measurements were continued for an additional five months. These recovery strains were divided into instantaneous elastic recovery strains and creep recovery strains.

The instantaneous elastic recovery strain was determined by taking strain readings just prior to and immediately after the loads were removed. Creep recovery strain was determined by considering that the total strain less the average shrinkage strain immediately after unloading was the zero reference point. Values of both instantaneous and creep recovery strains are shown in Table 7.

Curves representing the total strain less the average shrinkage strain from the time of unloading up to five months later are shown in Appendixes B through E for specimens having at least one gage functioning properly at the time of unloading. These curves indicate that creep recovery occurred at a high rate in the early weeks after unloading, then almost leveled off in about one month. These curves tend to indicate that a recovery period of five months is sufficient to obtain reasonable estimates of the maximum creep recovery.

A detailed discussion and summary of the findings obtained from the analysis of these data is contained in Chapter 5 of this report.

TABLE 7. INSTANTANEOUS RECOVERY AND CREEP RECOVERY STRAINS

Temperature	Curing Condition	Specimen	Pressure, psi		Instantaneous Recovery, ϵ_{ir}* Microunits		Creep Recovery After 5 Months, ϵ_{cr}* Microunits	
			Axial	Radial	Axial	Radial	Axial	Radial
75° F	As-Cast	E-39	527	0	-85	23	-8	6
		B-7	2179	0	-401	94	-68	19
		F-13	0	600	55	-74	8	-21
		H-22	0	3600	303	-548	66**	-102**
		E-5	562	600	-39	-53	-16	-16
		C-23	2139	600	-298	18	-65	2
		C-16x	1100	1200	-166	43	-38	7
		D-26	3449	1200	-495	-1	-89**	6**
		B-41	1092	2400	-178	-194	-40	-33
		F-9	2147	2400	-181	-199	-51	-54
		G-35	536	3600	233	-482	41	-121
		D-31	3472	3600	-275	-322	-49	-69
	Air-Dried	E-40	527	0	-100	27	-16	-2
		B-19	2179	0	-433	103	-88	16
		F-42	0	600	53	-81	1	-23
		H-14	0	3600	316	-	64**	-111**
		E-13	562	600	-51	-55	-16	-16
		C-11	2139	600	-385	15	-91	-16
		C-17	1100	1200	-70	-95	-24	-23
		D-44	3449	1200	-	-13	-131	-26
		B-42	1092	2400	-153	-222	-10	-34
		F-30	2147	2400	-184	-241	-67	-82
		G-30	536	3600	214	-	32	-118
		D-40	3472	3600	-315	-382	-96	-118

(Continued)

TABLE 7. (Continued)

Temperature	Curing Condition	Specimen	Pressure, psi		Instantaneous Recovery, ε_{ir}* Microunits		Creep Recovery After 5 Months, ε_{cr}* Microunits	
			Axial	Radial	Axial	Radial	Axial	Radial
150° F	As-Cast	B-4	561	0	**	22	**	8
		D-15	1102	0	-211	**	-72	**
		F-33	2123	0	**	**	-59	**
		A-35	0	600	**	-65	**	-34
		C-12	1032	1200	-143	**	-42	**
		D-2x	1086	2400	-200	51	-61	-13
		G-9	2268	2400	-199	-272	-95	-127
	Air-Dried	B-1	561	0	-96	21	-19	18
		D-22	1102	0	-234	47	-53	8
		F-34	2123	0	-431	**	-112	**
		D-3	0	600	99	**	**	**
		E-4	2259	600	-343	**	-118	**
		C-46x	1032	1200	-277	53	-86	14
		D-41	1086	2400	3	-368	31	-107
		G-19	2268	2400	-188	-249	-75	-104
		F-6	3474	3600	-295	**	-160	-**

* Compression is positive and tension is negative.
** Gage failed or gage range was exceeded.
x Radial pressure reduced to zero shortly after initial loading due to oil leak.

Table includes specimens having at least one gage functioning properly at the time of unloading.

CHAPTER 5. EVALUATION OF RECOVERY CHARACTERISTICS

The purpose of this chapter is to discuss the results of the analysis and evaluation of the strain data obtained after the loads were removed in the creep investigation described in Chapter 3. For purposes of evaluation and discussion, the recovery strains have been divided into instantaneous recovery strains and creep recovery.

The discussion has been subdivided into factors affecting recovery, relationships between creep and creep recovery characteristics, and the applicability of the principle of superposition of strains. For purposes of evaluation it was assumed that

(1) There was no significant batch-to-batch variation, a reasonably valid assumption since the tensile and compressive strengths did not vary significantly between batches.

(2) All axial loads applied from the same hydraulic pressure system were equal. This assumption was not entirely accurate since there were differences between loading units due to friction losses. However, the differences were very small and are assumed to be ineligible.

The recovery strain-time relationships for each specimen are shown in Appendices B through E. In these relationships the estimated shrinkage strains have been removed. Each relationship begins 364 days after loading, at which time the loads were removed.

FACTORS AFFECTING RECOVERY

Temperature

Instantaneous Recovery. No definite effect of temperature on the instantaneous recovery strain could be established (Fig 11). In some cases the instantaneous recovery strains were larger at 150° F than at 75° F while in other cases the instantaneous recovery strains were smaller at 150° F. However, in many of these cases the difference was quite small. Hence, it was concluded that temperature did not have an effect on the instantaneous recovery of the concrete specimens in this investigation. If, as discussed in Chapter 2,

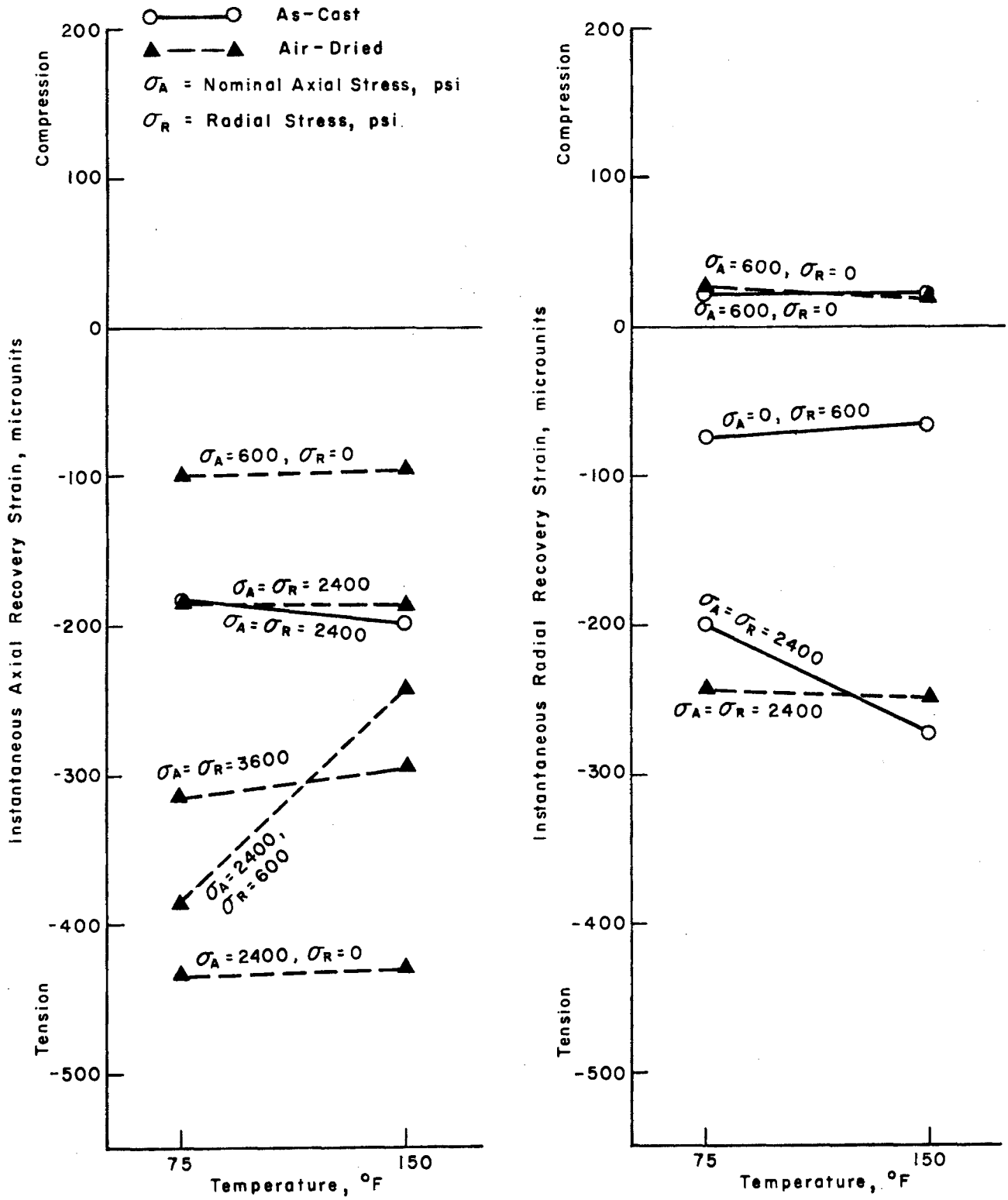

(a) Effect on axial recovery.

(b) Effect on radial recovery.

Fig 11. Effect of temperature on instantaneous axial and radial recovery strains.

instantaneous recovery is closely related to the strength of the concrete, then no effects of temperature would be expected since there were no significant strength differences for the two temperatures in this investigation (Table 4).

Creep Recovery. Previous work has indicated that creep recovery, defined as the recovery in excess of the instantaneous recovery at the time of unloading, was independent of the temperature at which the test was conducted but that the creep rate increased with increased temperature up to 160° F (Chapter 2). In this investigation, however, a definite temperature effect was evident, as shown in Figs 12 through 19, for different curing histories and different states of stress. For specimens loaded uniaxially at 600 psi (Fig 12), the magnitude of the recovery strains was larger for the specimens at 150° F than at 75° F; however, the differences were of no practical significance. At a higher stress level, 2400 psi, the effect of temperature was more pronounced (Fig 13). For the air-dried specimens, the creep recovery strains were larger at 150° F than at 75° F although the differences were small. The effect of temperature could not be evaluated for the biaxially loaded specimens (Figs 14 and 15) since most of the gages at 150° F had failed prior to unloading. For triaxially loaded specimens (Figs 16 through 19), the creep recovery strains for specimens at 150° F were substantially larger than those at 75° F for both the as-cast and the air-dried cases. Thus, it was concluded that, in general, the creep recovery strains were larger at 150° F than at 75° F.

Curing History

Instantaneous Recovery. The air-dried specimens generally showed larger instantaneous recovery strains than the as-cast specimens, as indicated in Fig 20, although the differences were small unless the stress levels were high. This can be related to the fact that as-cast specimens exhibited higher strengths than air-dried specimens.

Creep Recovery. The effect of the curing history on the creep recovery strains for different levels of temperature and at different states of stress is also shown in Figs 12 through 19.

For the uniaxially loaded specimens (Figs 12 and 13), the creep recovery strains in the direction of the applied stress for the air-dried specimens at both temperatures were larger than for the as-cast specimens, while no

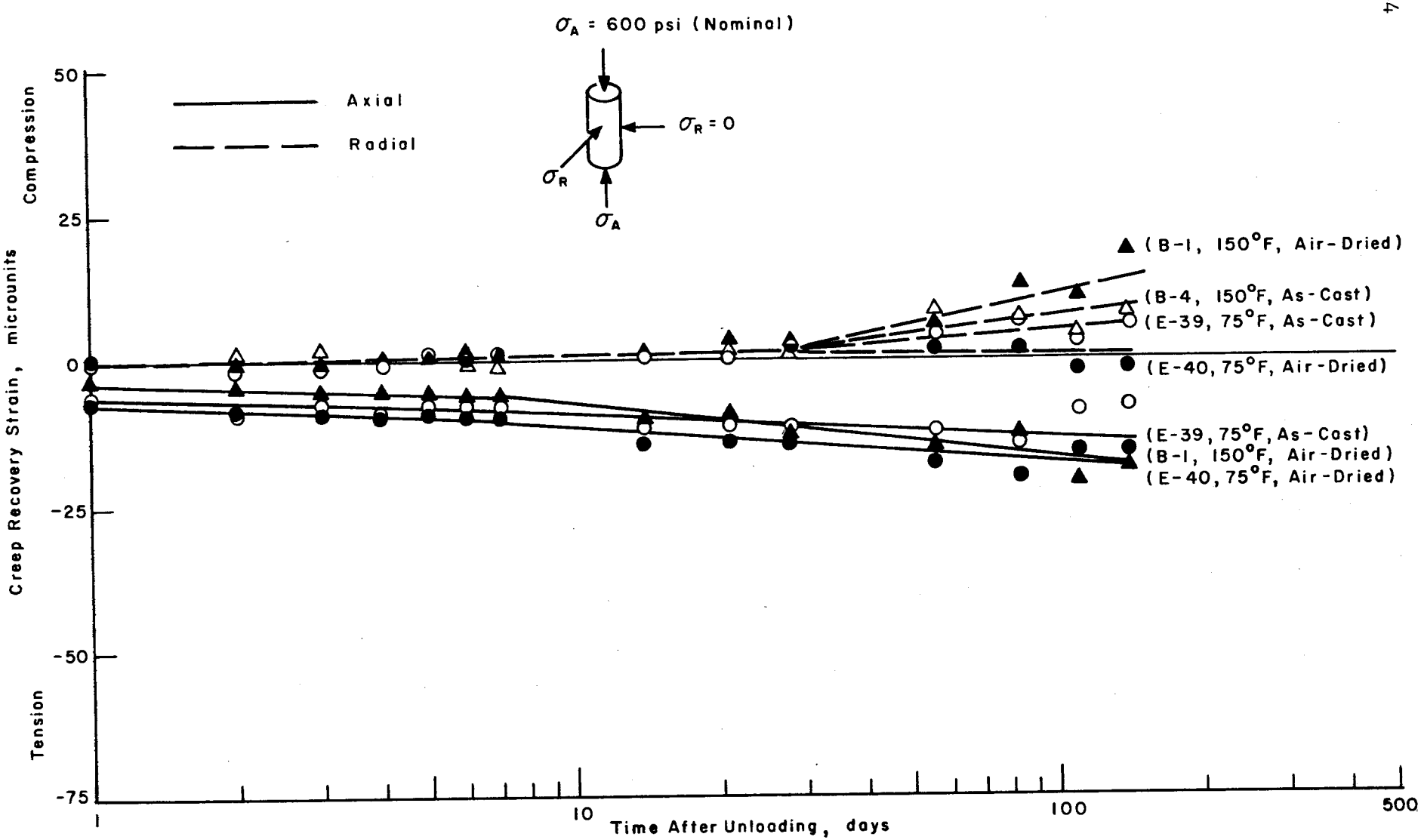

Fig 12. Effect of temperature and curing history on creep recovery for specimens loaded uniaxially at 600 psi.

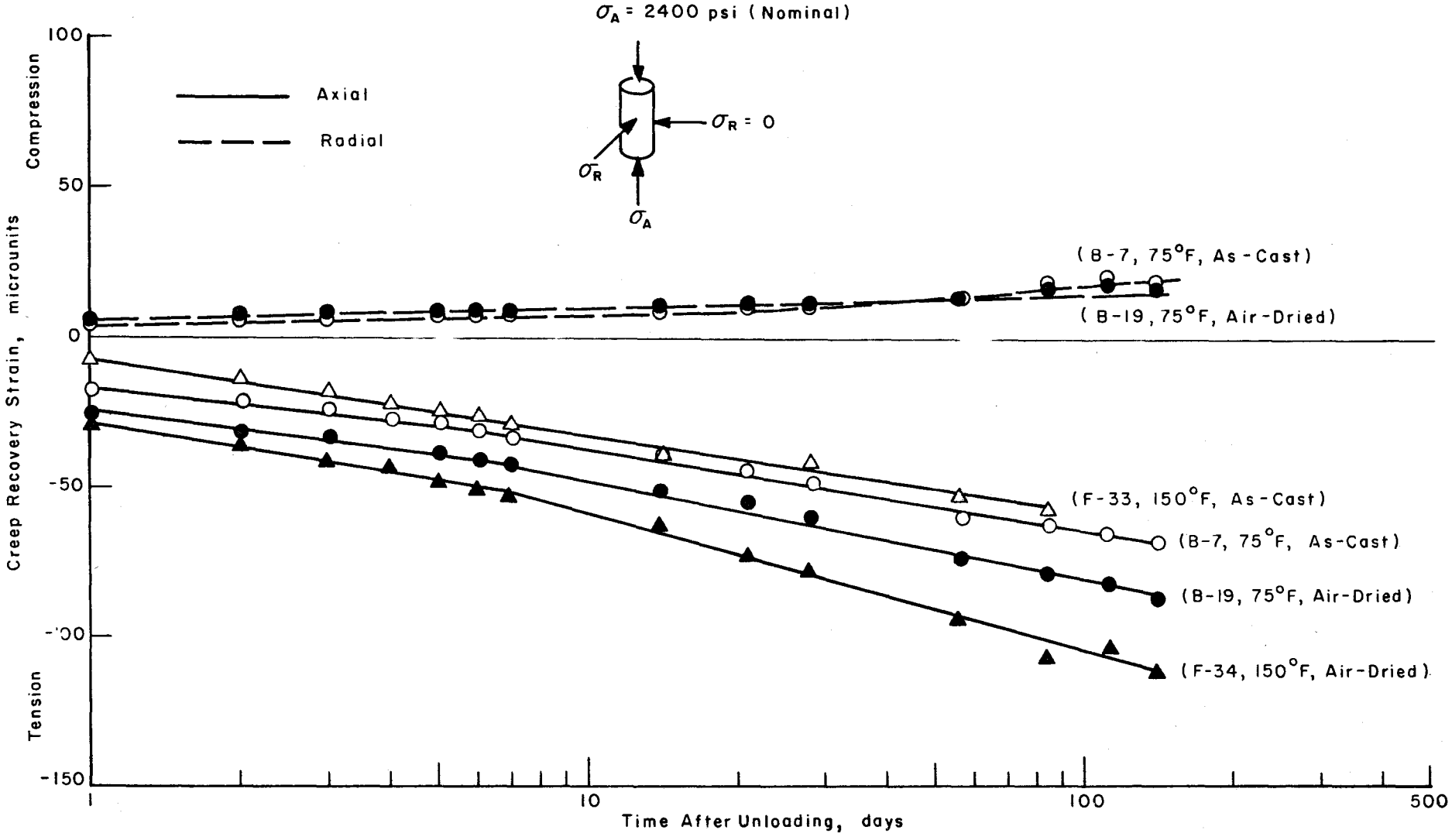

Fig 13. Effect of temperature and curing history on creep recovery for specimens loaded uniaxially at 2400 psi.

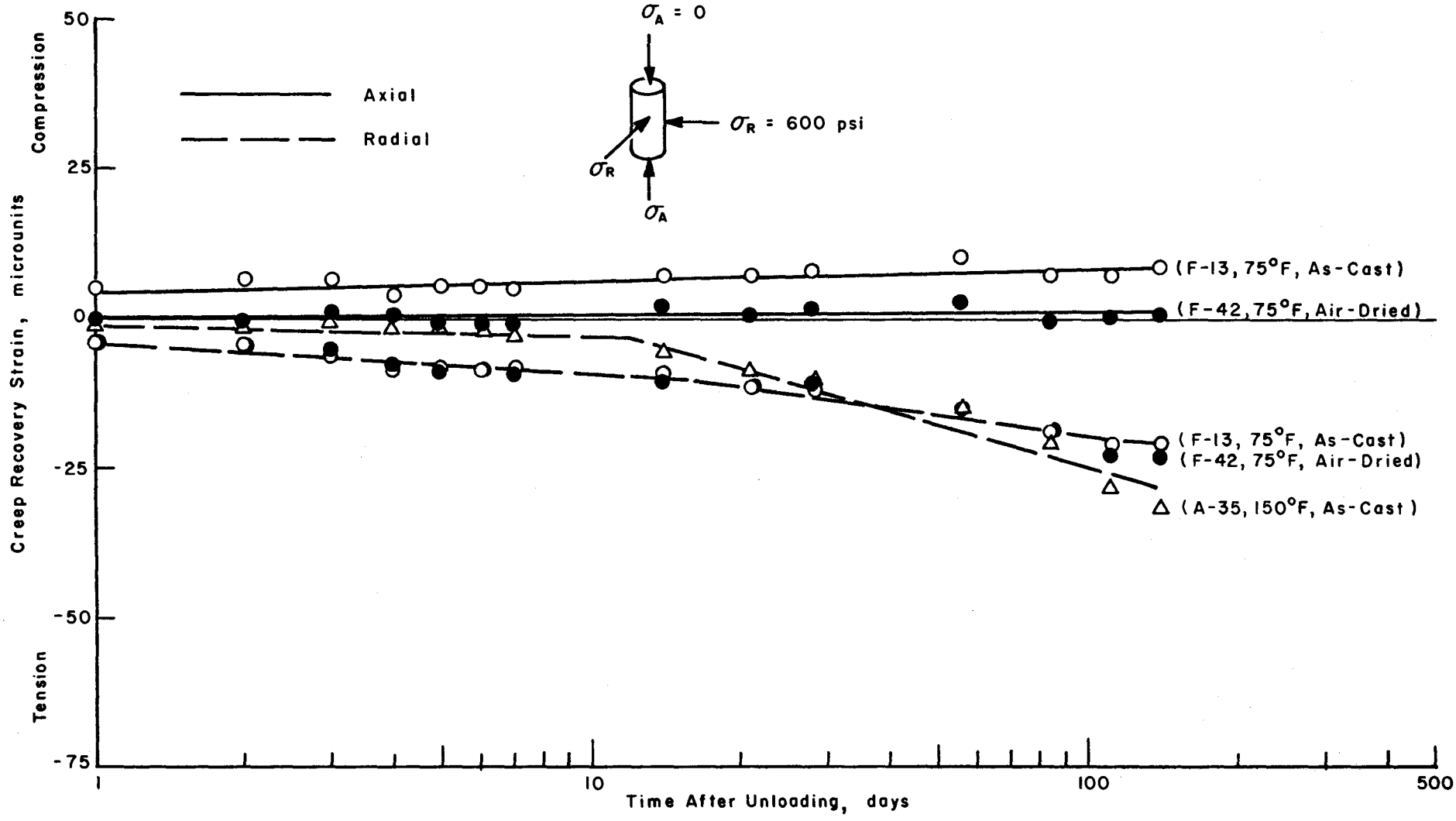

Fig 14. Effect of temperature and curing history on creep recovery for specimens loaded biaxially at 600 psi.

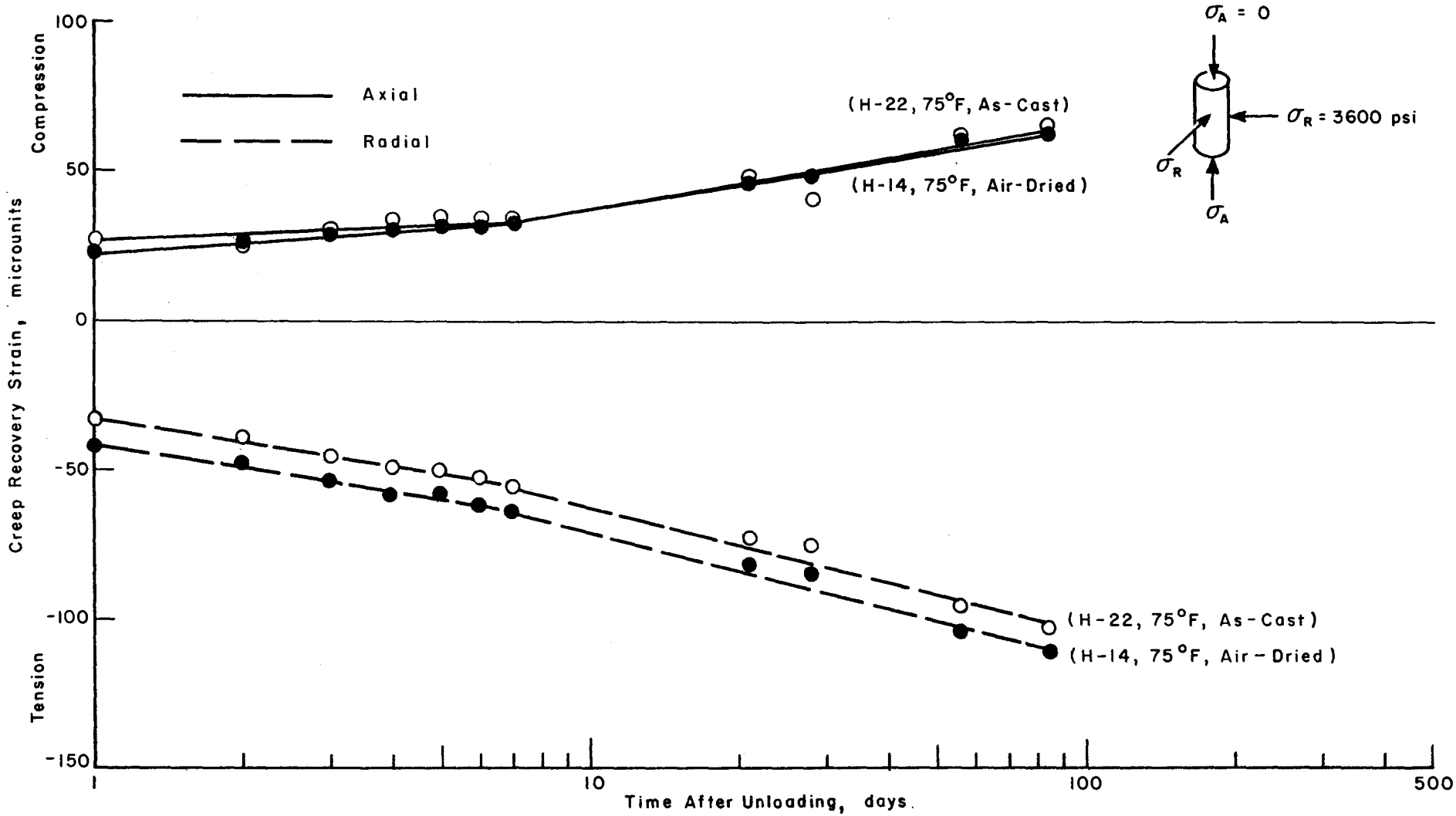

Fig 15. Effect of temperature and curing history on creep recovery for specimens loaded biaxially at 3600 psi.

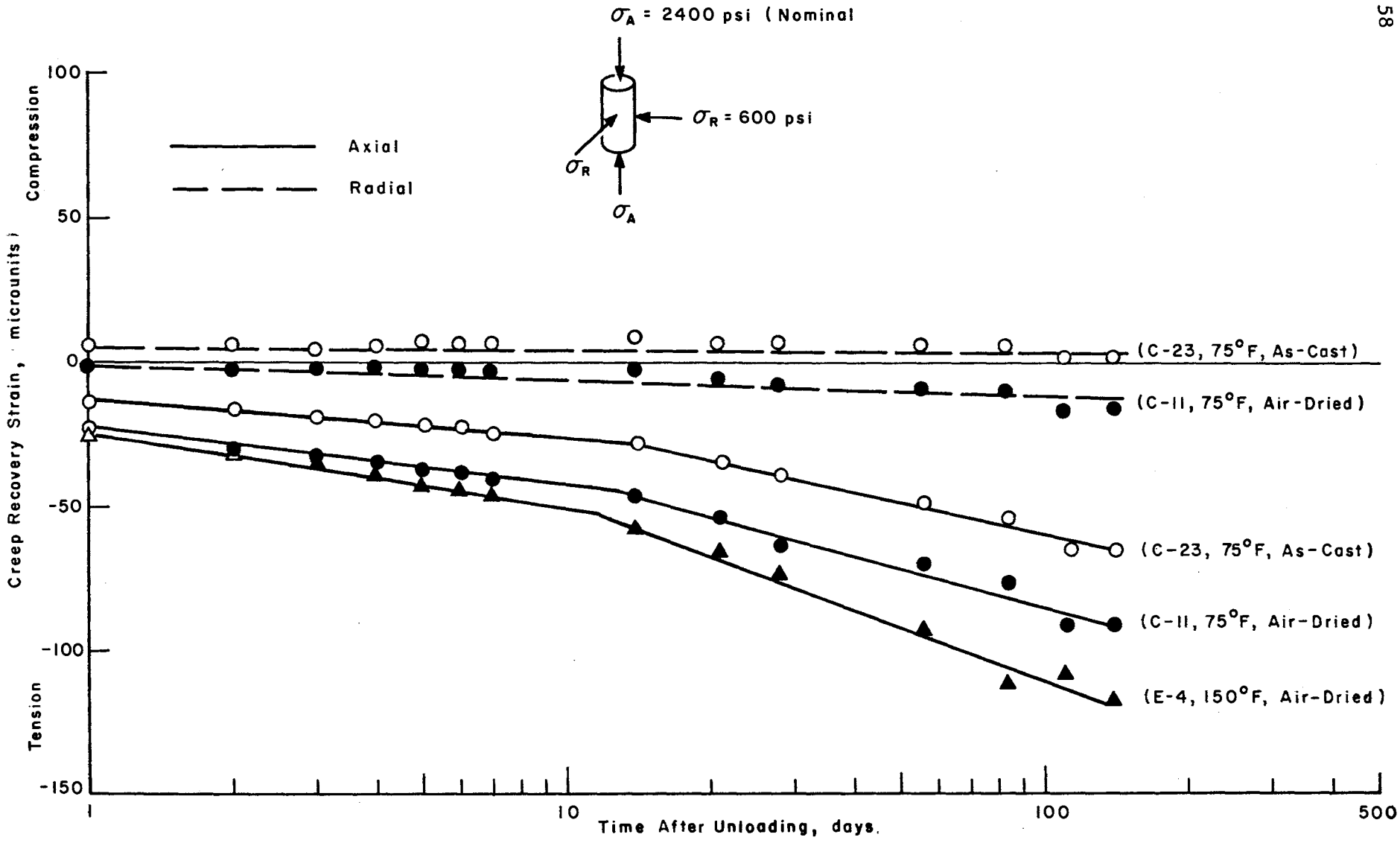

Fig 16. Effect of temperature and curing history on creep recovery for specimens loaded triaxially; σ_a = 2400 psi, σ_r = 600 psi.

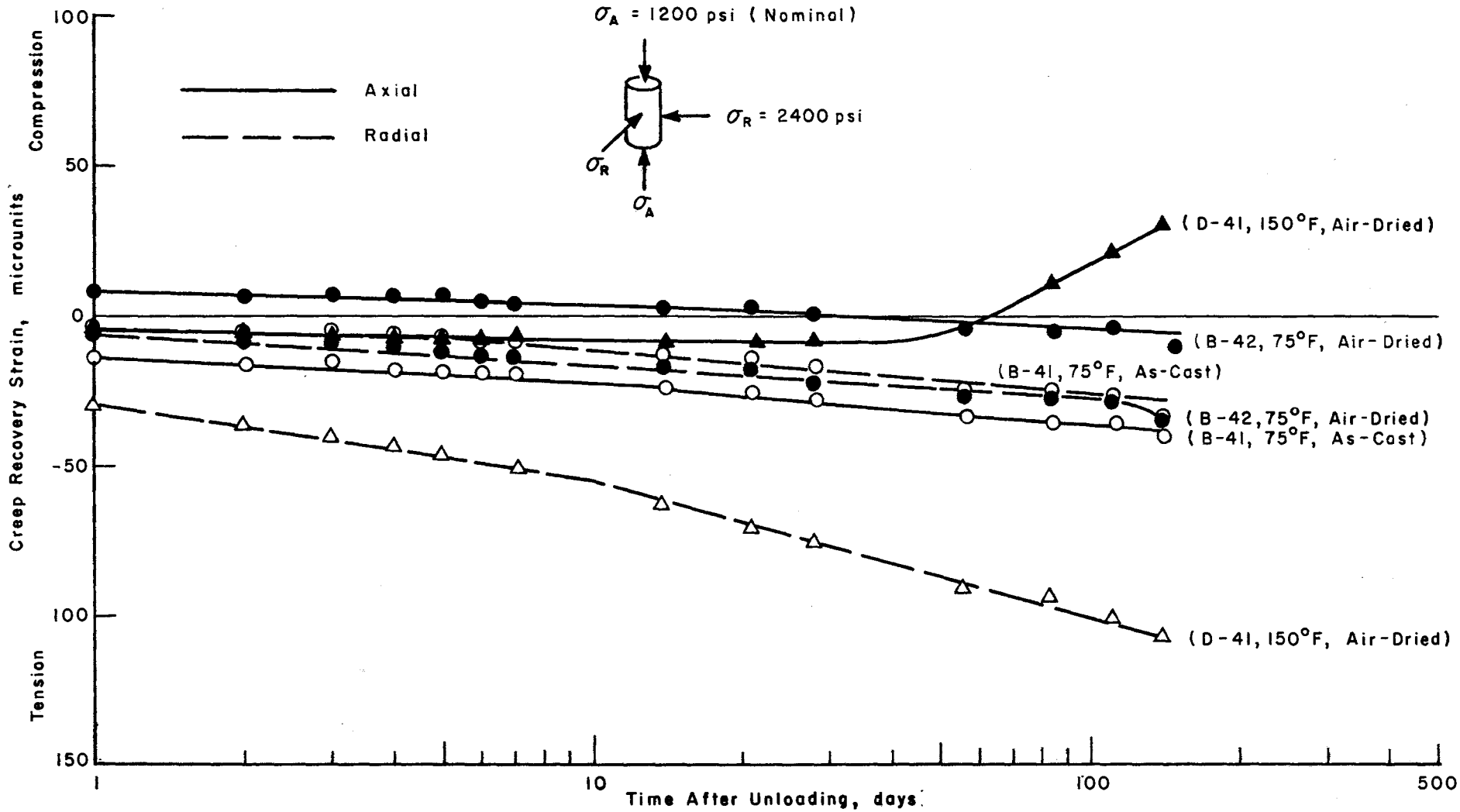

Fig 17. Effect of temperature and curing history on creep recovery for specimens loaded triaxially; σ_a = 1200 psi, σ_r = 2400 psi.

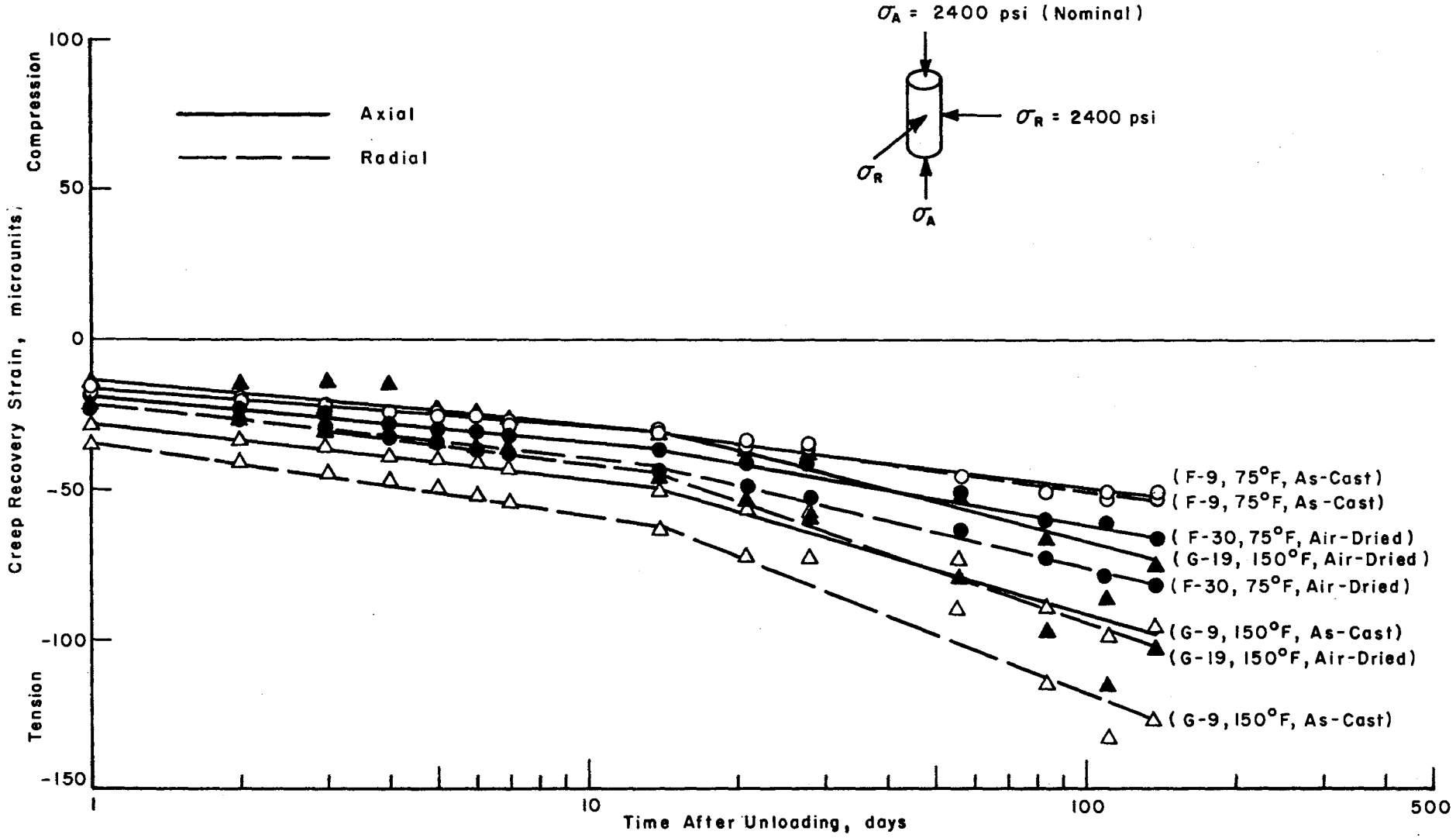

Fig 18. Effect of temperature and curing history on creep recovery for specimens loaded triaxially; $\sigma_a = \sigma_r = 2400$ psi.

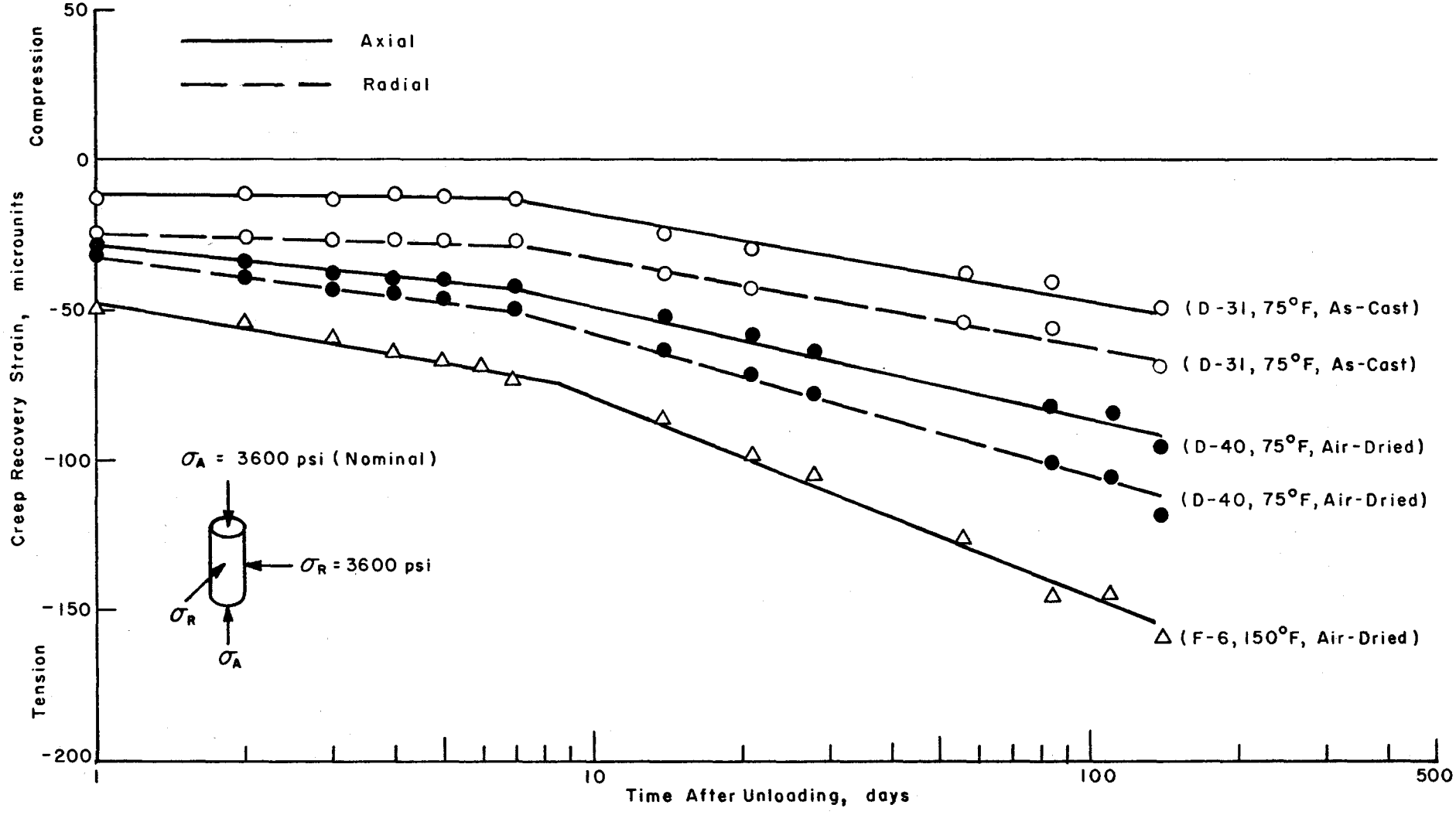

Fig 19. Effect of temperature and curing history on creep recovery for specimens loaded triaxially; $\sigma_a = \sigma_r = 3600$ psi.

significant differences were apparent in the direction perpendicular to the applied stress. The effect of curing history on the biaxially loaded specimens at 150° F could not be determined since most of the gages at this temperature failed prior to unloading. For biaxially loaded specimens at 75° F, the creep recovery strains in the direction of the applied stress were larger for the air-dried specimens than for the as-cast specimens, while smaller creep recovery strains were exhibited in the direction perpendicular to the applied stress by the air-dried specimens (Figs 14 and 15). For triaxial loading at 75° F (Figs 16 through 19), the air-dried specimens exhibited larger creep recovery strains than the as-cast specimens. At 150° F, only one set of specimens (Fig 18) survived through the recovery period, and it indicated that the creep recovery strains for the air-dried specimens were smaller than those for the as-cast specimens.

Thus, it can be concluded that the air-dried specimens exhibited larger creep recovery strains in the direction of the major stress while in the direction perpendicular to the major stress the creep recovery strains were smaller. The possible cause could be the fact that the as-cast specimens had higher strengths than the air-dried specimens, thus indicating that creep recovery strain might be related to the strength of concrete.

State of Stress

Instantaneous Recovery. The effect of stress level on the instantaneous recovery was similar to the effect of stress level on creep recovery, regardless of whether the stress condition was uniaxial, biaxial, or triaxial. Figures 21 through 23 indicate that instantaneous recovery was definitely a function of the magnitude of the stress removed. For the uniaxial and biaxial loading, it was concluded that there was a linear relationship between the instantaneous recovery and the magnitude of the removed stress since the relationships passed through the origin.

Creep Recovery. Previous investigations have shown conflicting results with regard to state of stress. Freudenthal and Roll (Ref 7) concluded that creep recovery is a function of the previously sustained stress, while Nasser and Neville (Ref 23) found that creep recovery was independent of the magnitude of the removed stress. The results of this experiment (Figs 24 through 26) indicated that creep recovery was dependent on the magnitude and the state of stress previously applied. For uniaxially and biaxially loaded

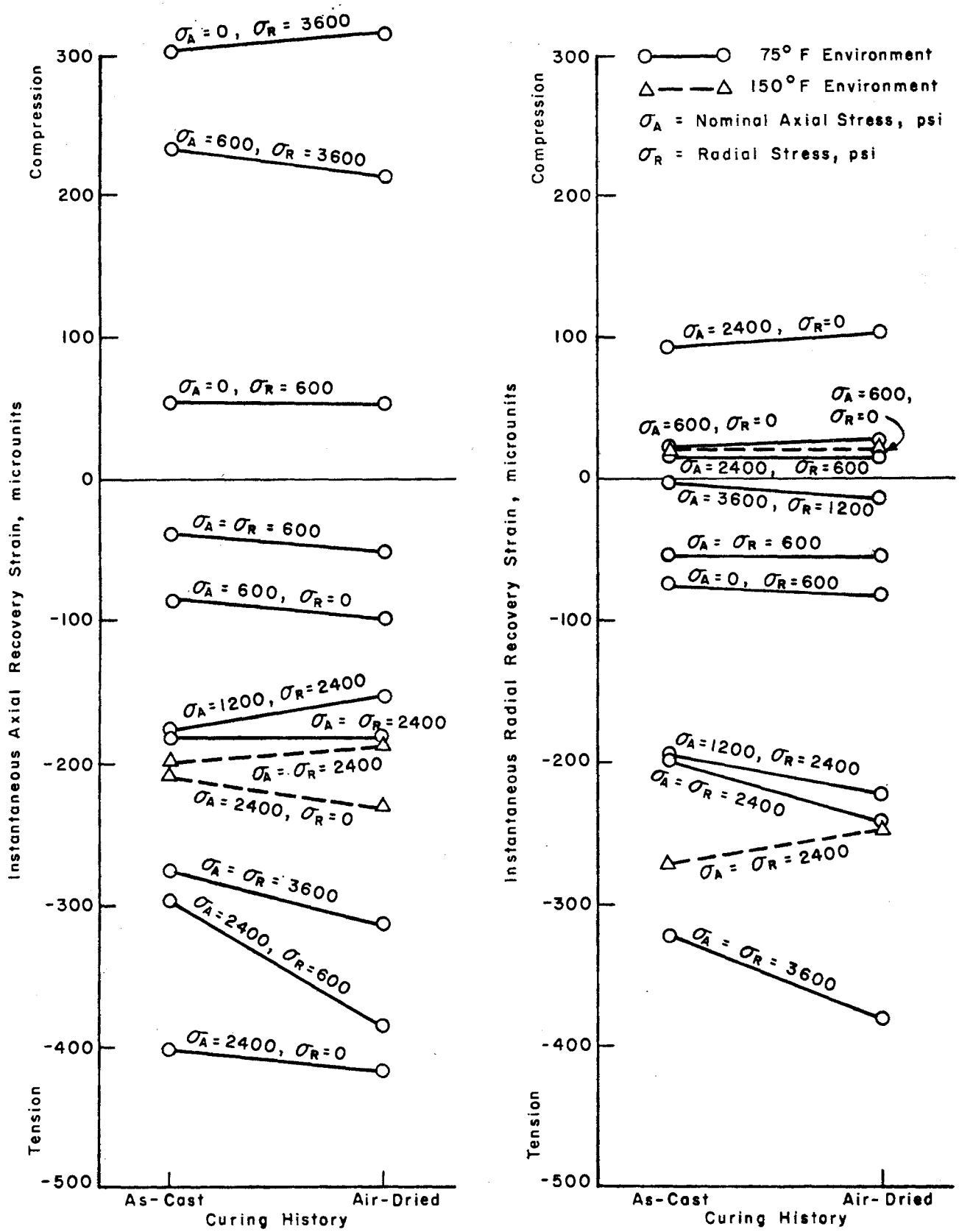

(a) Effect on axial recovery.

(b) Effect on radial recovery.

Fig 20. Effect of curing history on instantaneous axial and radial recovery strain.

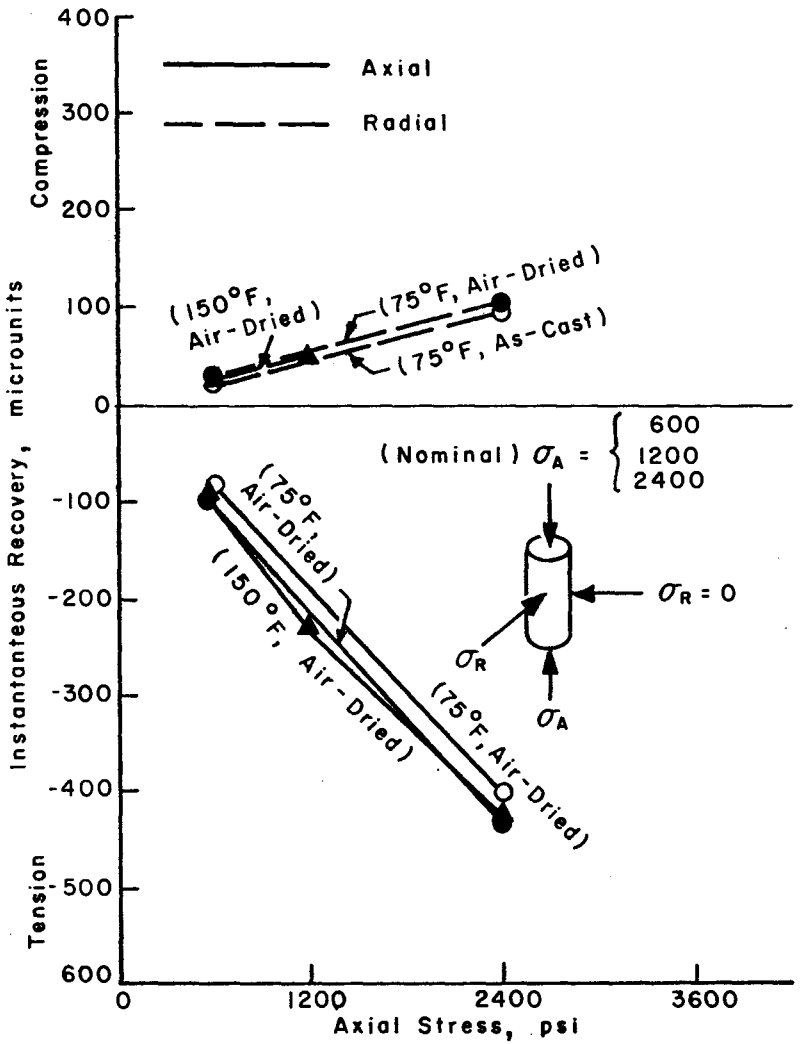

Fig 21. Effect of stress level on instantaneous recovery of uniaxially loaded specimens.

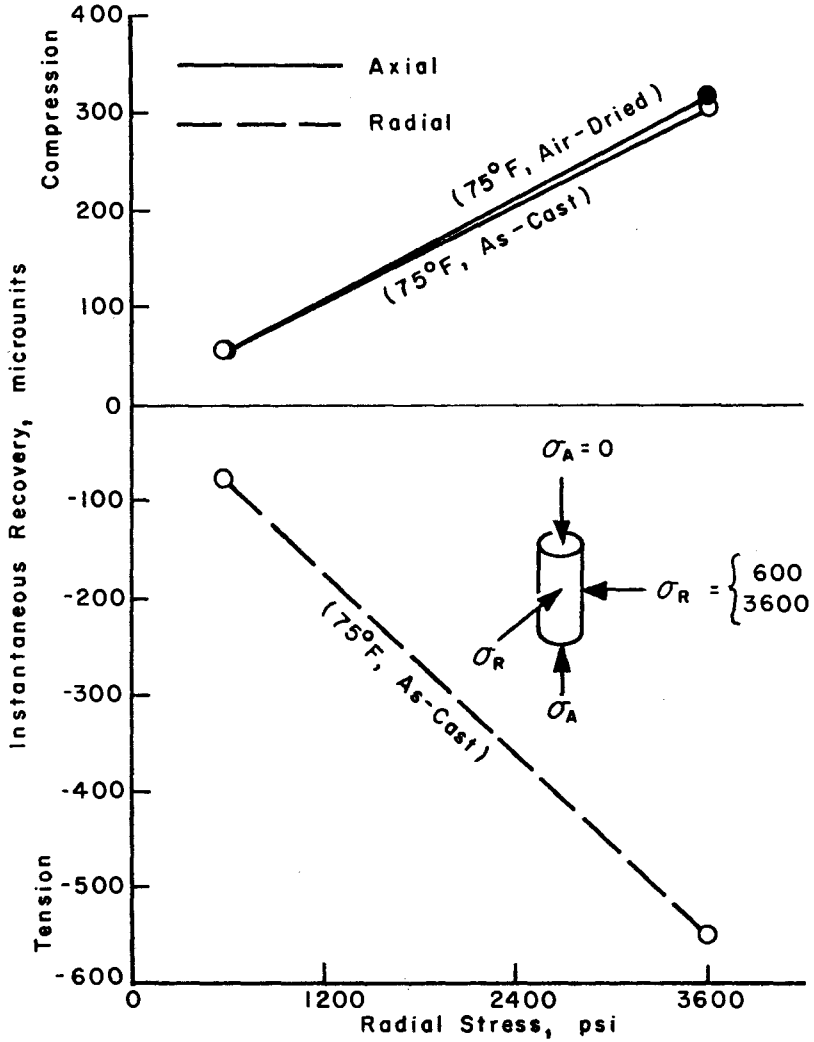

Fig 22. Effect of stress level on instantaneous recovery of biaxially loaded specimens.

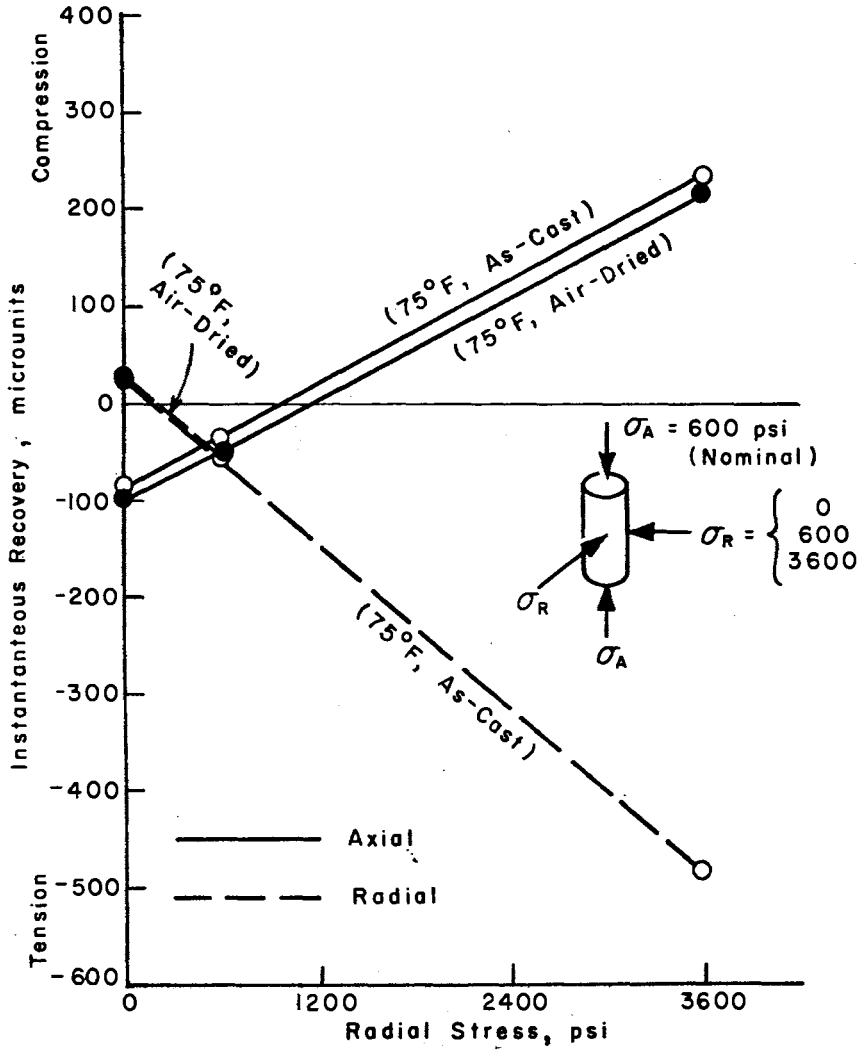

(a) Nominal axial stress of 600 psi.

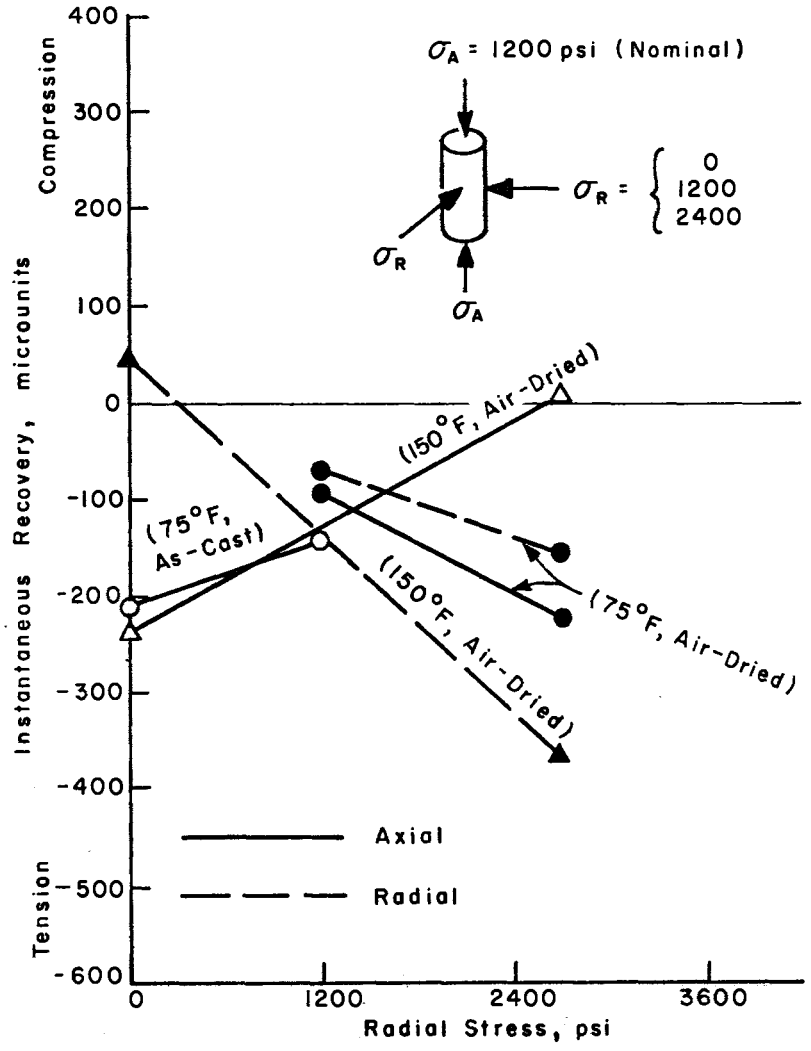

(b) Nominal axial stress of 1200 psi.

Fig 23. Effect of stress level on instantaneous recovery of triaxially loaded specimens.

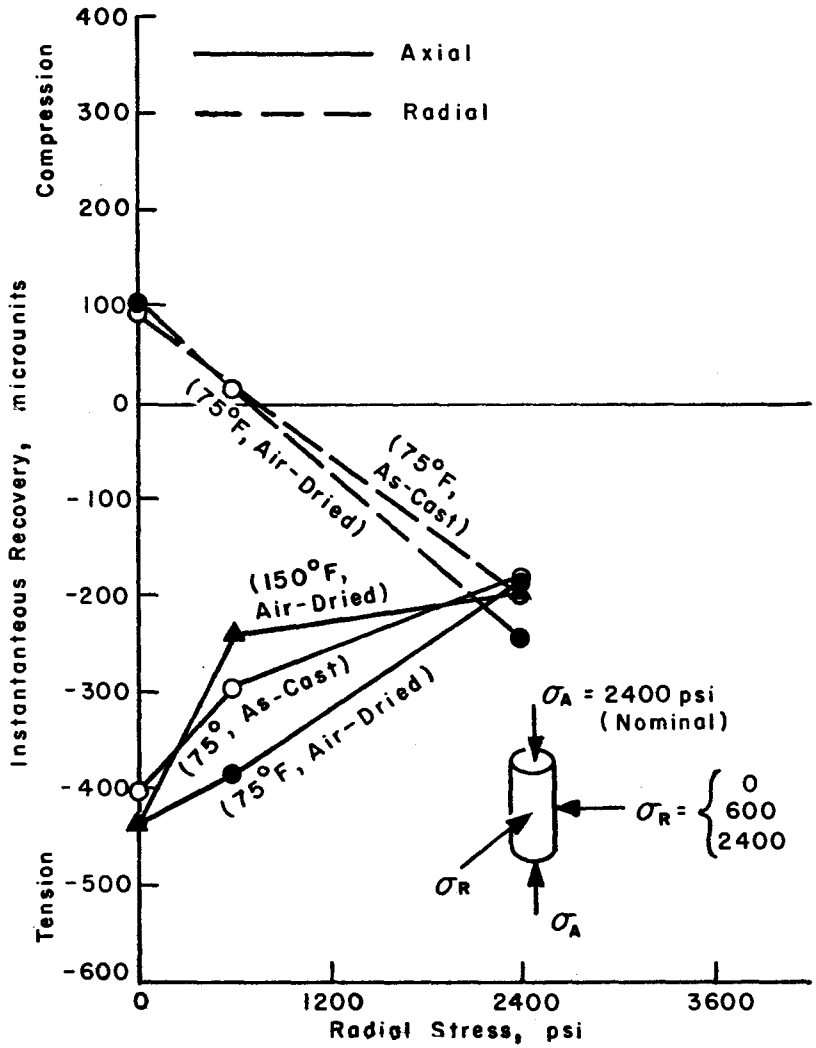

(c) Nominal axial stress of 2400 psi.

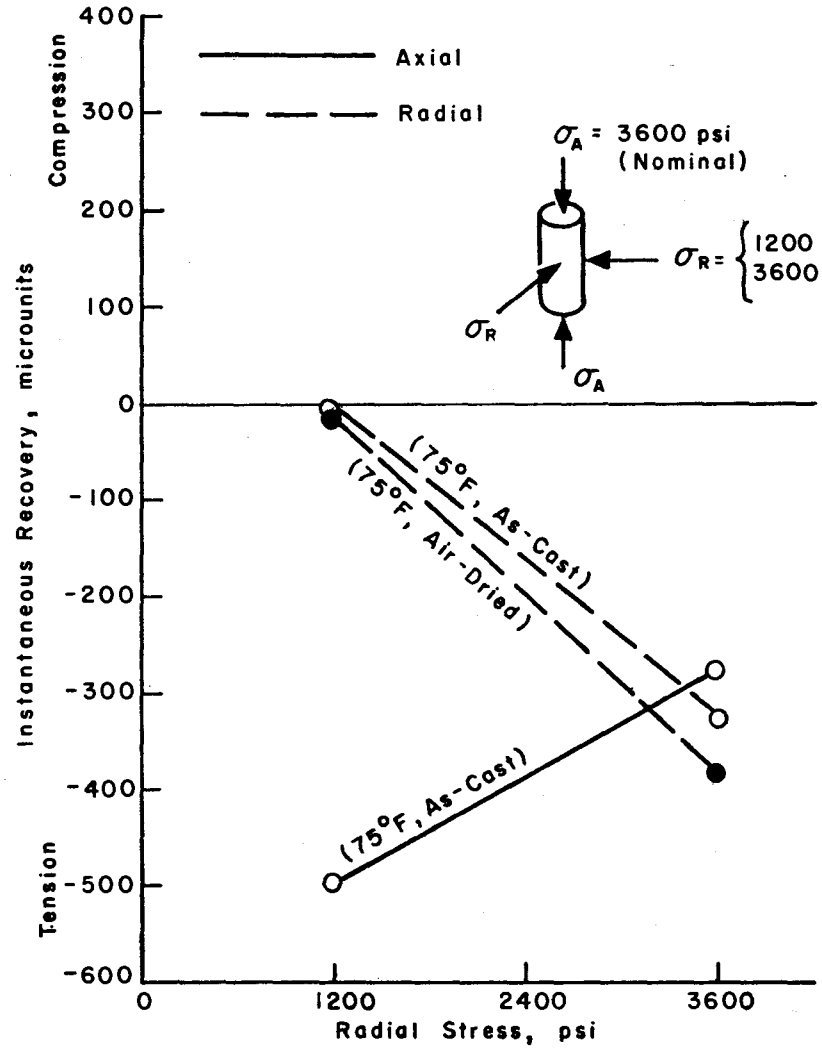

(b) Nominal axial stress of 3600 psi.

Fig 23. (Continued)

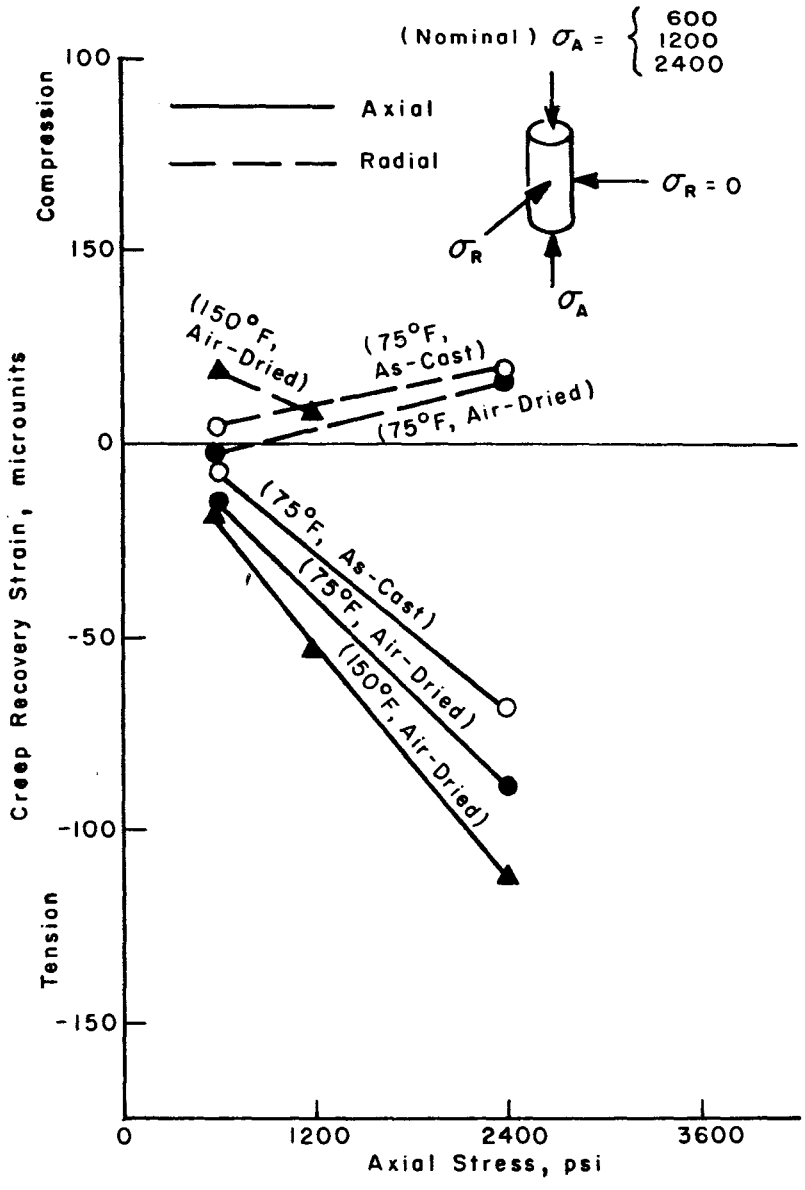

Fig 24. Effect of stress level on creep recovery of uniaxially loaded specimens after 140 days.

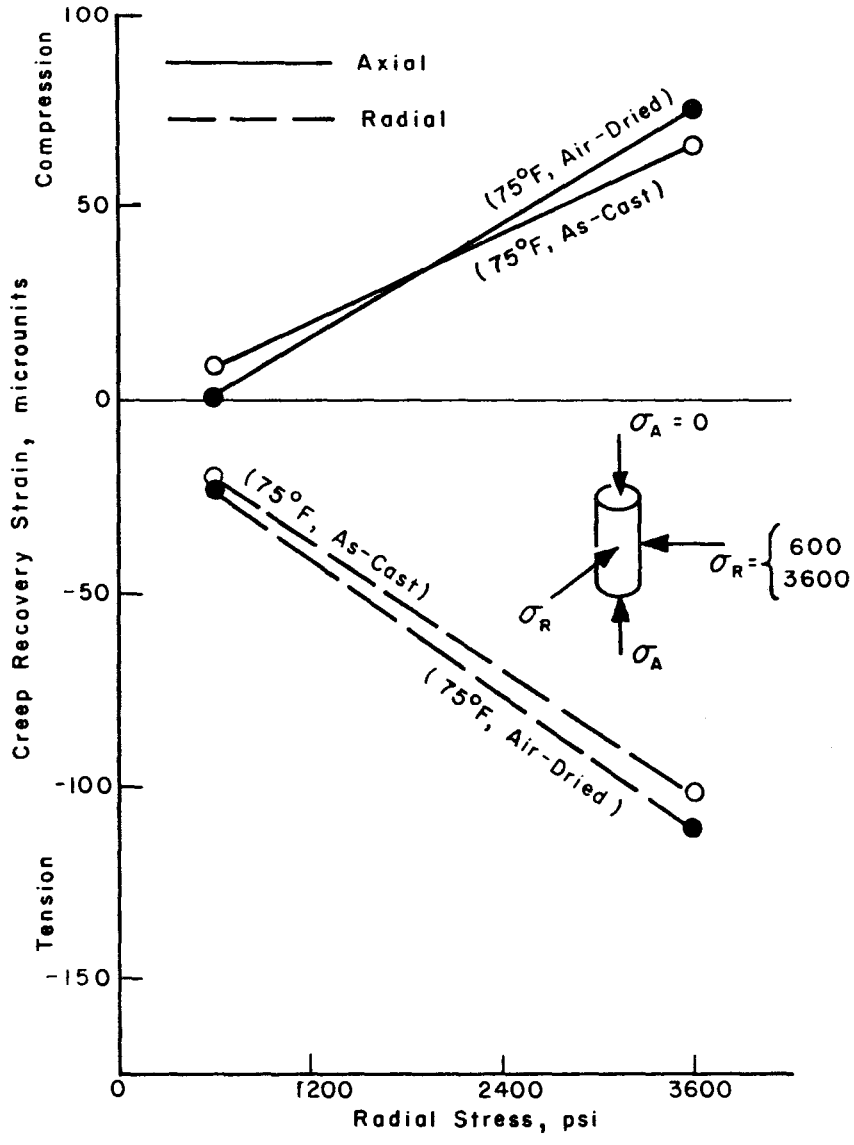

Fig 25. Effect of stress level on creep recovery of biaxially loaded specimens after 140 days.

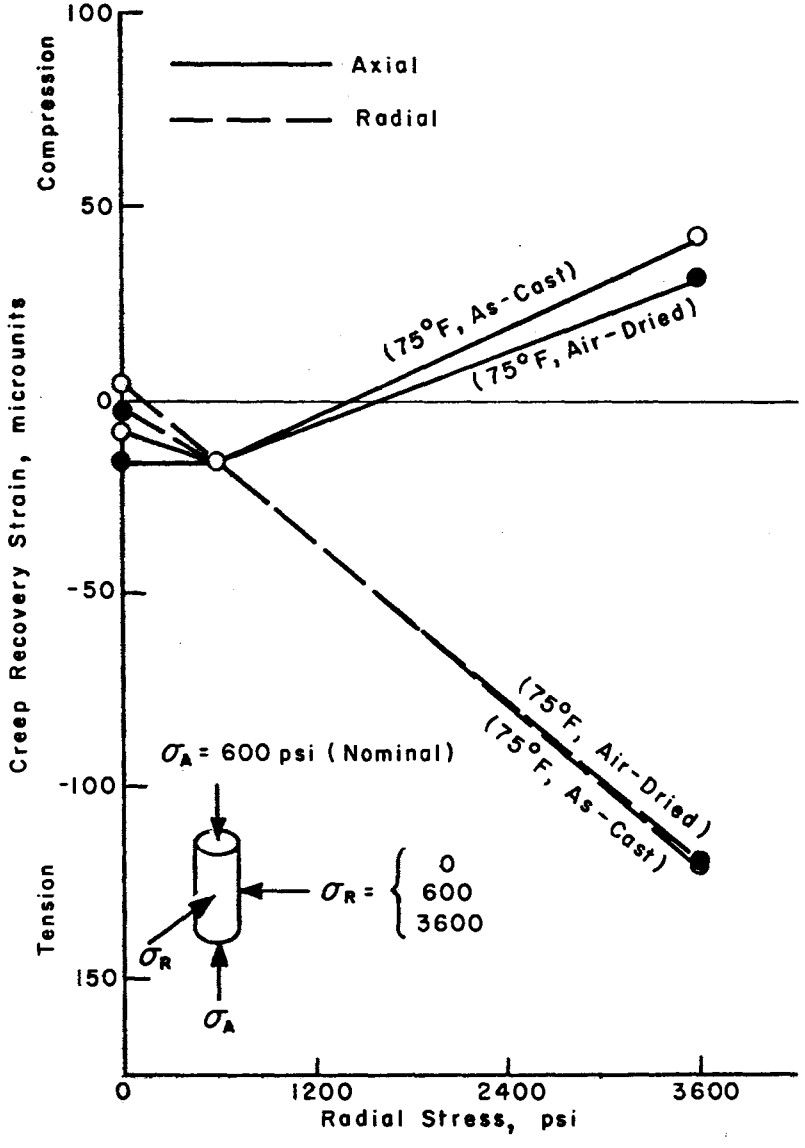

(a) Nominal axial stress of 600 psi.

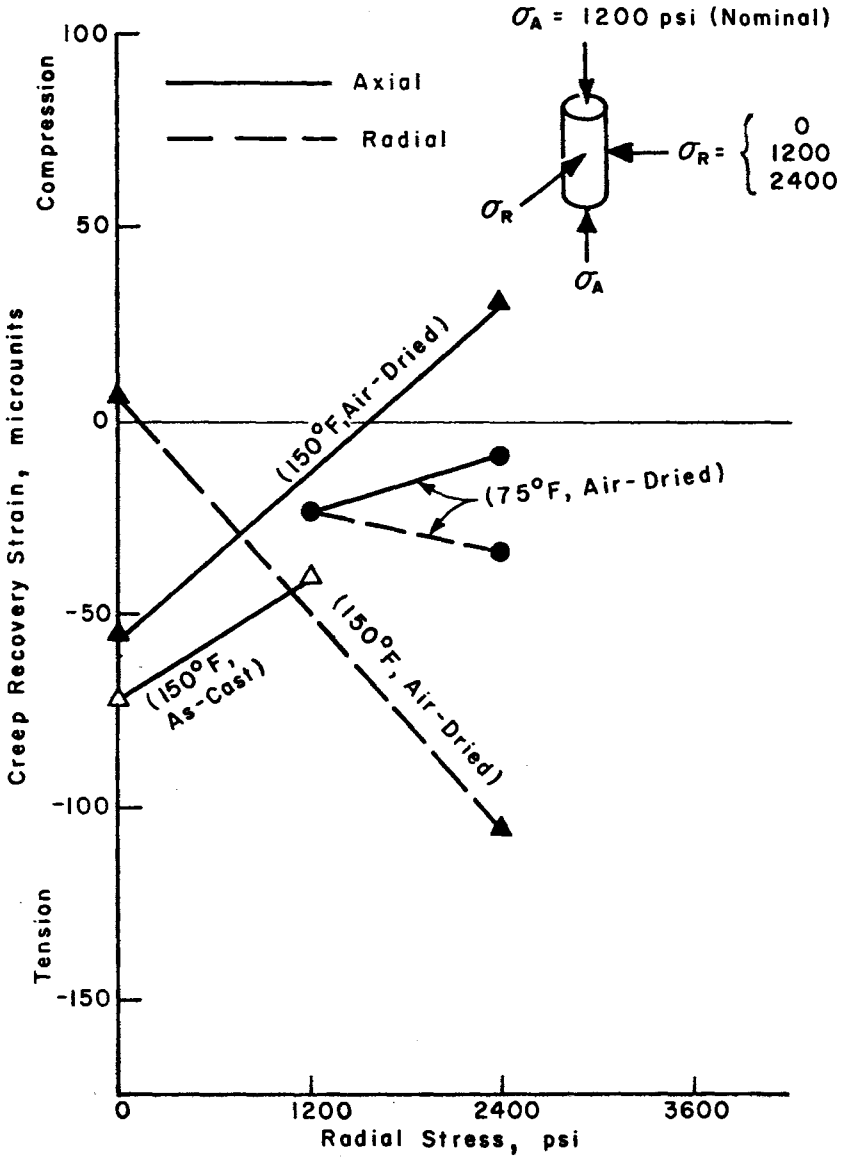

(b) Nominal axial stress of 1200 psi.

Fig 26. Effect of stress level on creep recovery of triaxially loaded specimens after 140 days.

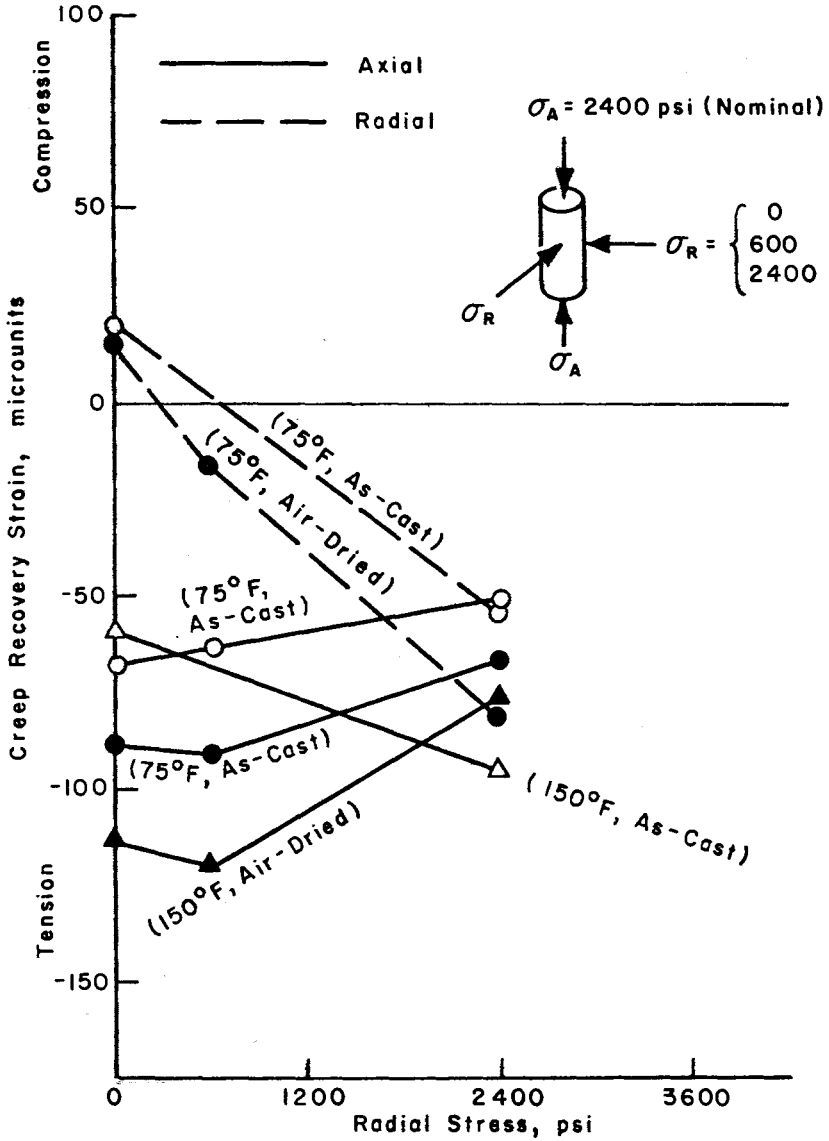

(c) Nominal axial stress of 2400 psi.

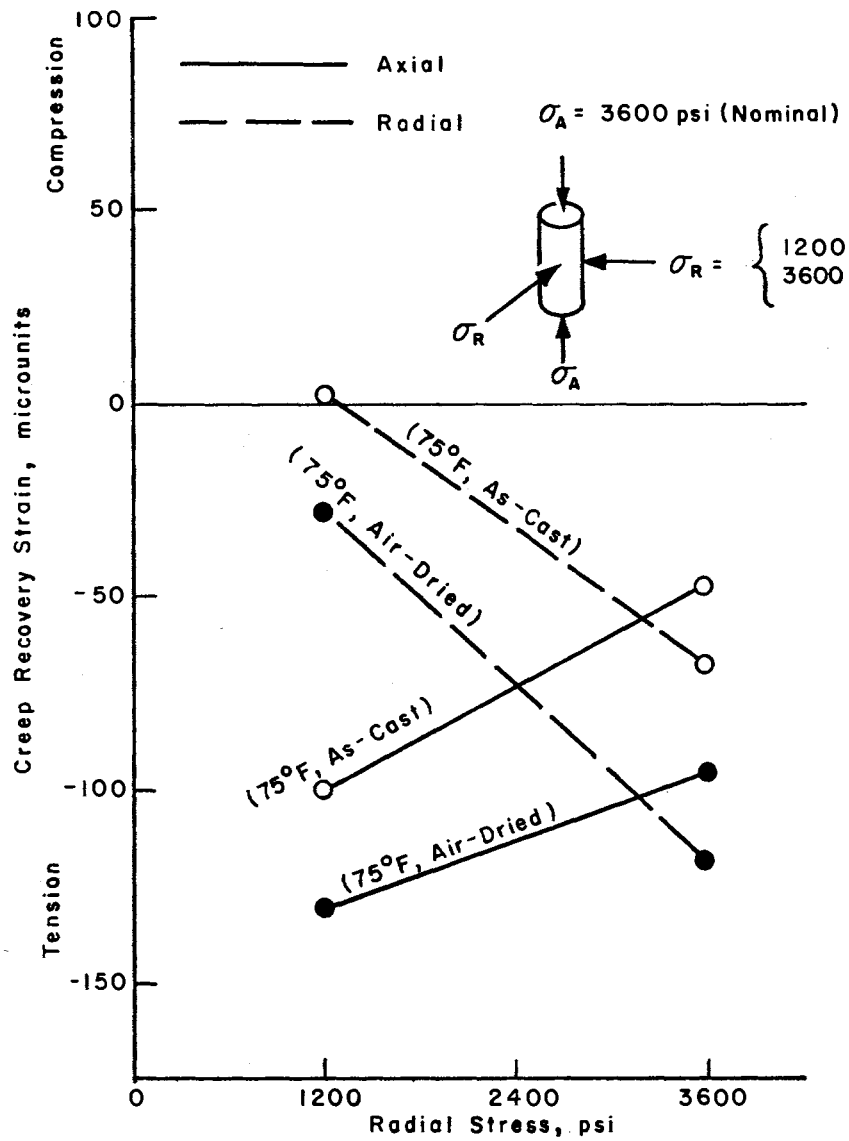

(d) Nominal axial stress of 3600 psi.

Fig 26. (Continued)

specimens (Figs 24 and 25), the recovery strains both in the direction of the removed stress and perpendicular to the direction of the removed stress were larger at the higher stress levels. This indicates that the magnitude of the creep recovery strains was related to the magnitude of the removed stress, but since the relationship did not pass through the origin, the relationship may not be linear.

For triaxially loaded specimens (Fig 26), the results indicate that when a large radial stress was removed, the result was a decrease in the magnitude of the axial creep recovery strain if the axial stress was large (Figs 26c and 26d) and an increase in the magnitude of the axial creep recovery strain if the axial stresses were relatively small (Figs 26a and 26b). At the same time, when the removed radial stress increased, the radial creep recovery showed a sharp increase in the tensile direction. These effects were similar to the effects observed for creep strain (Ref 1), but were opposite in direction.

RELATIONSHIP BETWEEN INSTANTANEOUS, CREEP, AND RECOVERY CHARACTERISTICS

Comparison of Instantaneous Recovery and Instantaneous Elastic Strains

Specimens at 75° F. For both the as-cast and the air-dried curing histories, two specimens were loaded uniaxially, two biaxially, and eight triaxially at the 75° F environment. For the uniaxial loading conditions, the ratios of the instantaneous recovery strain and the instantaneous strain of the as-cast specimens ranged from 0.885 to 1.042 (Table 8) with an average of 0.976, while for the air-dried specimens the ratios ranged from 0.990 to 1.143 with an average of 1.062. For the biaxial loading specimens, the ratios varied from 0.869 to 1.058, with an average of 0.966 for the as-cast specimens, while in the air-dried case, the ratios varied from 0.929 to 1.095, with an average of 1.014. For the triaxial loading conditions the variation was larger with the ratios varying from 0.886 to 1.800 for the as-cast specimens and from 0.714 to 1.594 for air-dried specimens, with an average of 1.041 and 1.021, respectively. The figures shown above for the triaxial loading conditions were evaluated excluding the ratios of specimens B-41 and B-42 in the axial direction, which had values of -22.250 and -38.250, respectively, and were obviously in error.

TABLE 8. RELATIONSHIP BETWEEN INSTANTANEOUS, CREEP, AND RECOVERY CHARACTERISTICS

Temperature	Curing Condition	Specimen	Stress, psi		ϵ_{ir}/ϵ_i		ϵ_{ir}/ϵ_c		$\epsilon_{cr}/\epsilon_{ir}$		Instant. Recovery Poisson's Ratio	Creep Recovery Poisson's Ratio
			Axial	Radial	Axial	Radial	Axial	Radial	Axial	Radial		
75° F	As-Cast	E-39	527	0	- .977	- .885	-.107	+ .600	+.094	+ .261	+.268	+ .750
		B-7	2179	0	-1.042	-1.000	-.211	- .452	+.170	+ .202	+.236	+ .279
		F-13	0	600	-1.058	-1.028	-.216	- .368	+.146	+ .284	+.264	+ .160
		H-22	0	3600	- .910	- .869	-.214	- .138	+.218	+ .186	+.217	+ .244
		E-5	562	600	-1.026	- .930	-.667	- .432	+.410	+ .302	+.355	-1.000
		C-23	2139	600	-1.053	-1.800	-.269	- .133	+.218	+ .111	+.260	+ .240
		C-16x	1100	1200	...	...	-.176	- .034	+.229	+ .163	+.258	+ .512
		D-26	3449	1200	-1.047	+ .083	-.239	- .231	+.180	-6.000	+.257	+ .298
		B-41	1092	2400	+22.250	- .886	-.118	- .214	+.225	+ .170	-.696	-3.203
		F-9	2147	2400	-1.017	-1.010	-.267	- .227	+.282	+ .271	-.058	- .237
		G-35	536	3600	- .914	- .920	-.233	- .197	+.176	+ .251	+.247	+ .204
		D-31	3472	3600	- .962	- .942	-.163	- .198	+.178	+ .214	+.342	+ .417
	Air-Dried	E-40	527	0	-1.075	-1.039	-.232	+ .118	+.160	- .074	+.266	- .125
		B-19	2179	0	-1.143	- .990	-.221	- .372	+.203	+ .155	+.239	+ .182
		F-42	0	600	-1.019	-1.095	-.030	- .284	+.019	+ .284	+.246	+ .021
		H-14	0	3600	- .929	...	-.181	...	+.203	...	...	+ .210
		E-13	562	600	-1.594	-1.078	-.356	- .208	+.314	+ .291	+.093	-1.000
		C-11	2139	600	-1.163	+ .714	-.229	+2.000	+.236	-1.067	+.245	+ .089
		C-17	1100	1200	- .933	- .941	-.686	- .511	+.343	+ .242	+.303	...
		D-44	3449	1200	...	- .813	...	- .228	...	+2.000	...	+ .124
		B-42	1092	2400	+38.250	- .847	-.043	- .264	+.065	+ .153	+.235	+ .102
		F-30	2147	2400	-1.076	-1.096	-.247	- .194	+.364	+ .340	+.235	+ .172
		G-30	536	3600	- .842	...	-.239	...	+.150	...	...	+ .182
		D-40	3472	3600	-1.057	-1.070	-.181	- .167	+.305	+ .309	+.367	+ .376

(Continued)

TABLE 8. (CONTINUED)

Temperature	Curing Condition	Specimen	Stress, psi		ϵ_{ir}/ϵ_i		ϵ_{ir}/ϵ_c		$\epsilon_{cr}/\epsilon_{ir}$		Instant. Recovery Poisson's Ratio	Creep Recovery Poisson's Ratio
			Axial	Radial	Axial	Radial	Axial	Radial	Axial	Radial		
150° F	As-Cast	B-4	561	0	...	-1.000	...	-.100	...	+.364	...	...
		D-15	1102	0	-1.039	...	-.369	...	+.341	...	...	...
		F-33	2123	0	...	...	...	...	...	...	...	...
		A-35	0	600	...	- .916	...	-.486	...	+.523	...	...
		C-12	1032	1200	-1.857	...	-.286	...	+.294	...	...	...
		D-2x	1086	2400	...	...	-.156	...	+.305	-.255	+.256	-.213
		G-9	2268	2400	-1.099	-1.138	-.348	-.360	+.477	+.467	+.370	+.361
	Air-Dried	B-1	561	0	- .941	- .840	-.167	...	+.198	+.857	+.217	+.947
		D-22	1102	0	- .918	- .870	-.262	+4.000	+.227	+.170	+.202	+.151
		F-34	2123	0	- .919	...	-.180	...	+.260	...	...	...
		D-3	0	600	-1.151	...	...	...	...	...	...	...
		E-4	2259	600	- .907	...	-.284	...	+.344	...	...	...
		C-46x	1032	1200	...	...	-.240	-.062	+.311	+.264	+.231	+.163
		D-41	1086	2400	- .130	- .963	-.237	-.214	+10.333	+.291	+.229	+.307
		G-19	2268	2400	- .990	- .984	-.254	-.266	+.399	+.418	+.357	+.375
		F-6	3474	3600	- .762	...	-.229	...	+.542	...	...	...

The overall average ratio of the instantaneous elastic recovery over the instantaneous strain for all the different loading conditions under the 75° F environment was 1.020. This indicated that the instantaneous elastic recovery at the time of unloading was, in general, higher than the instantaneous strain at the time of loading a year earlier for this specific environment and in this particular experiment.

Specimens at 150° F. At 150° F, four specimens were loaded axially, four biaxially, and five triaxially for both the as-cast and air-dried curing histories. Very few gages in the as-cast specimens lasted through the entire test period. Thus, a detailed evaluation of the creep recovery behavior of the as-cast specimens could not be made.

In the case of uniaxial loading, only two gages in as-cast specimens and five gages in air-dried specimens were functioning properly at the time of unloading. The values of the instantaneous elastic recovery obtained from these gages resulted in an average ratio of the instantaneous elastic recovery over the instantaneous strain of 1.020 and 0.898 for the as-cast and the air-dried cases, respectively. For each of the two different curing conditions under the biaxial loading, only one gage survived past the time of unloading and the resulting ratio of instantaneous recovery over instantaneous strain was 0.916 and 1.151 for the as-cast and the air-dried specimens, respectively. Under the triaxial loading condition, 50 and 20 percent mortality occured in the gages of the as-cast and the air-dried specimens, respectively. The instantaneous recovery over the instantaneous strain for the as-cast condition under the triaxial state of stress averaged 1.365 while that of the air-dried condition averaged 0.921.

It is difficult to evaluate the instantaneous recovery strains for specimens subjected to a temperature of 150° F during the creep and creep recovery periods since so many gages failed. In general, the instantaneous recovery strains were larger than the instantaneous strains for the as-cast specimens, with an average ratio of 1.175, and they were lower than the instantaneous strain for the air-dried specimens, with an average ratio of 0.922.

Comparison of Creep Recovery and Creep Strains

Specimens at 75° F. The creep strain recovered after a period of five months from the time of unloading for specimens at 75° F varied from 3 to 69 percent of the creep strain developed after one year of loading. The ratio

of creep recovery strain after five months to creep strain after one year did not show any systematic difference for different states of stress. This ratio varied from 0.034 to 0.667 and averaged 0.241 for the as-cast specimens, while it varied from 0.030 to 0.686 and averaged 0.256 for the air-dried specimens; thus, the air-dried specimens generally exhibited a larger recovery after 5 months, relative to the creep strain developed after one year, than did the as-cast specimens.

Specimens at 150° F. The values of creep recovery strains after a period of five months for specimens at 150° F were more uniform than for specimens at 75° F. The creep recovery strains varied from 6 to 49 percent of the creep strain developed after one year under load. For the as-cast specimens, the ratio of the creep recovery strain after five months to the creep strain after one year varied from 0.100 to 0.486 and averaged 0.301, while in the air-dried case, it varied from 0.062 to 0.284 and averaged 0.216. Unlike specimens at 75° F, the average values shown here indicated that the as-cast specimens recovered a larger percentage of the creep strain developed after one year than did the air-dried specimens.

Comparison of Creep Recovery and Instantaneous Recovery Strains

Specimens at 75° F. At 75° F the creep recovery strains after a period of five months were quite small in comparison to the instantaneous elastic recovery, in contrast to the creep strain, which in some cases exceeded the magnitude of the instantaneous elastic strain. The ratio of the creep recovery after five months over the instantaneous elastic recovery varied from 0.094 to 0.410 and averaged 0.218 for as-cast specimens, while it varied from 0.019 to 0.364 and averaged 0.230 for the air-dried specimens.

Specimens at 150° F. For specimens at 150° F, the creep recovery strain after a period of five months was also small in comparison to the instantaneous elastic recovery; however, the ratios were larger than at 75° F. The ratio of the creep recovery after five months to the instantaneous elastic recovery for the as-cast specimens varied from 0.294 to 0.523 and averaged 0.396, while for the air-dried specimens the ratios varied from 0.170 to 0.857 and averaged 0.357. These average values indicated that the as-cast specimens also showed a higher average ratio of creep recovery strain over the instantaneous recovery strain than the air-dried specimens, in contrast to specimens at 75° F.

RECOVERY POISSON'S RATIO

Instantaneous Recovery

The air-dried specimens resulted in a smaller average Poisson's ratio than the as-cast specimens.

Excluding the hydrostatically loaded specimens, the instantaneous recovery Poisson's ratios for all specimens at 75° F ranged from 0.217 to 0.269 and averaged 0.251 and 0.246 for the as-cast and the air-dried specimens, respectively.

Excluding the hydrostatically loaded specimens, Poisson's ratio for instantaneous recovery could be evaluated for only one as-cast specimen and three air-dried specimens at 150° F. For the as-cast specimen, the elastic recovery Poisson's ratio was 0.256. This value was essentially equal to those of the same curing condition but under the 75° F environment, and it was even closer to the average values of the elastic Poisson's ratio at loading time for the same curing condition and under both environments. For the air-dried specimens, the average instantaneous recovery Poisson's ratio was 0.216. This value was lower than the instantaneous recovery Poisson's ratio of the air-dried specimens at 75° F and was also smaller than the elastic Poisson's ratio of the air-dried specimens at the time of loading at both temperatures. In general, it can be concluded that the instantaneous recovery Poisson's ratio was not affected by temperature or by state of stress, but was affected by curing history, and that Poisson's ratios for the instantaneous recovery strains were essentially equal to the values of the elastic Poisson's ratios at the time of loading.

Creep Recovery

A Poisson's effect was also noticed in the recovery period. The creep recovery Poisson's ratio for each specimen under the 75° F environment was calculated and recorded in Table 8. Excluding the hydrostatically loaded specimens and specimens penetrated by oil, the creep recovery Poisson's ratio five months after unloading varied from 0.160 to 0.279 and averaged 0.233 for as-cast specimens, while it varied from 0.021 to 0.210 and averaged 0.130 for the air-dried specimens. Similar to previous Poisson's ratios calculated at different stages of the test, the average creep recovery Poisson's ratio of the air-dried specimens was also smaller than that of the as-cast specimens.

It was not possible to make any valid judgment of the creep recovery Poisson's ratio of specimens at 150° F due to the large percentage of gage failures. Excluding hydrostatically loaded specimens and specimens penetrated by oil, only two values of creep recovery Poisson's ratio could be obtained, 0.151 and 0.307. Both of these values were for air-dried specimens and both seem to be within the expected range of creep recovery Poisson's ratio of concrete.

APPLICABILITY OF THE PRINCIPLE OF SUPERPOSITION OF STRAIN

Based on the previously discussed analysis, it would appear that the principle of superposition of creep strains as a means of evaluating and estimating recovery strains should be carefully examined for accuracy. As discussed in Chapter 2, many investigators have investigated and discussed the validity and accuracy of the principle of superposition, and most of them (Refs 5, 14, and 33) concluded that it overestimated the measured creep recovery strains. Although originally this investigation was not designed to investigate this point, the nature of the experiment allowed a crude evaluation of the validity of superposition to be conducted.

Figures 27 and 28 compare the estimated creep recovery strains with the measured creep recovery strains for specimens which were cured for 90 days, loaded for one year, and then unloaded. The estimated creep recovery strains were obtained from the creep strains for the specimens which were loaded at an age of 365 days by applying the principle of superposition of strain. These two figures clearly indicate that the estimated creep strains were substantially larger than the measured creep strains and indicate that the principle of superposition overestimates creep recovery strains. Even though there was a difference of 90 days between the time that specimens H-5 and H-24 were loaded, 365 days after casting, and the time that specimens E-39 and B-7 were unloaded, 454 days after casting, it is felt that the difference between the estimated and measured creep recovery strains was so large that the 90-day difference in age would not have any significant effect. Therefore, it is concluded that the use of superposition of creep strains as a means of estimating recovery strains is not accurate and should not be used unless large errors can be tolerated.

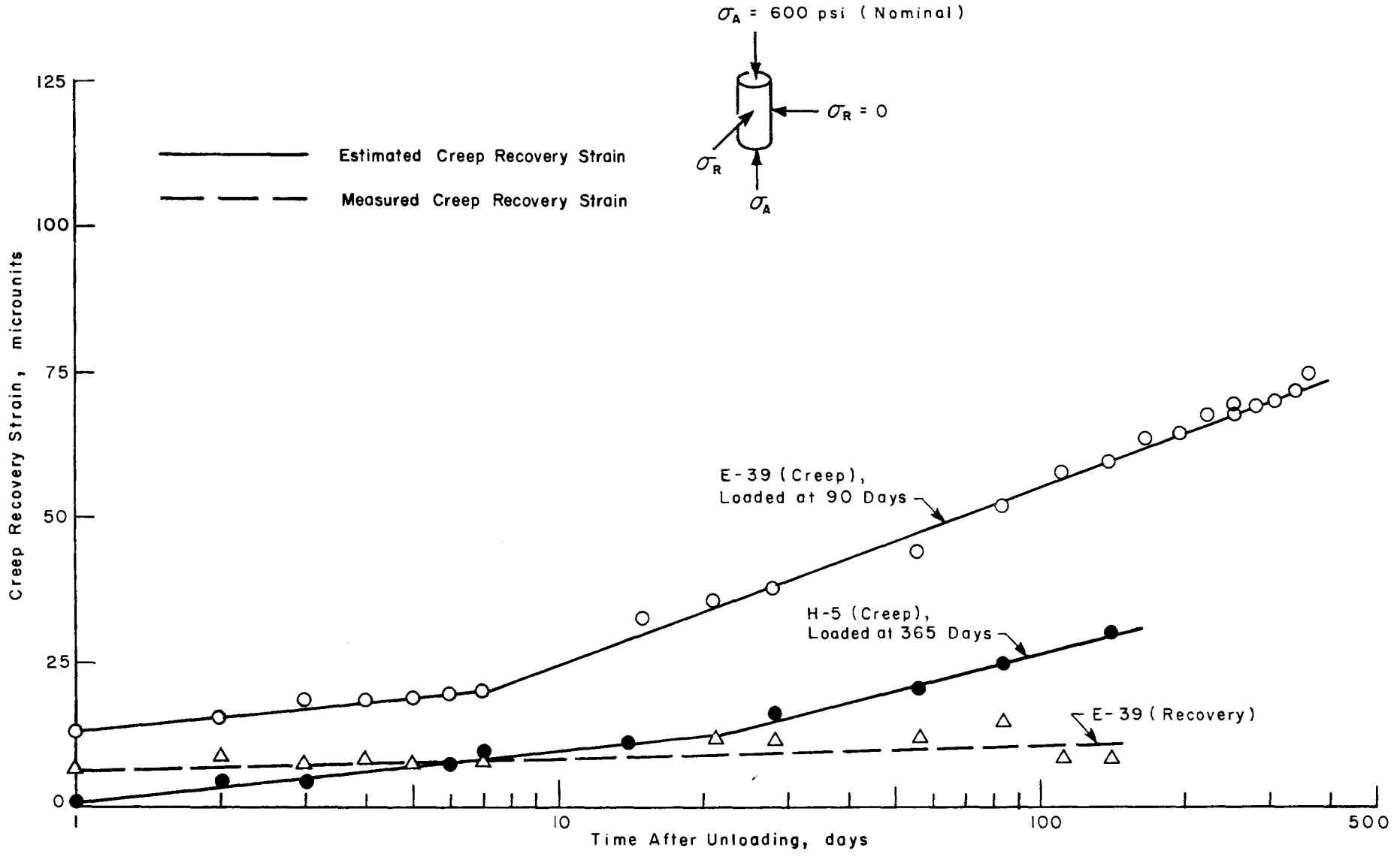

Fig 27. Estimated and measured creep recovery strain for as-cast specimens loaded uniaxially at 600 psi.

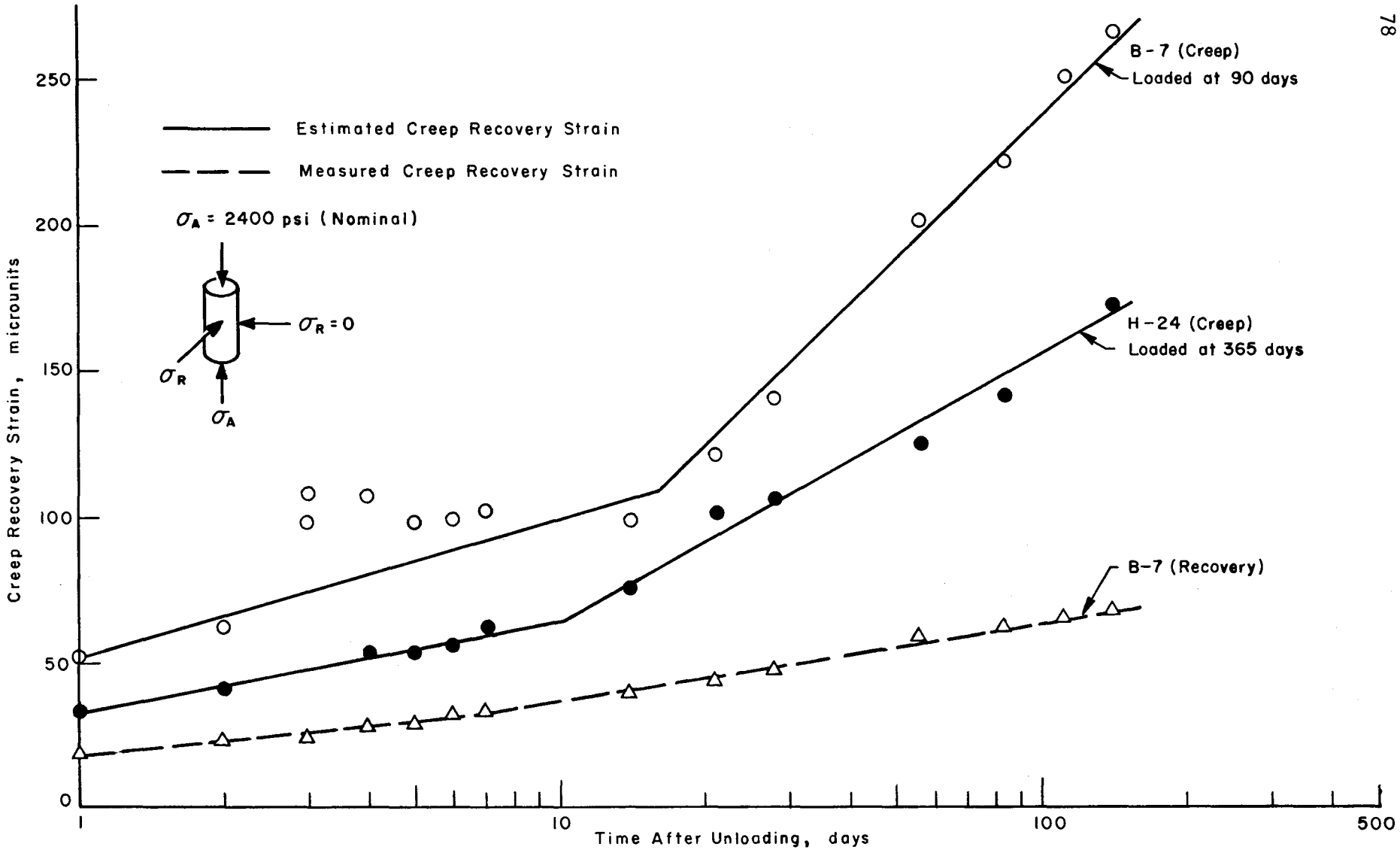

Fig 28. Estimated and measured creep recovery strain for as-cast specimens loaded uniaxially at 2400 psi.

CHAPTER 6. CONCLUSIONS AND RECOMMENDATIONS

This chapter summarizes the findings and conclusions of the evaluation of the recovery data obtained from the experimental investigation described in Chapter 3, in which the concrete was subjected to compressive stresses, two curing histories, and two temperatures during the loading and unloading periods. In addition, recommendations based on the results of this research are included.

CONCLUSIONS

Instantaneous Recovery

(1) Instantaneous recovery was not affected by temperature but was linearly related to the previously sustained stress for stress levels less than about 55 percent of the ultimate strength of the concrete.

(2) Instantaneous recovery strains of air-dried specimens were larger than of as-cast specimens, which probably can be related to the fact that the as-cast specimens exhibited higher strengths.

(3) The instantaneous recovery strains at the time of unloading were generally higher than the instantaneous elastic strains at the time of loading a year earlier, especially at 75° F.

(4) The instantaneous recovery Poisson's ratio was not affected by temperature or state of stress but was larger for the as-cast specimens than for the air-dried specimens. Poisson's ratio for instantaneous recovery varied from 0.202 to 0.269.

Creep Recovery

(1) Creep recovery strains were affected by temperature, curing history, and stress conditions. The creep recovery strains were larger at 150° F than at 75° F and for the air-dried specimens than for the as-cast specimens. The magnitude of the creep recovery strains was also related to the magnitude of the previously sustained stress.

(2) At 75° F, the ratio of the creep recovery strain 5 months after unloading to the creep strains 12 months after loading was greater for the air-dried specimens than for the as-cast specimens; however, at 150° F, the ratio was greater for the as-cast specimens than for the air-dried specimens.

(3) The creep recovery strains were small in comparison to the instantaneous recovery strains, in contrast to the fact that during the loading period the creep strains were large in comparison to the instantaneous strains and in some cases exceeded the magnitude of the instantaneous strains. At 75° F, the ratio of creep recovery strain five months after unloading to the instantaneous recovery strain was larger for the air-dried specimens than for the as-cast specimens; however, at 150° F, the ratio was larger for the as-cast specimens than for the air-dried specimens.

(4) Creep recovery Poisson's ratio was larger for the as-cast specimens than for the air-dried specimens. The instantaneous recovery Poisson's ratio varied from 0.202 to 0.269, while the average creep recovery Poisson's ratio was smaller, varying from 0.021 to 0.307.

(5) The principle of superposition of strains overestimates the actual creep recovery strains and thus should not be used unless a relatively large error can be tolerated.

RECOMMENDATIONS

Based on the above conclusions, the following recommendations are made for further studies of the creep and recovery behavior of concrete.

(1) Additional study should be conducted to investigate the effects of higher stress level, particularly on instantaneous recovery, which showed a linear relationship up to the level investigated in this study.

(2) The effects of a wider range of temperature during the loading period and a range of concrete strengths should be studied to determine whether any definite relationships exist between these parameters and the creep and creep recovery behavior of concrete.

(3) The effect of curing time prior to loading on creep behavior should be investigated more thoroughly.

(4) The creep behavior under loading periods in excess of 12 months should be studied since the service life of a reactor vessel is many years.

(5) Concretes should be studied over a range of moisture content to determine if there is any correlation between moisture content and the creep recovery of concrete.

(6) The prediction of the magnitude of creep recovery strains by means of equations which are a function of creep strain, time of loading, level of stress, and curing history should be considered.

REFERENCES

1. Ali, I., and C. E. Kesler, "Rheology of Concrete: A Review of Research," Bulletin 476, Engineering Experiment Station, University of Illinois, 1965.

2. Arnstein, A., and M. Reiner, "Creep of Cement, Cement-Mortar and Concrete," Civil Engineering and Public Works Review, Vol 40, London, pp 198-202.

3. Bingham, E. C., and M. Reiner, "Rheological Properties of Cement and Cement Mortar-Stone," Physics, Vol 4, March 1933, pp 88-96.

4. Chaung, J. W., T. W. Kennedy, and E. S. Perry, "An Approach to Estimating Long-Term Multiaxial Creep Behavior from Short-Term Uniaxial Creep Results," Union Carbide Report No. 2864-3, Department of Civil Engineering, The University of Texas at Austin, June 1970.

5. Davies, R. D., "Some Experiments on the Applicability of the Principle of Superposition to the Strains of Concrete Subjected to Changes of Stress, with Particular Reference to Prestressed Concrete," Magazine of Concrete Research, Vol 9, No. 27, London, November 1957, pp 161-172.

6. Freudenthal, A. M., The Inelastic Behavior of Engineering Materials and Structures, John Wiley and Sons, Inc., New York, 1950, 587 pp.

7. Freudenthal, A. M., and F. Roll, "Creep and Creep Recovery of Concrete Under High Compressive Stress," American Concrete Institute Journal, Proceedings, Vol 54, June 1958, pp 1111-1142.

8. Freyssinet, E., "The Deformation of Concrete," Magazine of Concrete Research, London, Vol 3, No. 8, December 1951, pp 49-56.

9. Glanville, W. H., and F. G. Thomas, "Further Investigations on the Creep or Flow of Concrete Under Load," Building Research Technical Paper No. 21, London, 1939.

10. Glucklich, J., "Rheological Behavior of Hardened Cement Paste Under Low Stresses," American Concrete Institute Journal, Proceedings, Vol 56, October 1959, pp 327-338.

11. Gopalakrishnan, K. S., A. M. Neville, and A. Ghali, "A Hypothesis on Mechanism of Creep of Concrete with Reference to Multiaxial Compression," American Concrete Institute Journal, Proceedings, Vol 67, January 1970, pp 29-35.

12. Hannant, D. J., "Creep and Creep Recovery of Concrete Subjected to Multiaxial Compressive Stress," American Concrete Institute Journal, Proceedings, Vol 66, May 1969, pp 391-394.

13. Illston, J. M., "Components of Creep in Mature Concrete," American Concrete Institute Journal, Proceedings, Vol 65, March 1968, pp 219-227.

14. Jessop, E. L., M. A. Ward, and A. M. Neville, "Relation Between Creep and Creep Recovery in Cement Paste," Journal of Materials, JMLSA, Vol 6, No. 1, March 1971, pp 188-217.

15. Kennedy, T. W., "Loss of Axial Load Due to Friction in the Loading Ram," Union Carbide Subcontract 2864, unpublished research, Department of Civil Engineering, The University of Texas at Austin, August 15, 1968.

16. Kennedy, T. W., "Pilot Test 1," Union Carbide Subcontract 2864, unpublished research, Department of Civil Engineering, The University of Texas at Austin, July 21, 1968.

17. Kennedy, T. W., "Pilot Test 2," Union Carbide Subcontract 2864, unpublished research, Department of Civil Engineering, The University of Texas at Austin, August 2, 1968.

18. Kennedy, T. W., and E. S. Perry, "An Experimental Approach to the Study of the Creep Behavior of Plain Concrete Subjected to Triaxial Stresses and Elevated Temperatures," Union Carbide Report No. 2864-1, Department of Civil Engineering, The University of Texas at Austin, June 1970.

19. Lead, F. M., and C. R. Lee, "Shrinkage and Creep in Concrete," Symposium on Shrinkage and Cracking of Cementive Materials, Society of Chemical Industry, London, 1947, pp 17-22.

20. Lorman, W. R., "Theory of Concrete Creep," Proceedings, American Society for Testing Materials, Vol 90, 1940, pp 1082-1102.

21. Lynam, C. G., "Growth and Movement in Portland Cement Concrete," Oxford University Press, London, 1934.

22. McHenry, D., "A New Aspect of Creep in Concrete and Its Application to Design," Proceedings, American Society for Testing Materials, Vol 43, 1943, pp 1069-1084.

23. Nasser, K. W., and A. M. Neville, "Creep of Concrete at Elevated Temperatures," American Concrete Institute Journal, Proceedings, Vol 62, December 1965, pp 1567-1579.

24. Neville, A. M., "Creep Recovery of Mortars Made with Different Cements," American Concrete Institute Journal, Proceedings, Vol 56, August 1959, pp 167-174.

25. Neville, A. M., "Theories of Creep in Concrete," American Concrete Institute Journal, Proceedings, Vol 52, September 1955, pp 47-60.

26. Neville, A. M., Properties of Concrete, Sir Isaac Pitman and Sons, London, 1963.

27. Powers, T. C., "Mechanism of Shrinkage and Reversible Creep of Hardened Cement Paste," International Conference on the Structure of Concrete, Paper G1, London, 1965.

28. Roll, Fredric, "Long Time Creep Recovery of Highly Stressed Concrete Cylinders," Symposium on Creep of Concrete, SP-9, American Concrete Institute, Detroit, 1964, pp 95-114.

29. Ross, A. D., "Creep of Concrete Under Variable Stress," American Concrete Institute Journal, Proceedings, Vol 54, March 1958, pp 739-758.

30. Ross, A. D., "Experiments on the Creep of Concrete Under Two-Dimensional Stresses," Magazine of Concrete Research, No. 16, London, June 1954, pp 3-10.

31. Seed, H. B., "Creep and Shrinkage in Reinforced Concrete Structures," Engineering, London, September 26, 1947.

32. Thomas, F. G., "Creep of Concrete Under Load," International Association of Testing Materials, 1937.

33. U. S. Bureau of Reclamation, "A 10-Year Study of Creep Properties of Concrete," Concrete Laboratory Report No. SP-38, July 28, 1953.

34. Vogt, F., "On the Flow and Extensibility of Concrete," Stockholm, 1935, 24 pp.

35. York, G. P., T. W. Kennedy, and E. S. Perry, "Experimental Investigation of Creep in Concrete Subjected to Multiaxial Compressive Stresses at Elevated Temperatures," Union Carbide Report No. 2864-2, Department of Civil Engineering, The University of Texas at Austin, June 1970.

APPENDIX A

COMPRESSIVE AND TENSILE STRENGTH DATA

TABLE A.1. 365-DAY COMPRESSIVE STRENGTHS*

Curing History: As-Cast

Specimen	Remarks	Temp., °F	Load, lb	Strength, psi	Average Strength, psi
A-26	Good cap	75	248,970	8805	8836
A-45	Fair cap	75	250,720	8867	
A-6	Very poor cap	150	189,720	6710	7596
A-40	Fair cap	150	239,810	8481	
G-3	Fair cap	75	225,530	7977	8190
G-24	Good cap	75	237,620	8404	
G-8	Good cap	150	241,030	8525	8313
G-34	Good cap	150	229,040	8101	
H-3	Cap 90% effective	75	192,270	6800	
H-26	Cap 80% effective	75	185,840	6573	6930
H-42	Good cap	75	209,670	7416	
I-19	Cap 80% effective	75	189,930	6717	7342
I-24	Good cap	75	225,260	7967	
I-8	Good cap	150	210,670	7451	7658
I-10	Good cap	150	222,390	7865	

Curing History: Air-Dried

Specimen	Remarks	Temp., °F	Load, lb	Strength, psi	Average Strength, psi
A-24	Good cap	75	207,820	7350	7480
A-34	Good Cap	75	215,190	7611	
A-33	Very poor cap	150	198,350	7015	7009
A-44	Very poor cap	150	198,000	7003	
G-6	Fair cap (cracks)	75	222,340	7864	7809
G-46	Good cap	75	219,230	7754	
G-22	Good cap	150	225,350	7970	7863
G-31	Good cap	150	219,300	7756	
H-10	Good cap	75	193,250	6836	
H-27	Cap 70% effective	75	177,140	6265	6856
H-44	Good cap	75	211,100	7466	
I-33	Good cap	75	218,650	7733	7586
I-38	Good cap	75	210,310	7438	
I-5	Good cap	150	197,540	6987	7171
I-31	Good cap	150	207,940	7354	

* Compressive strengths at earlier ages are tabulated in Appendix B of Ref 35.

TABLE A.2. 538-DAY COMPRESSIVE STRENGTHS

Curing History: As-Cast

Specimen	Remarks	Temp., °F	Load, lb	Strength, psi	Average Strength, psi
A-3	Good cap	75	249,600	8828	8425
A-21	Good cap	75	266,710	9933	
A-2	Good cap	150	214,100	7572	9131
A-46	Good cap	150	262,310	9277	
G-4	Good cap	75	241,640	8546	9006
G-13	Good cap	75	267,650	9466	
G-2	Good cap	150	225,610	7979	8265
G-44	Good cap	150	241,740	8550	
H-18	Good cap	75	202,250	7154	7531
H-41	Good cap	75	216,170	7647	
H-43	Good cap	75	220,280	7792	
I-7	Good cap	75	204,850	7256	7122
I-41	Good cap	75	200,370	7088	
I-2	Good cap	150	210,410	7443	7466
I-3	Good cap	150	211,700	7989	

Curing History: Air-Dried

Specimen	Remarks	Temp., °F	Load, lb	Strength, psi	Average Strength, psi
A-30	Good cap	75	242,360	8572	8569
A-31	Good cap	75	242,170	8565	
A-10	Cap 75% effective	150	211,000	7463	7940
A-27	Good cap	150	237,960	8416	
G-27	Good cap	75	229,560	8119	8072
G-92	Good cap	75	226,890	8025	
G-32	Good cap	150	213,460	7550	7549
G-41	Good cap	150	213,380	7547	
H-2	Good cap	75	206,365	7300	7469
H-12	Good cap	75	215,884	7637	
I-37	Good cap	150	222,085	7856	7856

TABLE A.3. 538-DAY TENSILE STRENGTHS*

Curing History: As-Cast

Specimen	Temp., °F	Load, lb	Strength, psi	Average Strength, psi
B-25	75	64,800	573	601
B-28	75	71,050	628	
B-27	150	53,800	476	599
B-39	150	81,600	722	
C-33	75	65,600	580	593
C-38	75	69,200	612	
C-3	150	62,300	551	553
C-37	150	62,800	555	
E-12	75	62,400	552	548
E-27	75	61,500	544	
E-26	150	65,300	577	621
E-46	150	75,200	665	
F-2	75	48,000	424	486
F-14	75	62,000	598	
F-11	150	69,000	610	613
F-96	150	69,500	615	

Curing History: Air-Dried

Specimen	Temp., °F	Load, lb	Strength, psi	Average Strength, psi
B-8	75	89,250	789	763
B-43	75	83,200	736	
B-17	150	65,000	575	657
B-40	150	83,500	738	
C-14	75	78,000	690	739
C-24	75	89,000	787	
C-4	150	68,300	604	581
C-9	150	63,000	557	
E-30	75	78,500	694	647
E-34	75	67,700	599	
E-6	150	72,600	642	607
E-20	150	64,600	571	
F-37	75	80,800	714	691
F-41	75	75,400	667	
F-7	150	86,200	762	663
F-32	150	63,800	564	

* Tensile strengths at earlier ages are tabulated in Appendix C in Ref 35.

APPENDIX B

TOTAL STRAIN LESS SHRINKAGE STRAIN CURVES DURING THE UNLOADING PERIOD FOR AS-CAST SPECIMENS AT 75^{o} F

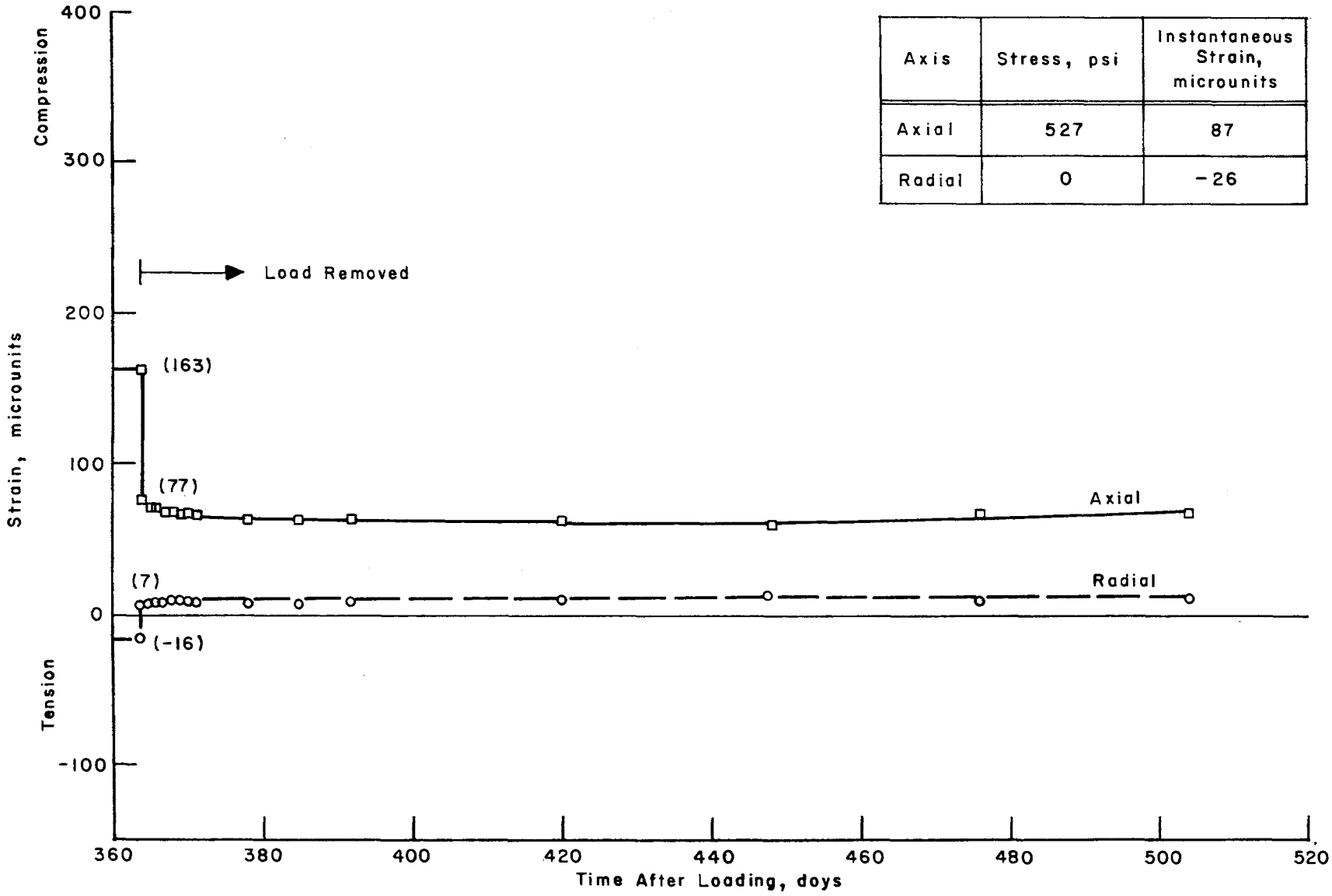

Axis	Stress, psi	Instantaneous Strain, microunits
Axial	527	87
Radial	0	-26

Fig B.1. Total strain less shrinkage strain after unloading for specimen E-39.

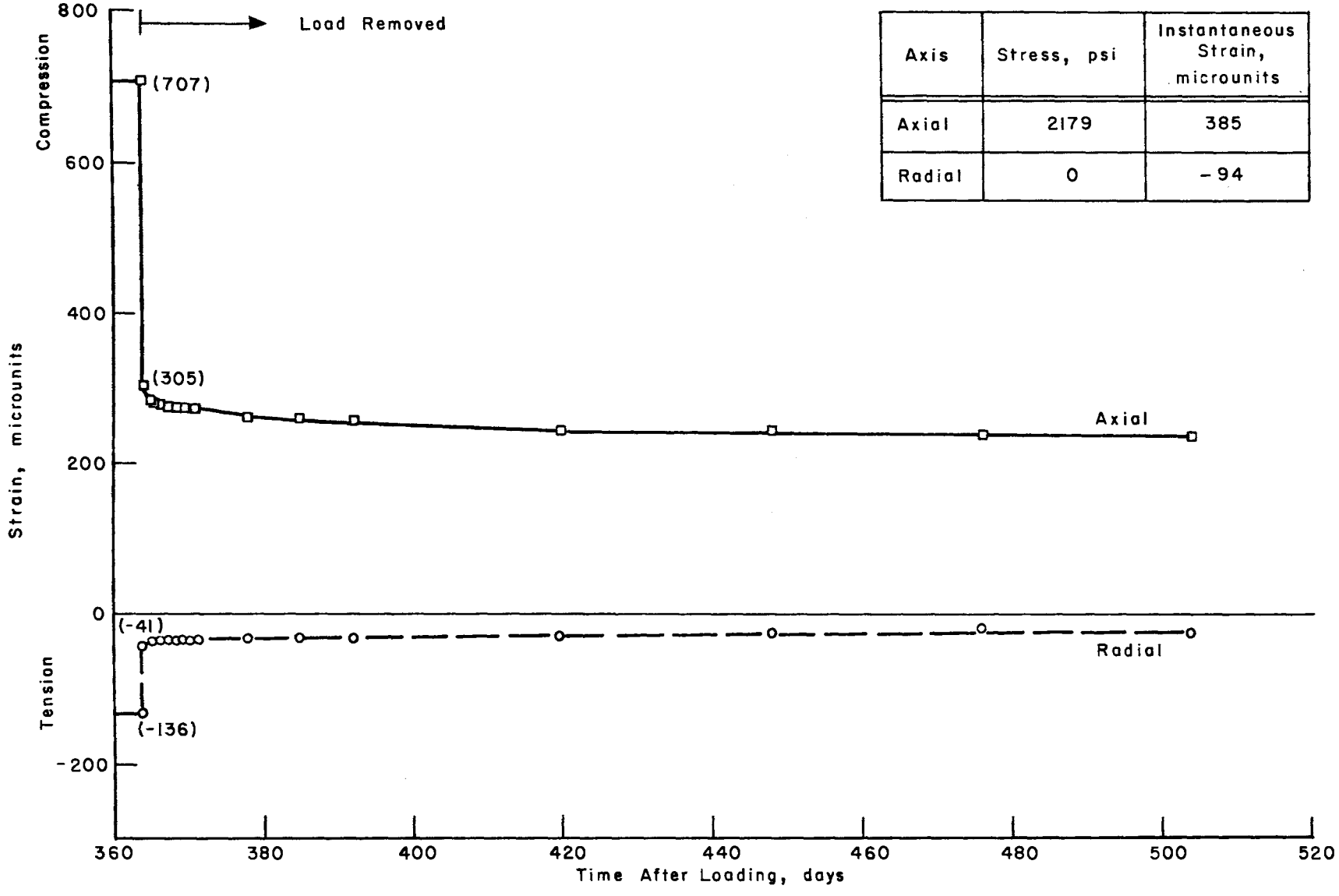

Axis	Stress, psi	Instantaneous Strain, microunits
Axial	2179	385
Radial	0	-94

Fig B.2. Total strain less shrinkage strain after unloading for specimen B-7.

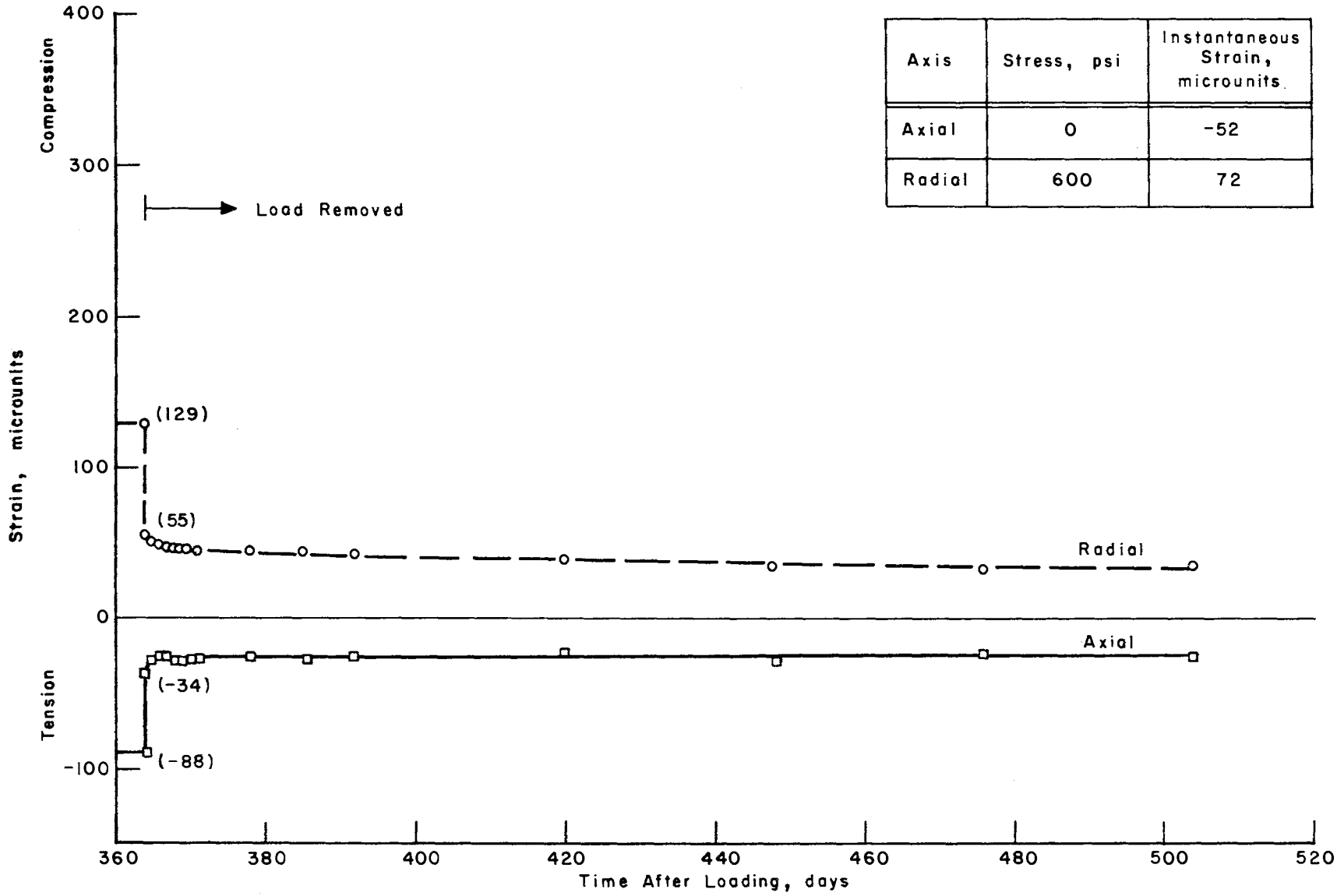

Axis	Stress, psi	Instantaneous Strain, microunits
Axial	0	-52
Radial	600	72

Fig B.3. Total strain less shrinkage strain after unloading for specimen F-13.

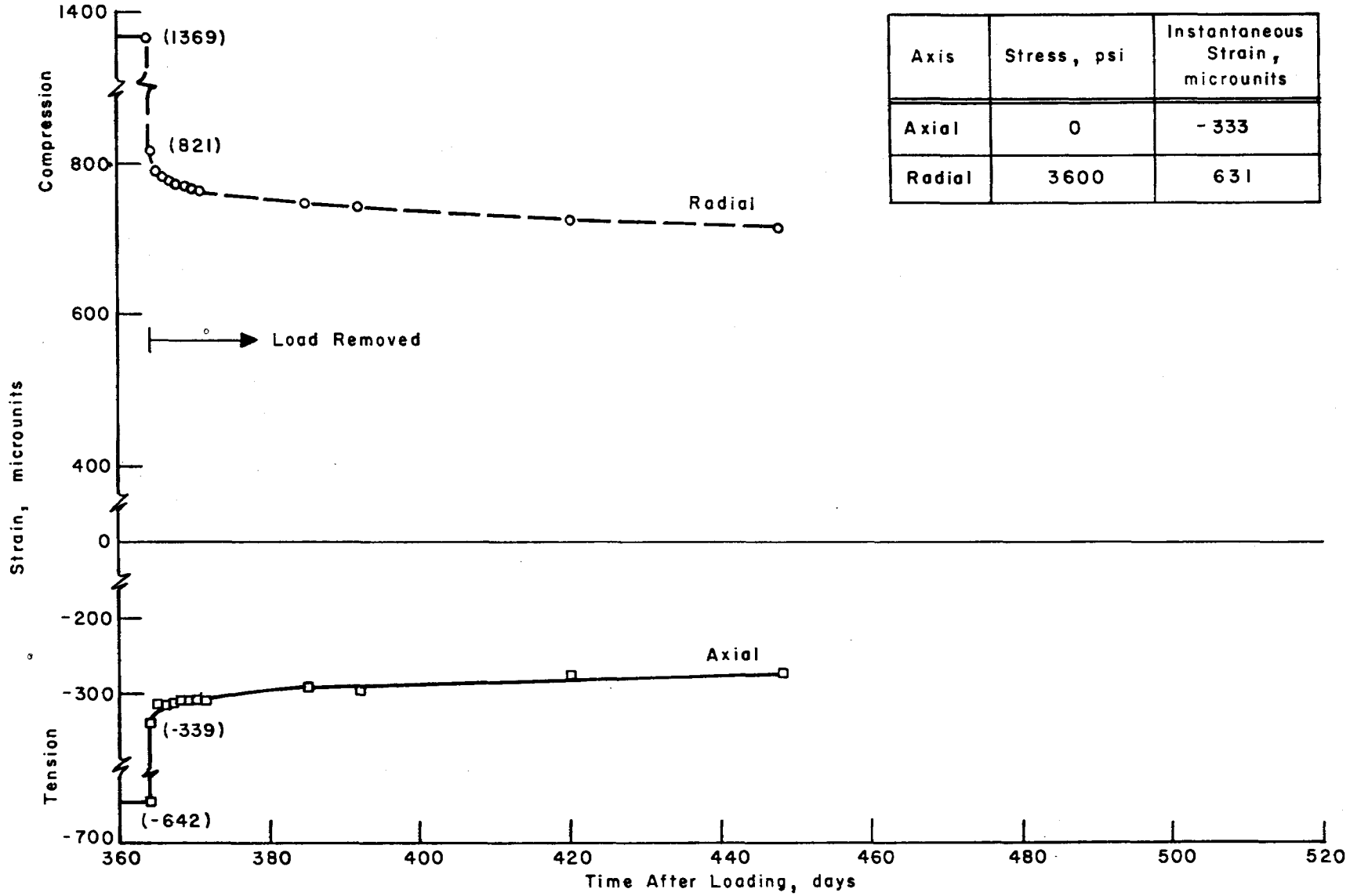

Axis	Stress, psi	Instantaneous Strain, microunits
Axial	0	-333
Radial	3600	631

Fig B.4. Total strain less shrinkage strain after unloading for specimen H-22.

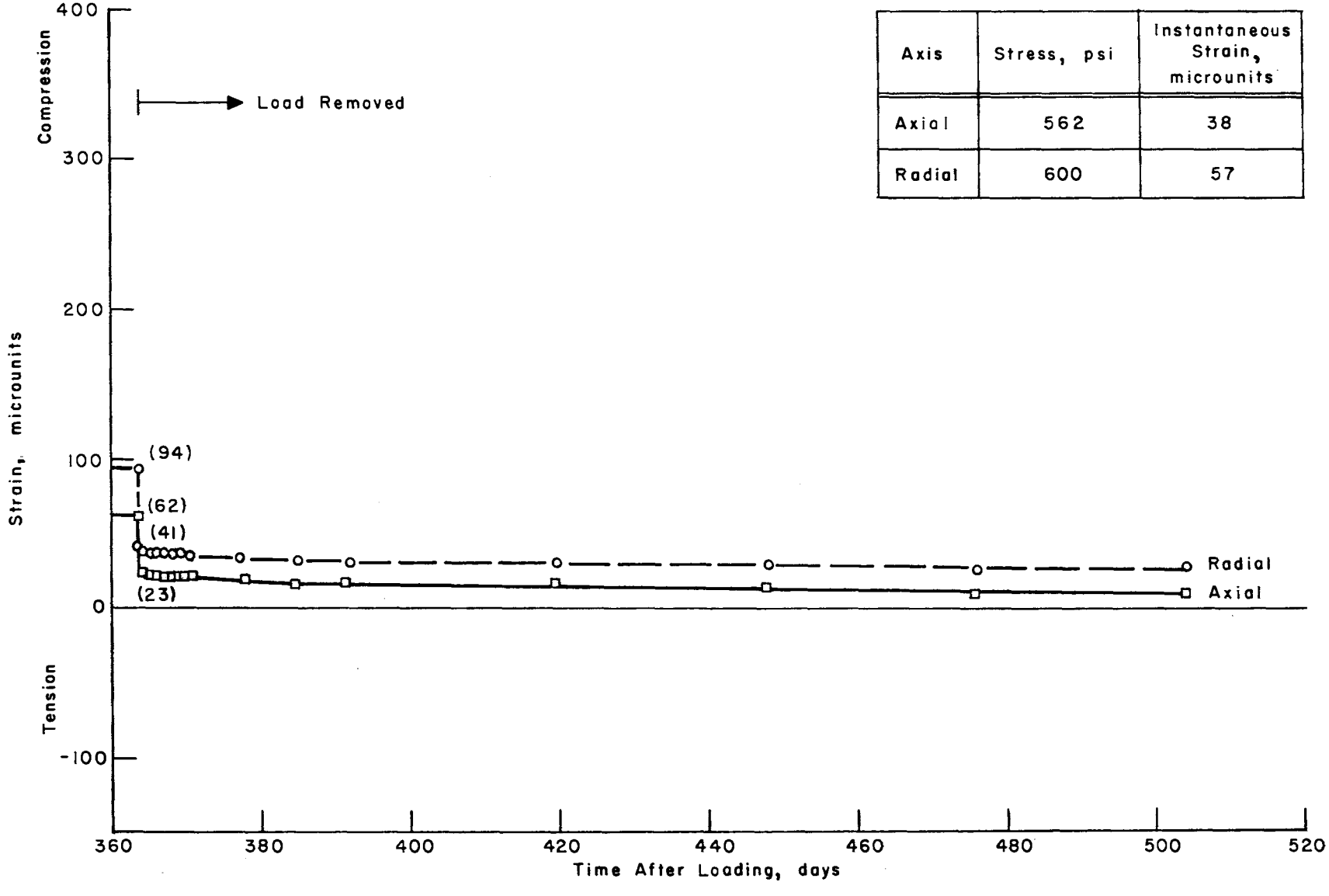

Axis	Stress, psi	Instantaneous Strain, microunits
Axial	562	38
Radial	600	57

Fig B.5. Total strain less shrinkage strain after unloading for specimen E-5.

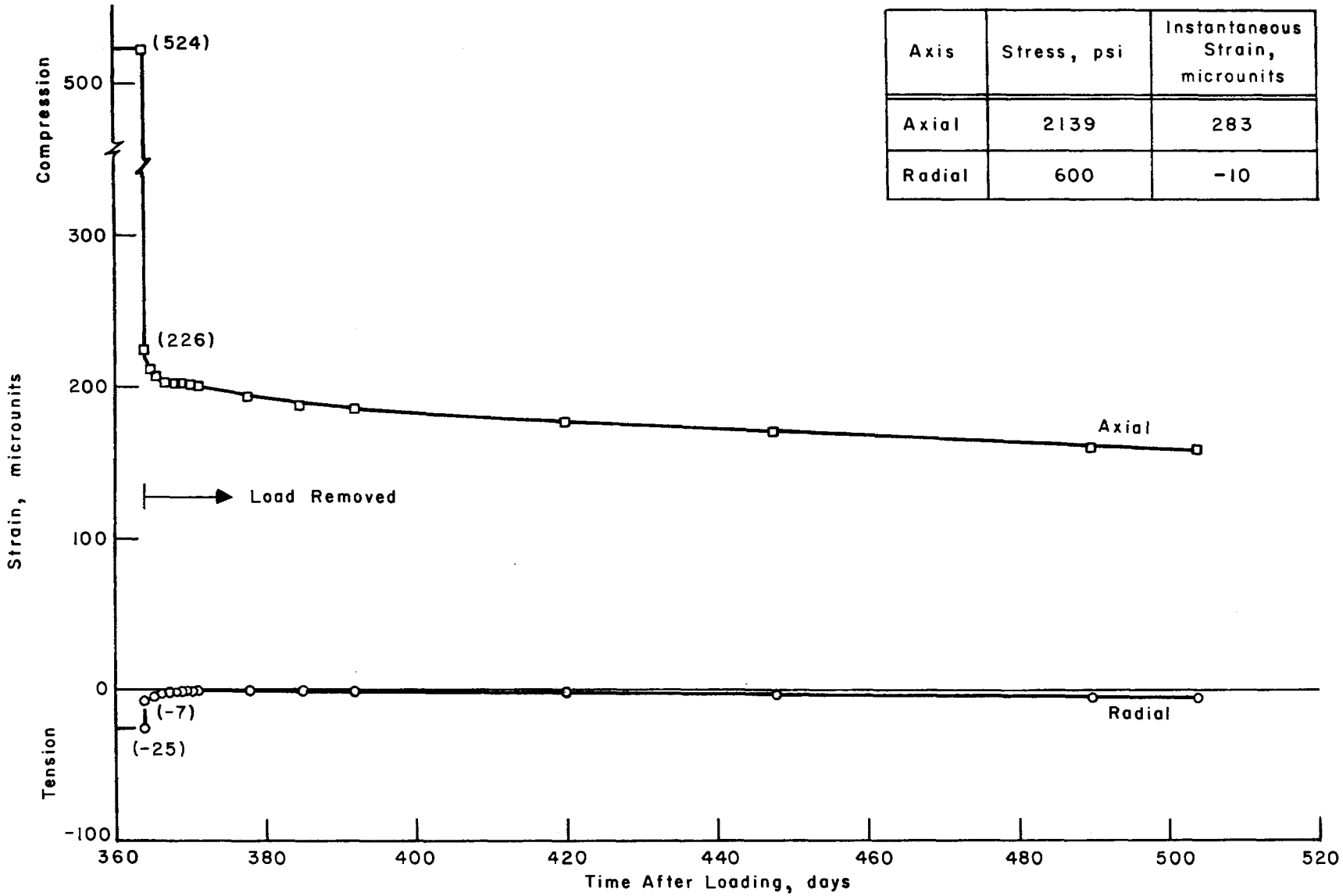

Fig B.6. Total strain less shrinkage strain after unloading for specimen C-23.

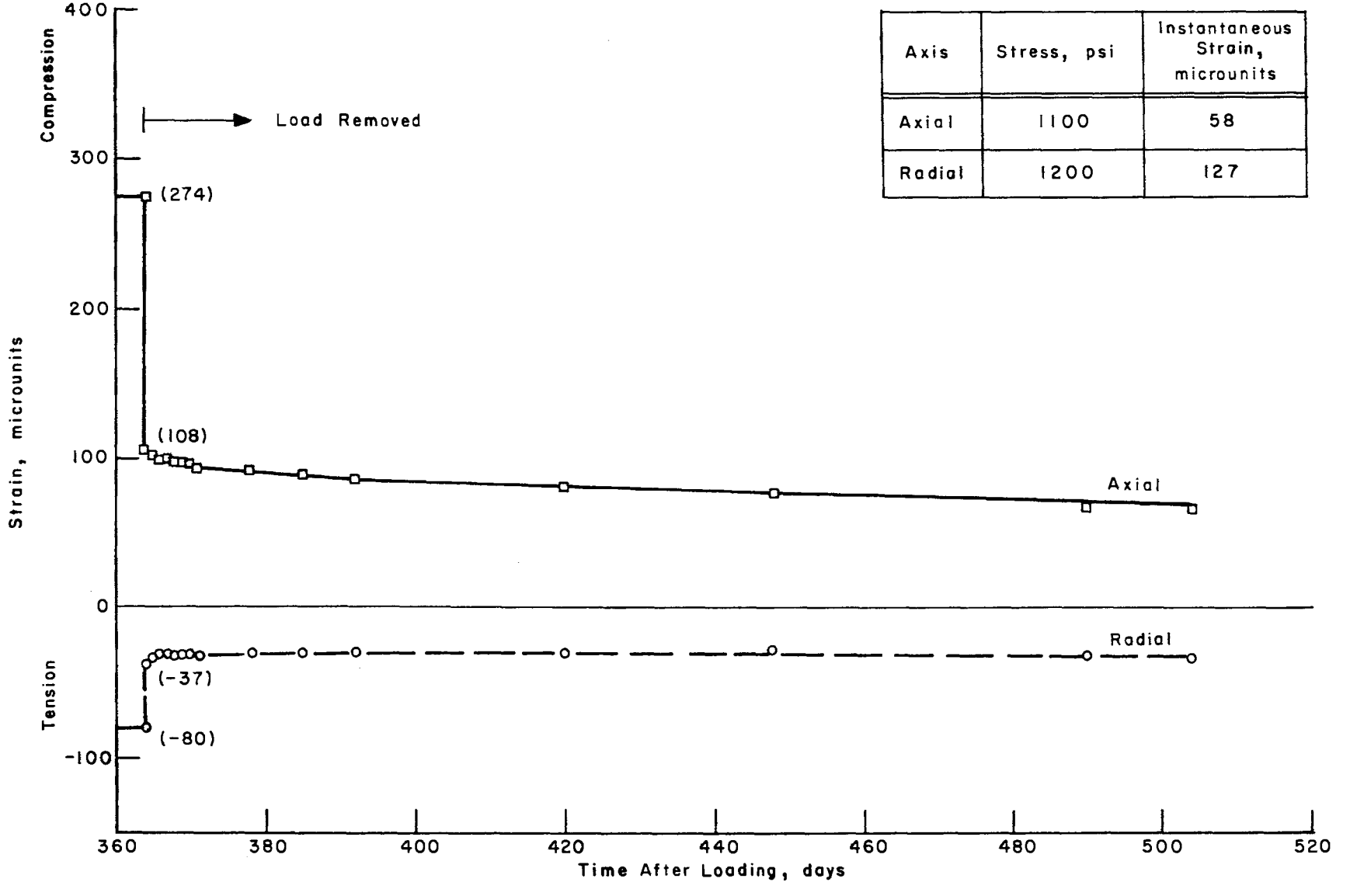

Axis	Stress, psi	Instantaneous Strain, microunits
Axial	1100	58
Radial	1200	127

Fig B.7. Total strain less shrinkage strain after unloading for specimen C-16.

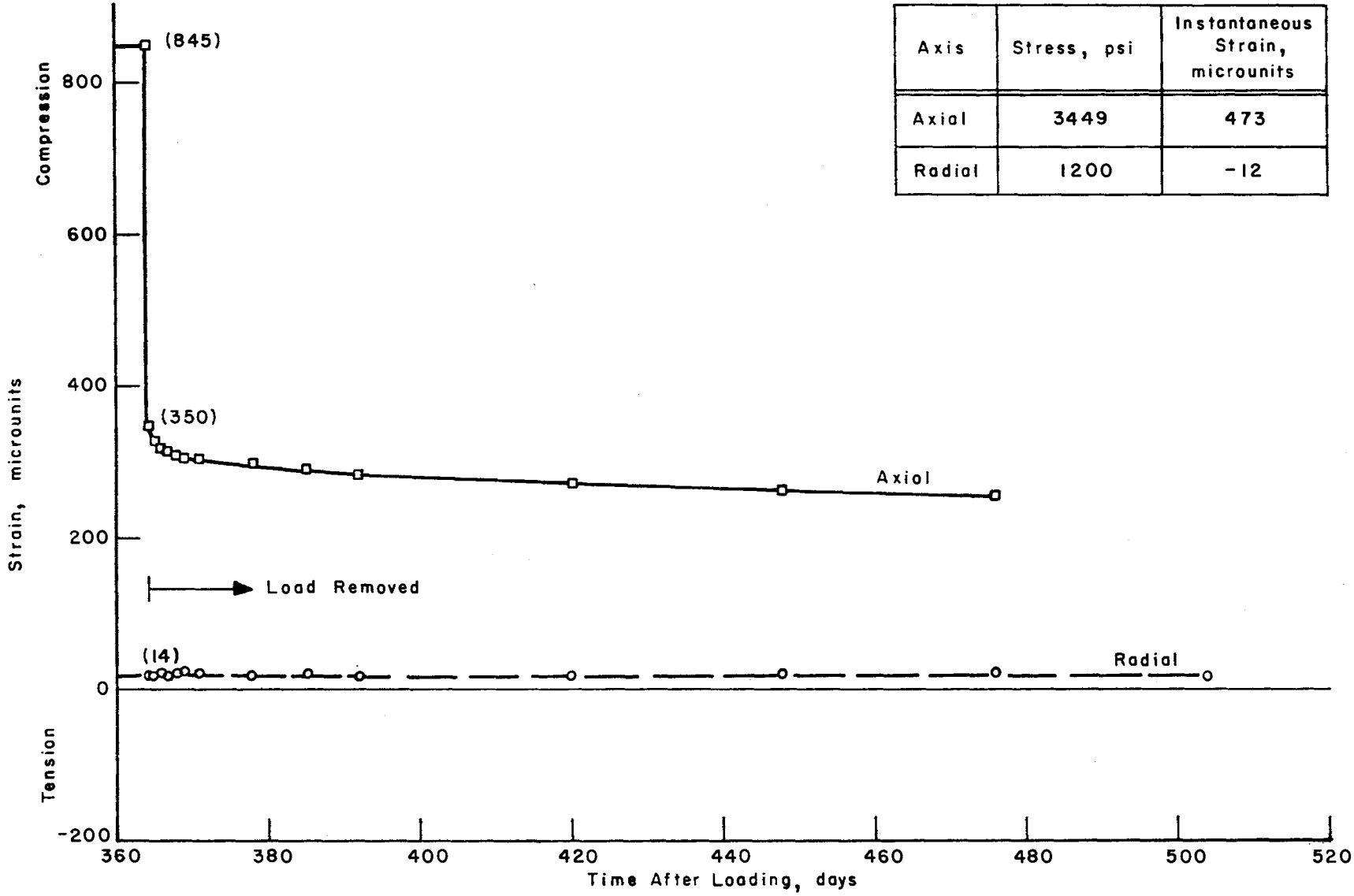

Fig B.8. Total strain less shrinkage strain after unloading for specimen D-26.

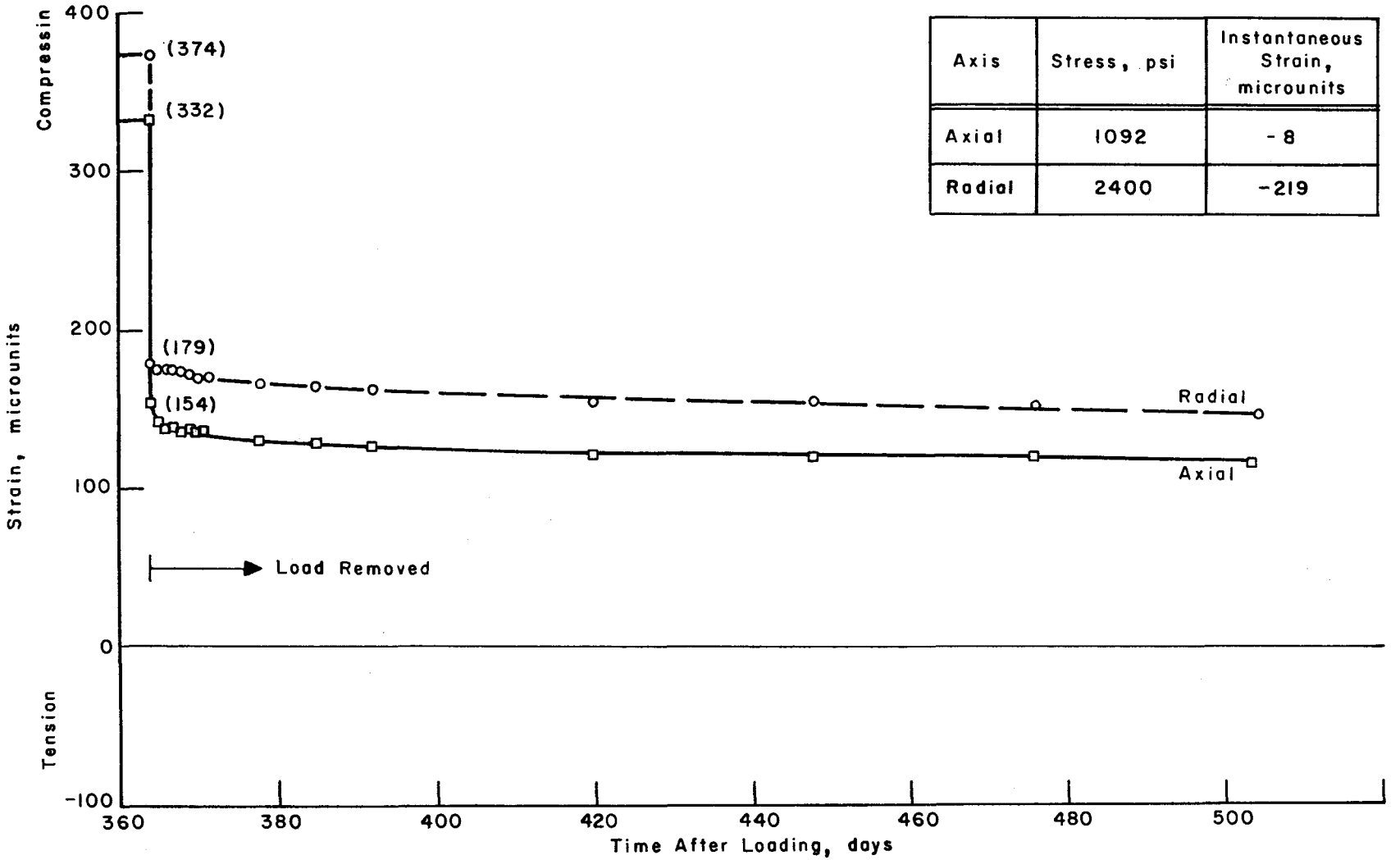

Axis	Stress, psi	Instantaneous Strain, microunits
Axial	1092	- 8
Radial	2400	-219

Fig B.9. Total strain less shrinkage strain after unloading for specimen B-41.

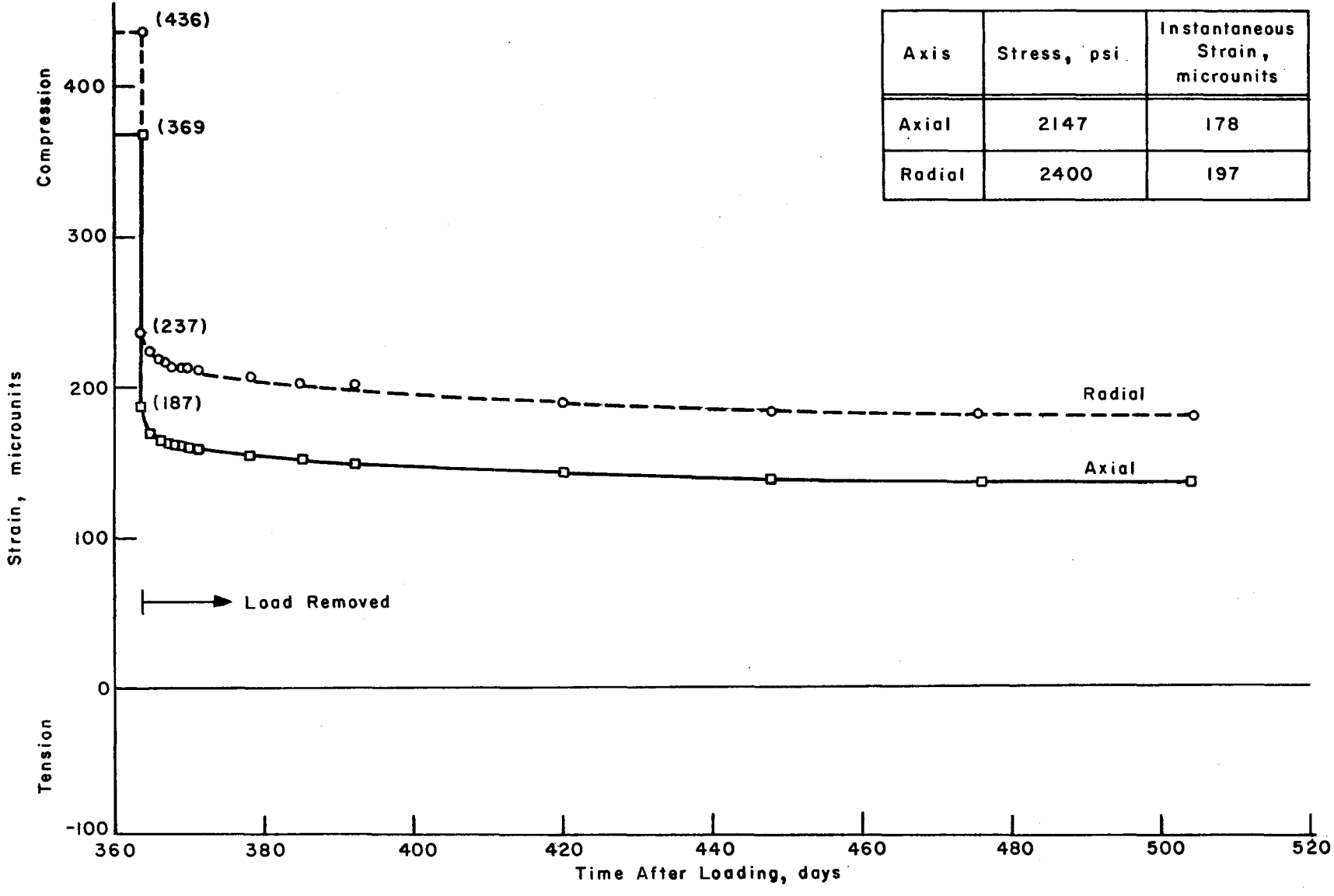

Axis	Stress, psi	Instantaneous Strain, microunits
Axial	2147	178
Radial	2400	197

Fig B.10. Total strain less shrinkage strain after unloading for specimen F-9.

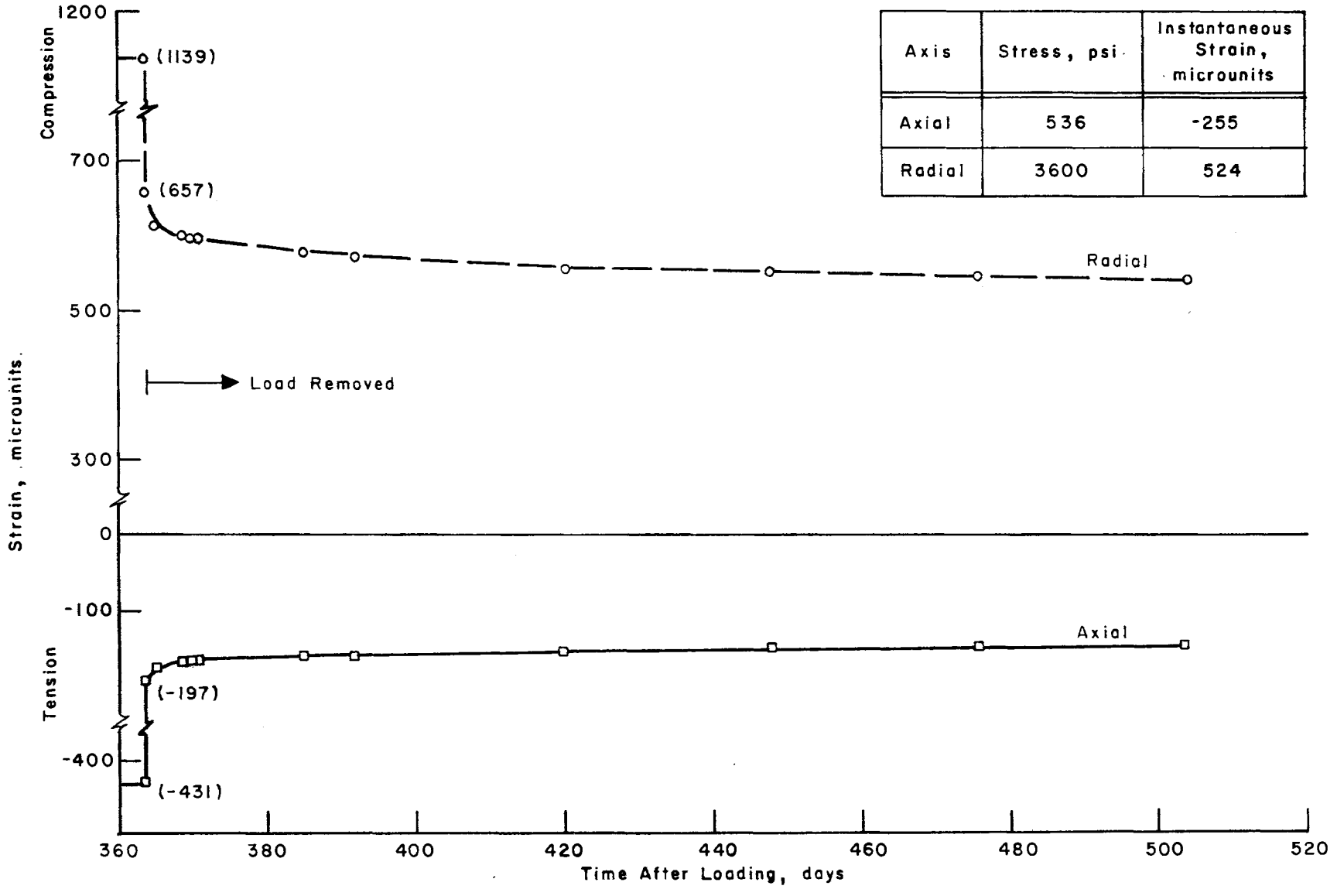

Fig B.11. Total strain less shrinkage strain after unloading for specimen G-35.

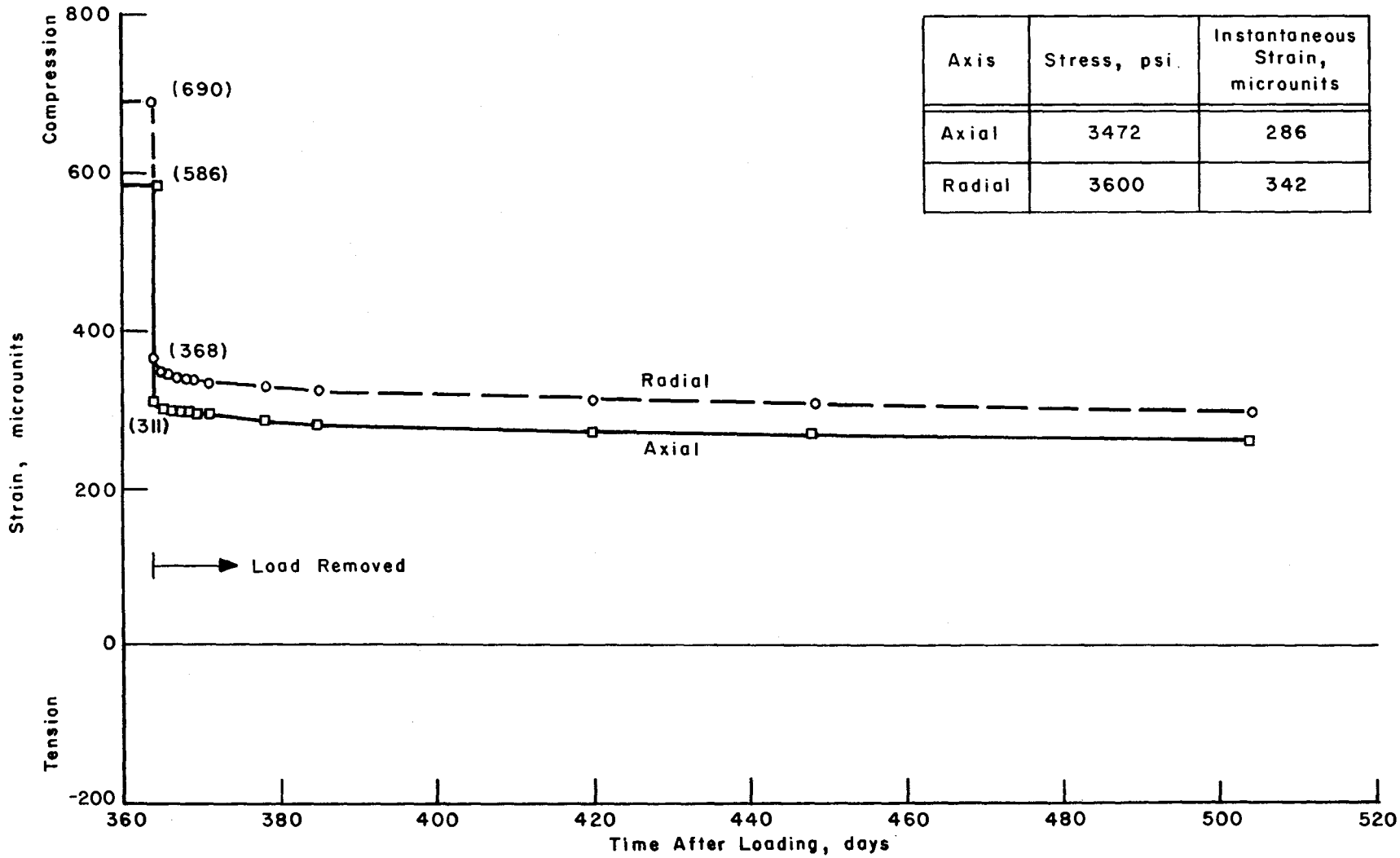

Axis	Stress, psi	Instantaneous Strain, microunits
Axial	3472	286
Radial	3600	342

Fig B.12. Total strain less shrinkage strain after unloading for specimen D-31.

APPENDIX C

TOTAL STRAIN LESS SHRINKAGE STRAIN CURVES AFTER UNLOADING FOR AIR-DRIED SPECIMENS AT 75° F

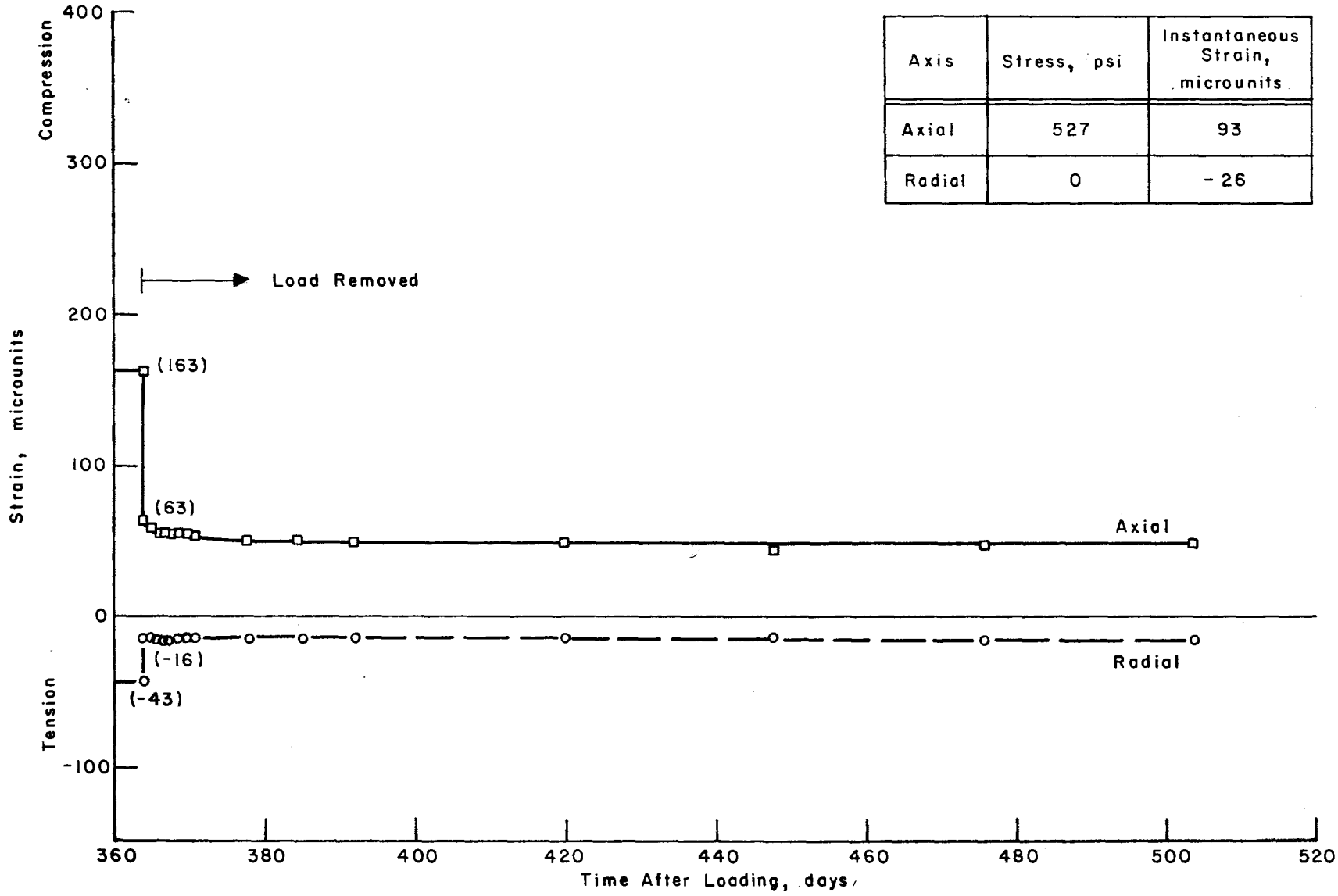

Axis	Stress, psi	Instantaneous Strain, microunits
Axial	527	93
Radial	0	- 26

Fig C.1. Total strain less shrinkage strain after unloading for specimen E-40.

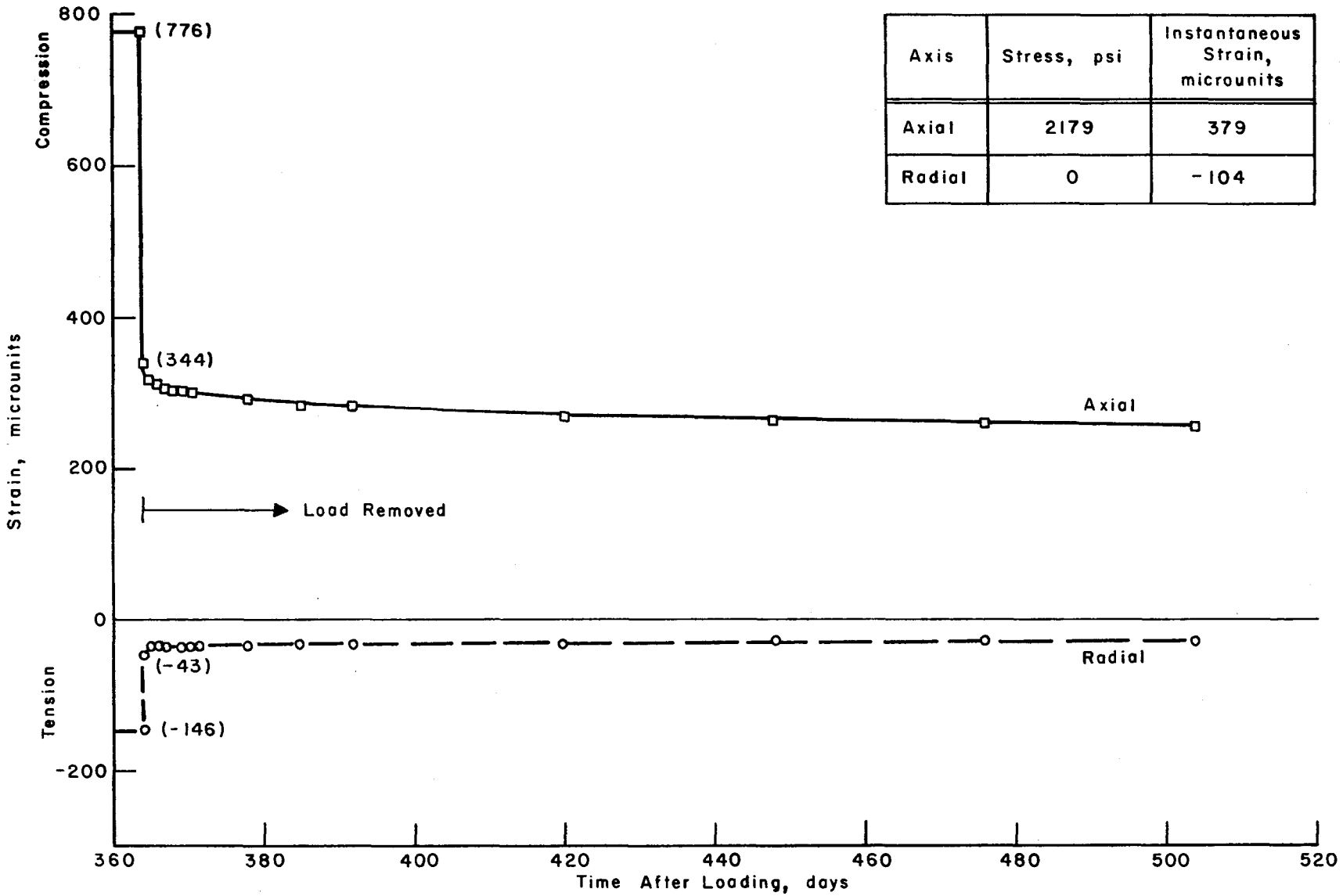

Axis	Stress, psi	Instantaneous Strain, microunits
Axial	2179	379
Radial	0	-104

Fig C.2. Total strain less shrinkage strain after unloading for specimen B-19.

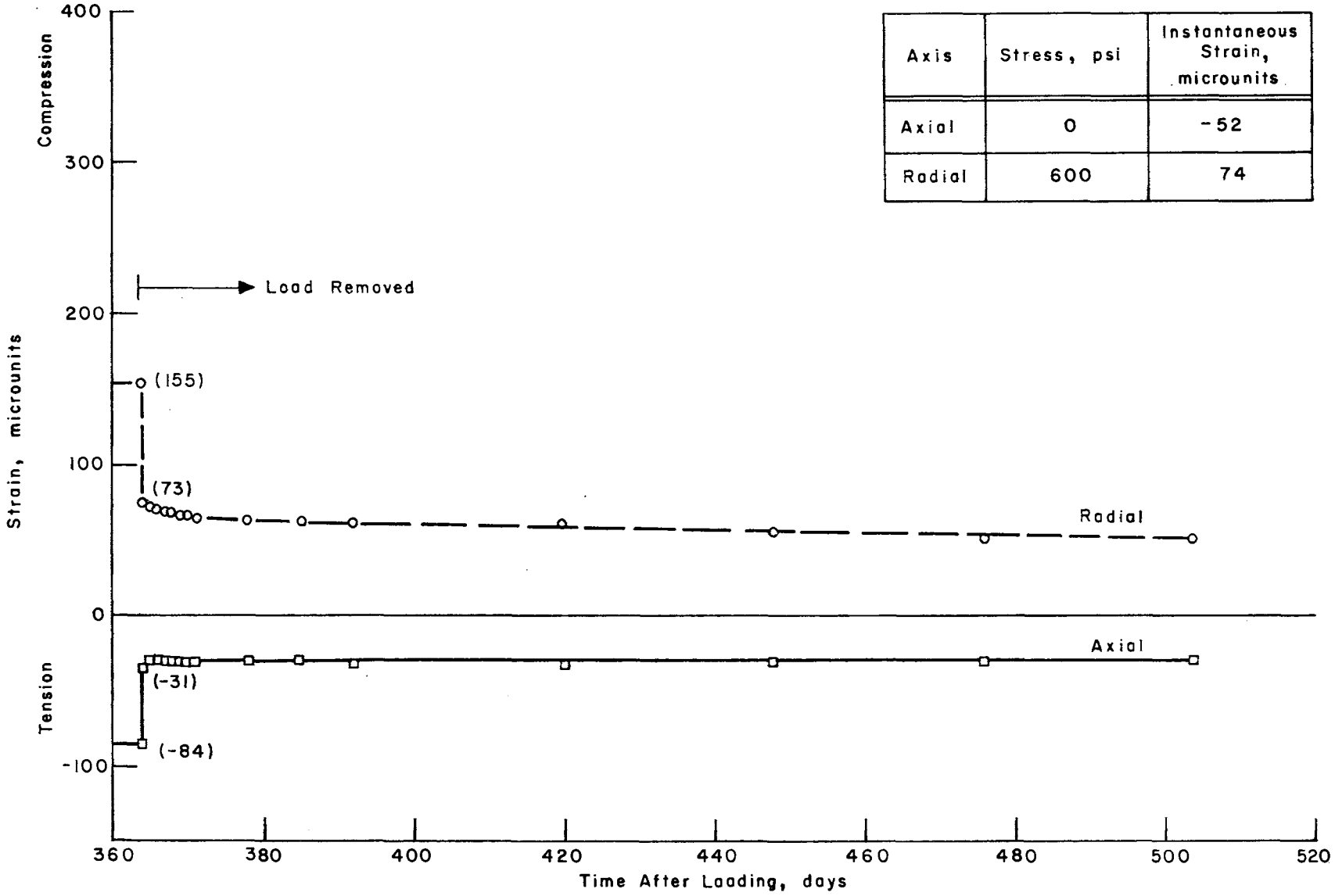

Axis	Stress, psi	Instantaneous Strain, microunits
Axial	0	-52
Radial	600	74

Fig C.3. Total strain less shrinkage strain after unloading for specimen F-42.

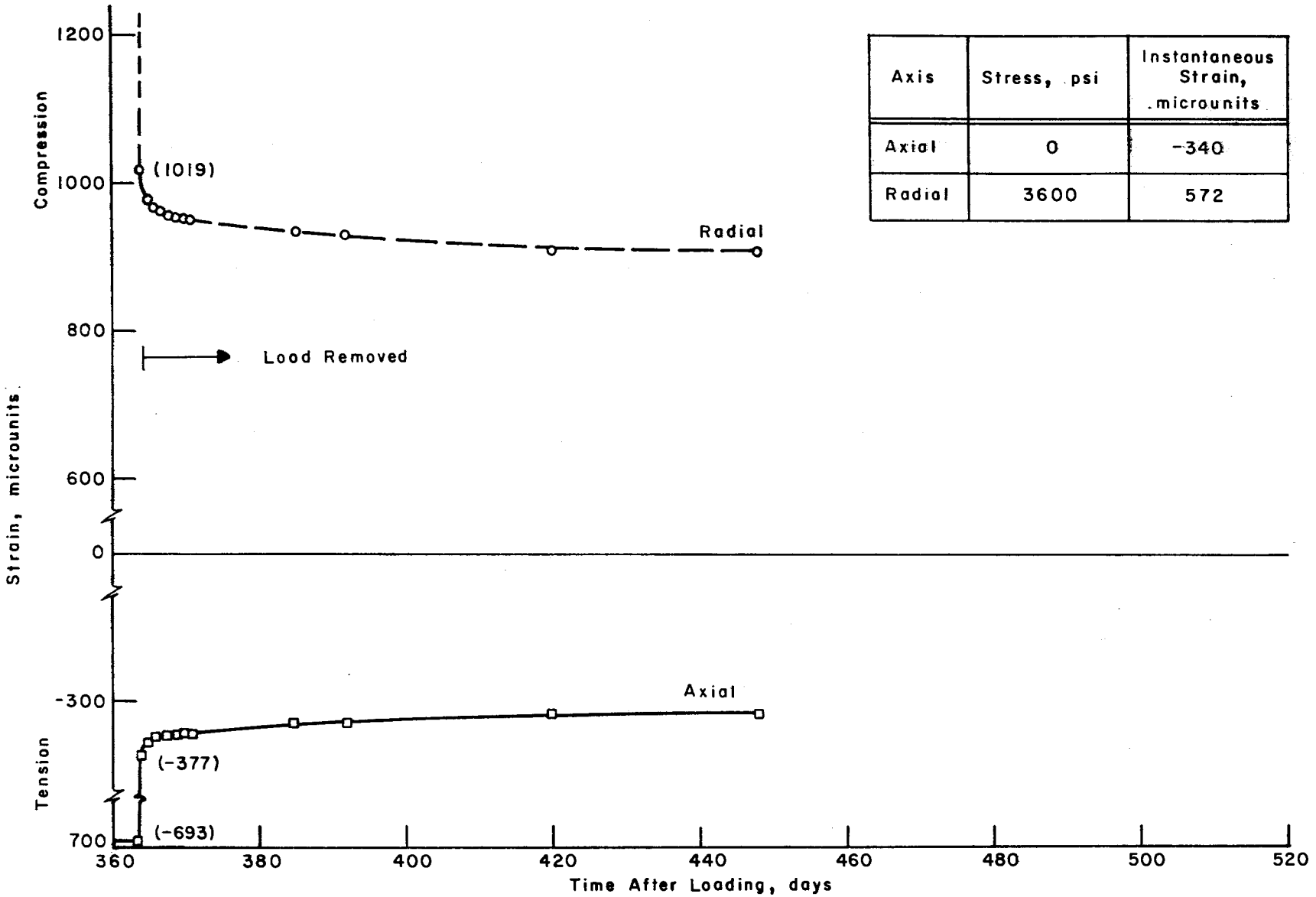

Axis	Stress, psi	Instantaneous Strain, microunits
Axial	0	-340
Radial	3600	572

Fig C.4. Total strain less shrinkage strain after unloading for specimen H-14.

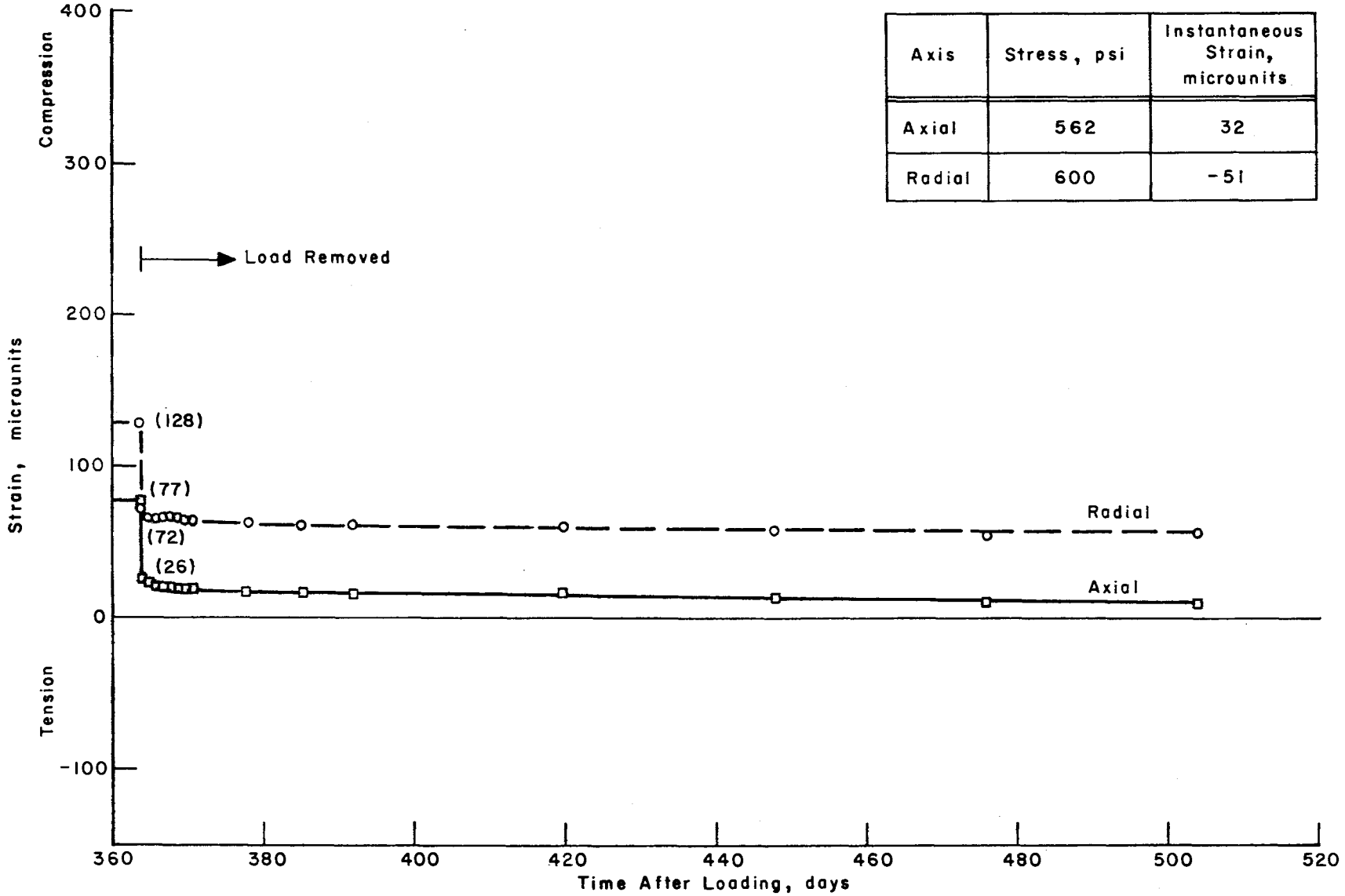

Axis	Stress, psi	Instantaneous Strain, microunits
Axial	562	32
Radial	600	-51

Fig C.5. Total strain less shrinkage strain after unloading for specimen E-13.

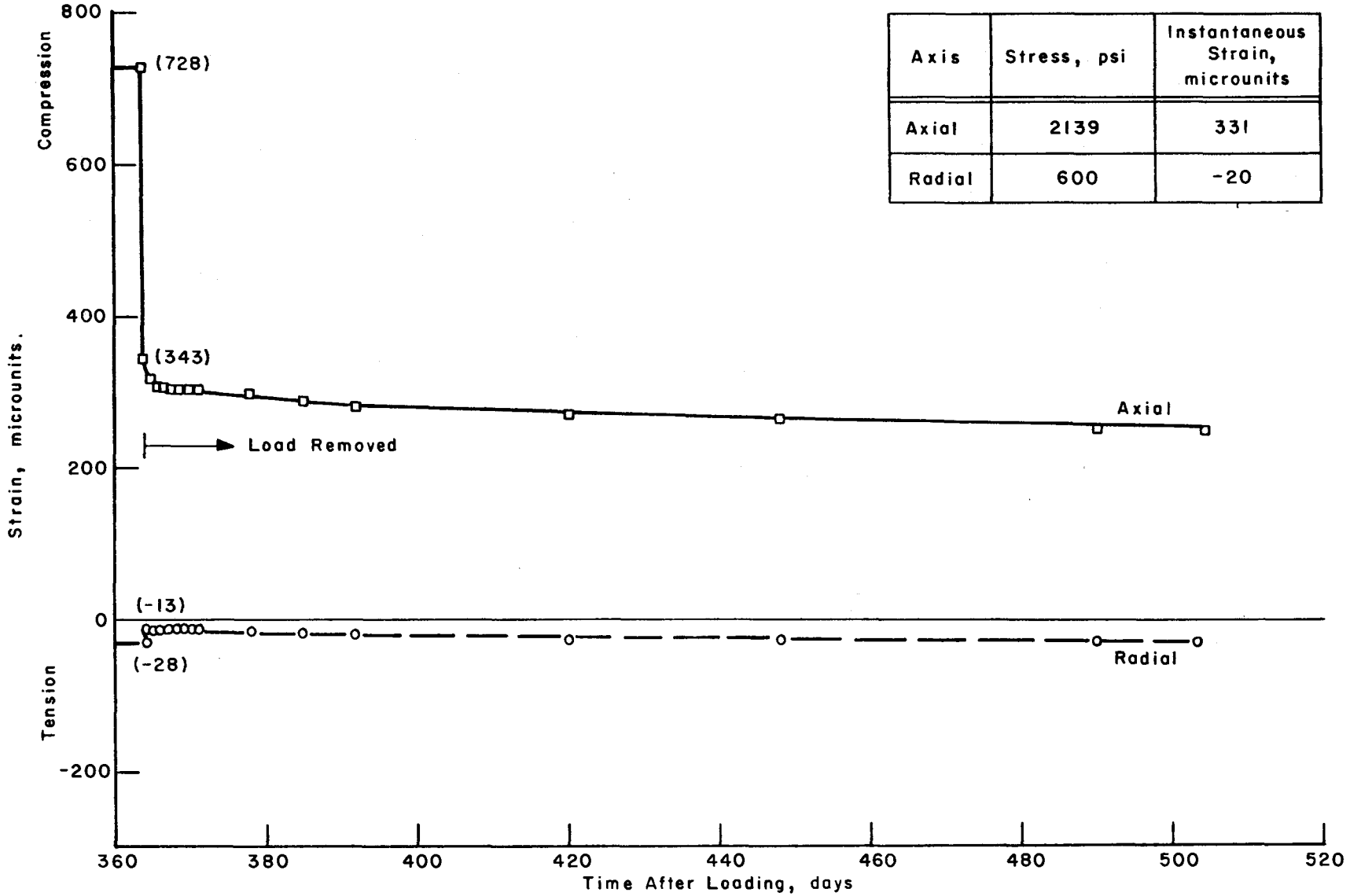

Axis	Stress, psi	Instantaneous Strain, microunits
Axial	2139	331
Radial	600	-20

Fig C.6. Total strain less shrinkage strain after unloading for specimen C-11.

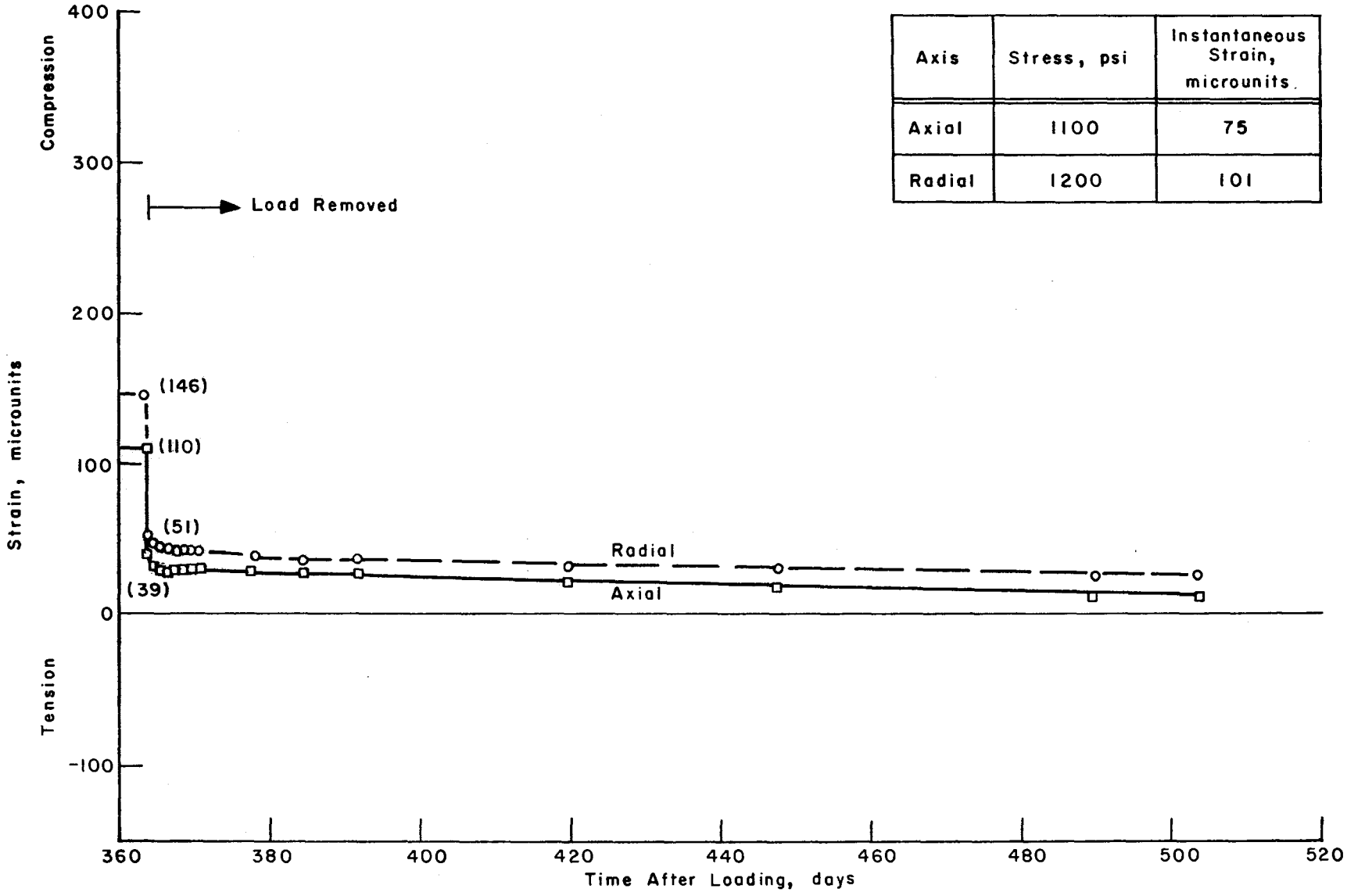

Axis	Stress, psi	Instantaneous Strain, microunits.
Axial	1100	75
Radial	1200	101

Fig C.7. Total strain less shrinkage strain after unloading for specimen C-17.

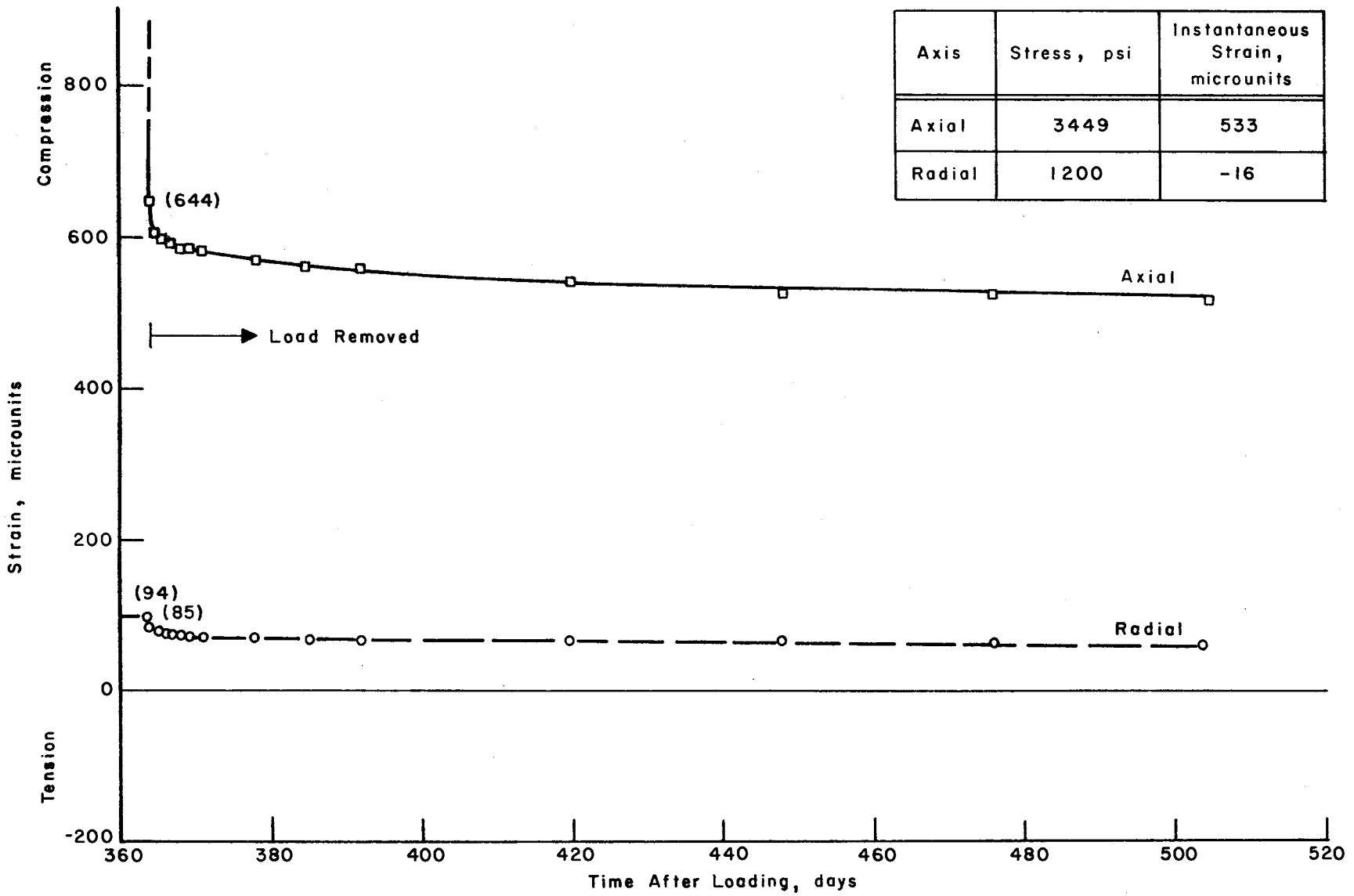

Fig C.8. Total strain less shrinkage strain after unloading for specimen D-44.

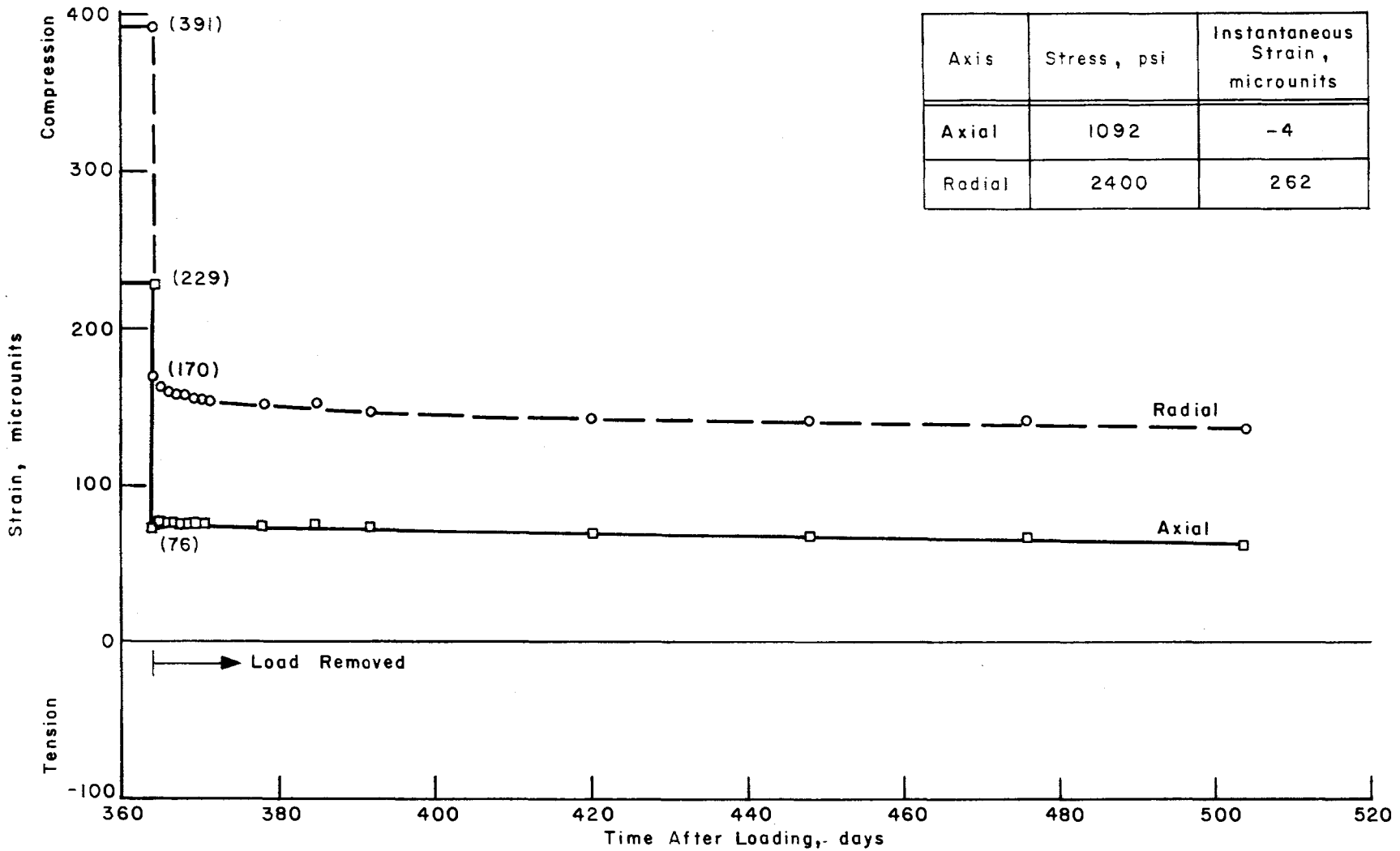

Fig C.9. Total strain less shrinkage strain after unloading for specimen B-42.

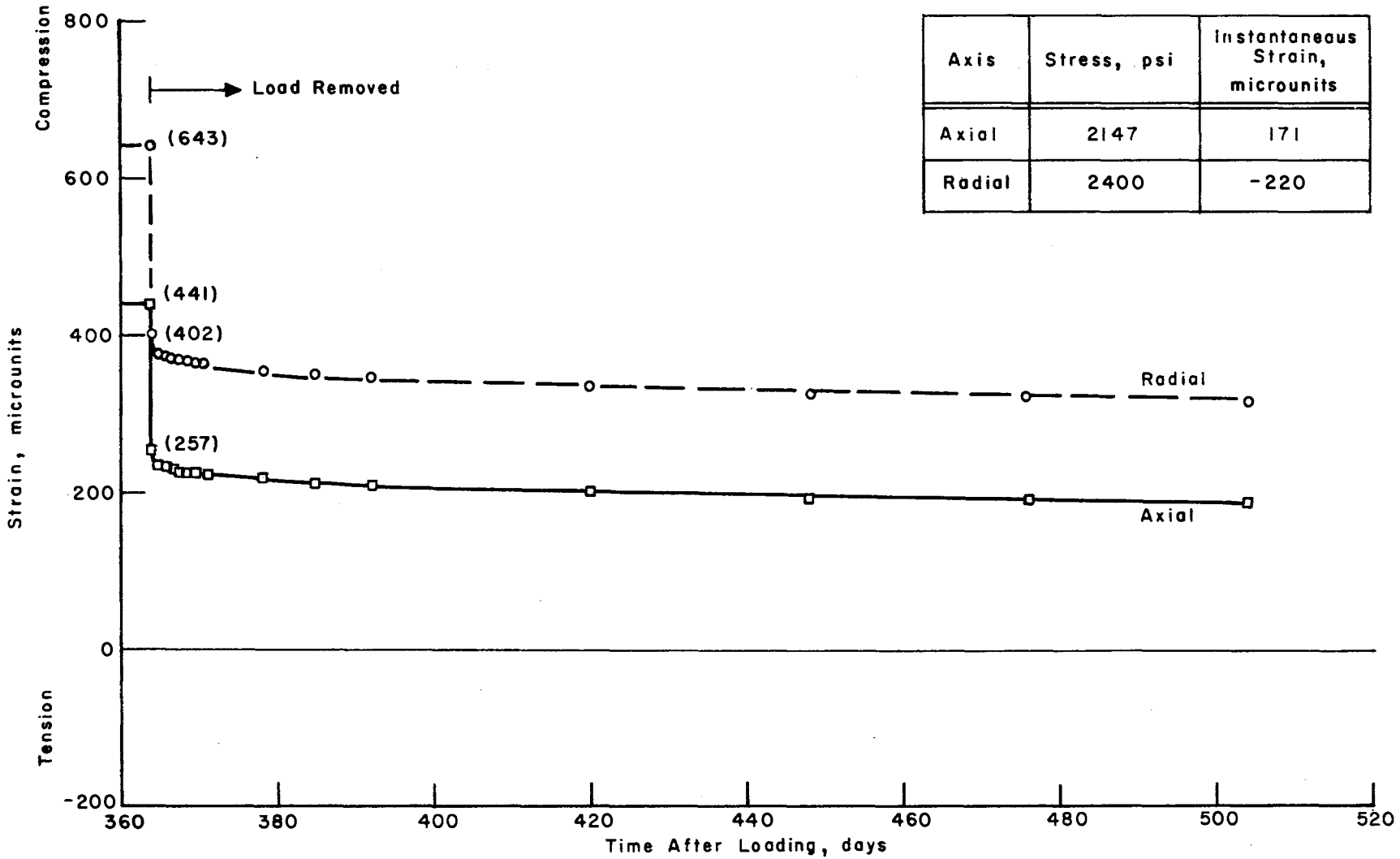

Axis	Stress, psi	Instantaneous Strain, microunits
Axial	2147	171
Radial	2400	-220

Fig C.10. Total strain less shrinkage strain after unloading for specimen F-30.

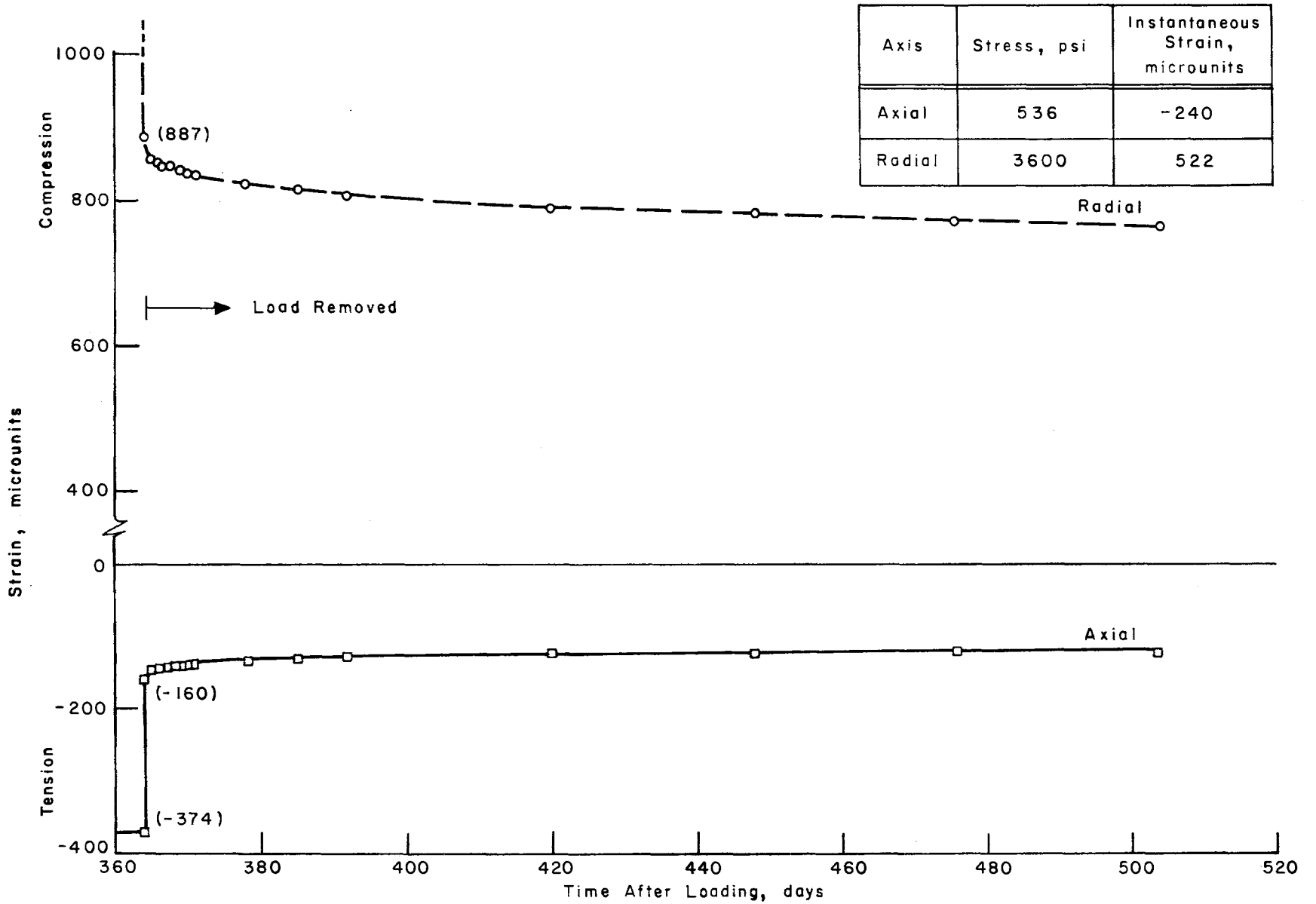

Fig C.11. Total strain less shrinkage strain after unloading for specimen G-30.

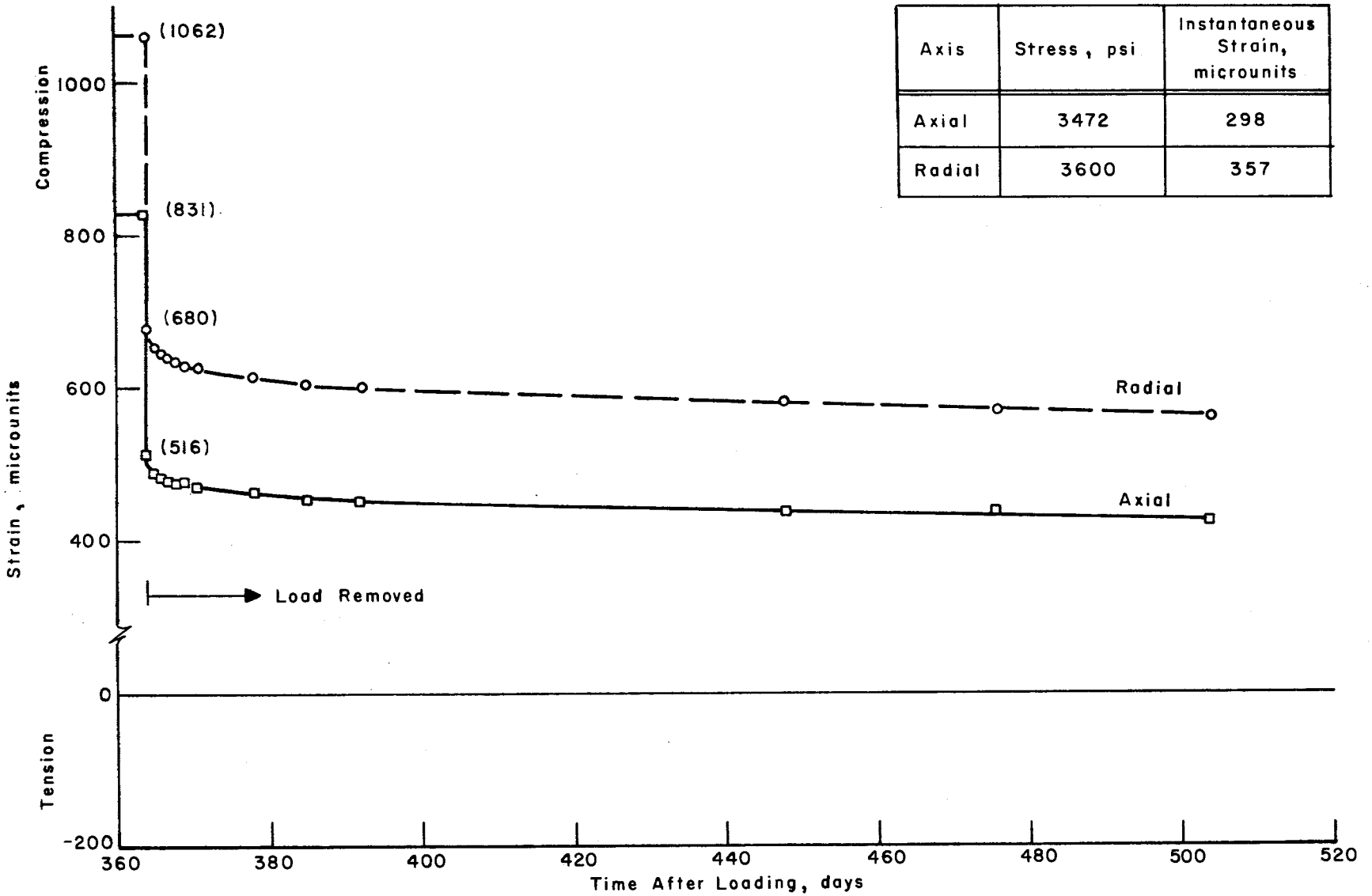

Axis	Stress, psi	Instantaneous Strain, microunits
Axial	3472	298
Radial	3600	357

Fig C.12. Total strain less shrinkage strain after unloading for specimen D-40.

APPENDIX D

TOTAL STRAIN LESS SHRINKAGE STRAIN CURVES AFTER UNLOADING FOR AS-CAST SPECIMENS AT 150° F

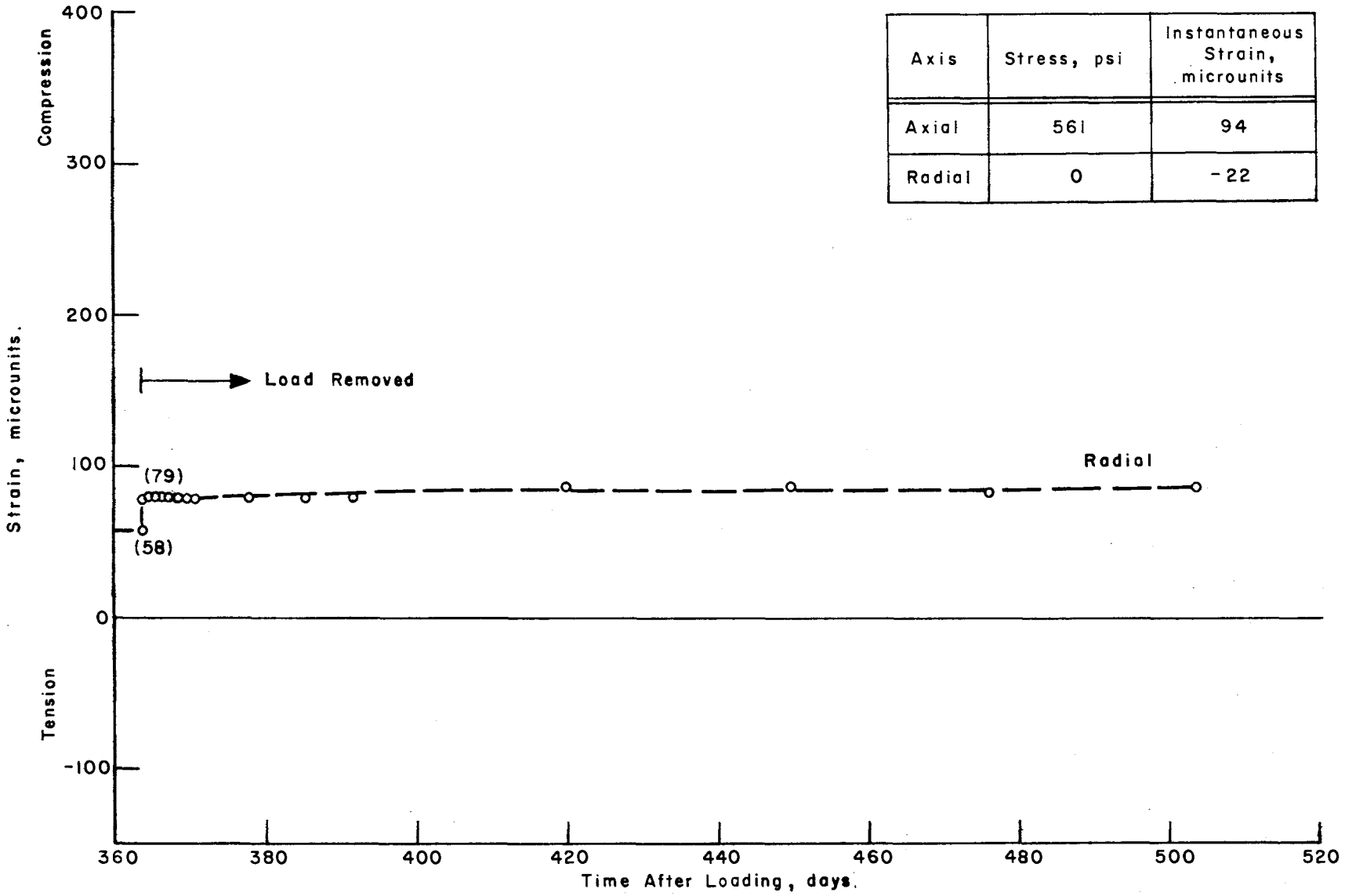

Axis	Stress, psi	Instantaneous Strain, microunits
Axial	561	94
Radial	0	-22

Fig D.1. Total strain less shrinkage strain after unloading for specimen B-4.

Axis	Stress, psi	Instantaneous Strain, microunits
Axial	1102	203
Radial	0	−53

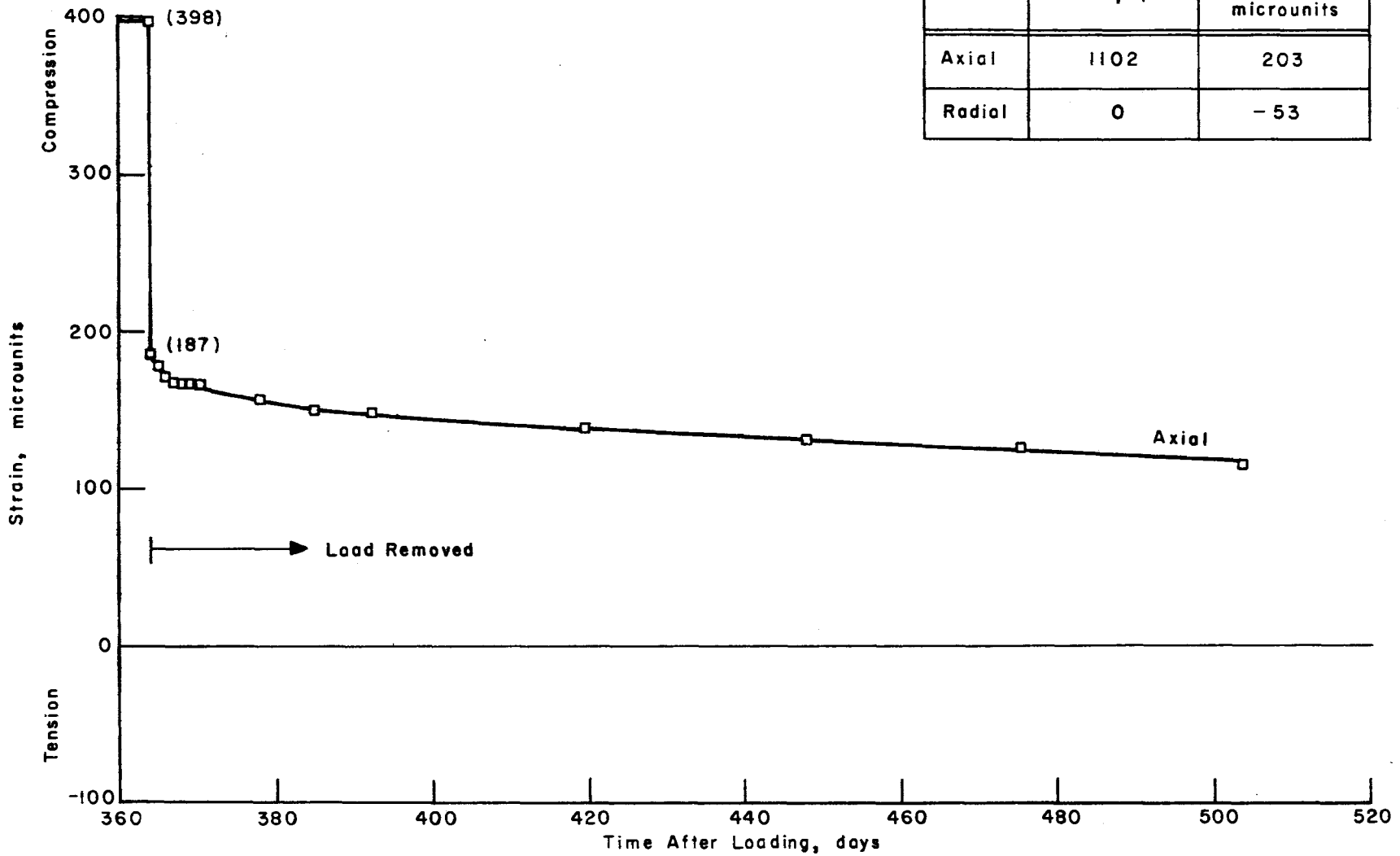

Fig D.2. Total strain less shrinkage strain after unloading for specimen D-15.

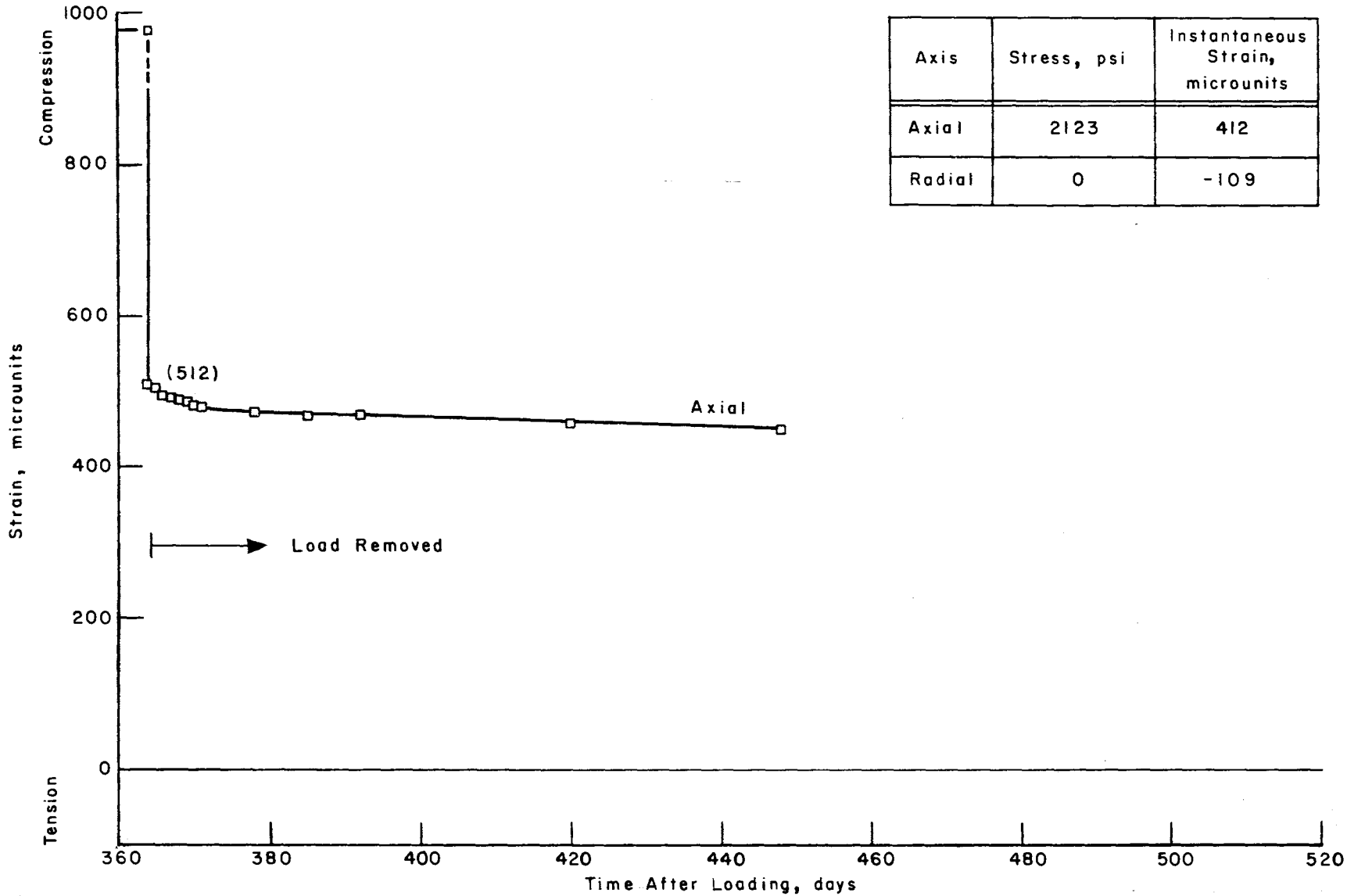

Axis	Stress, psi	Instantaneous Strain, microunits
Axial	2123	412
Radial	0	-109

Fig D.3. Total strain less shrinkage strain after unloading for specimen F-33.

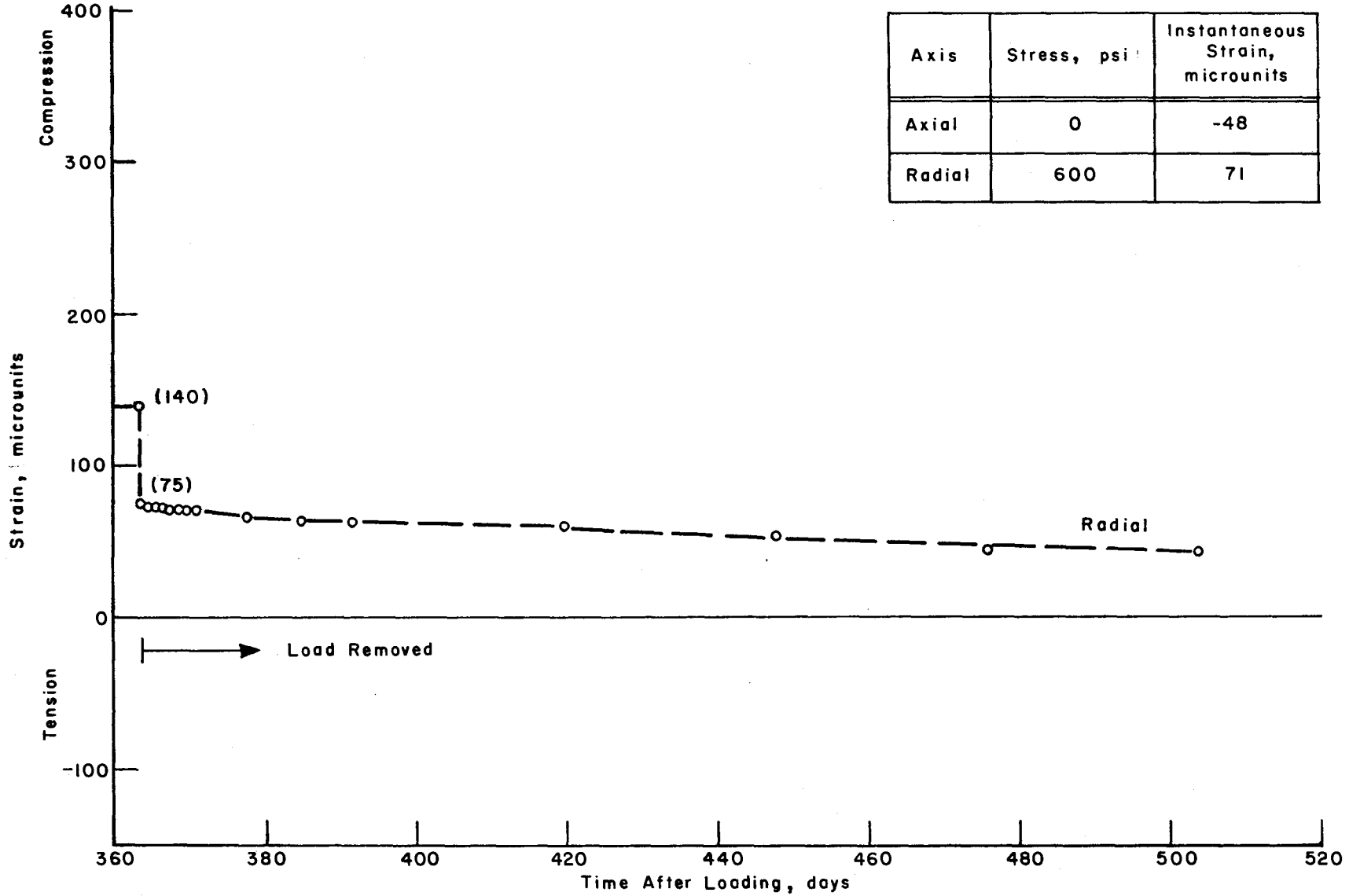

Fig D.4. Total strain less shrinkage strain after unloading for specimen A-35.

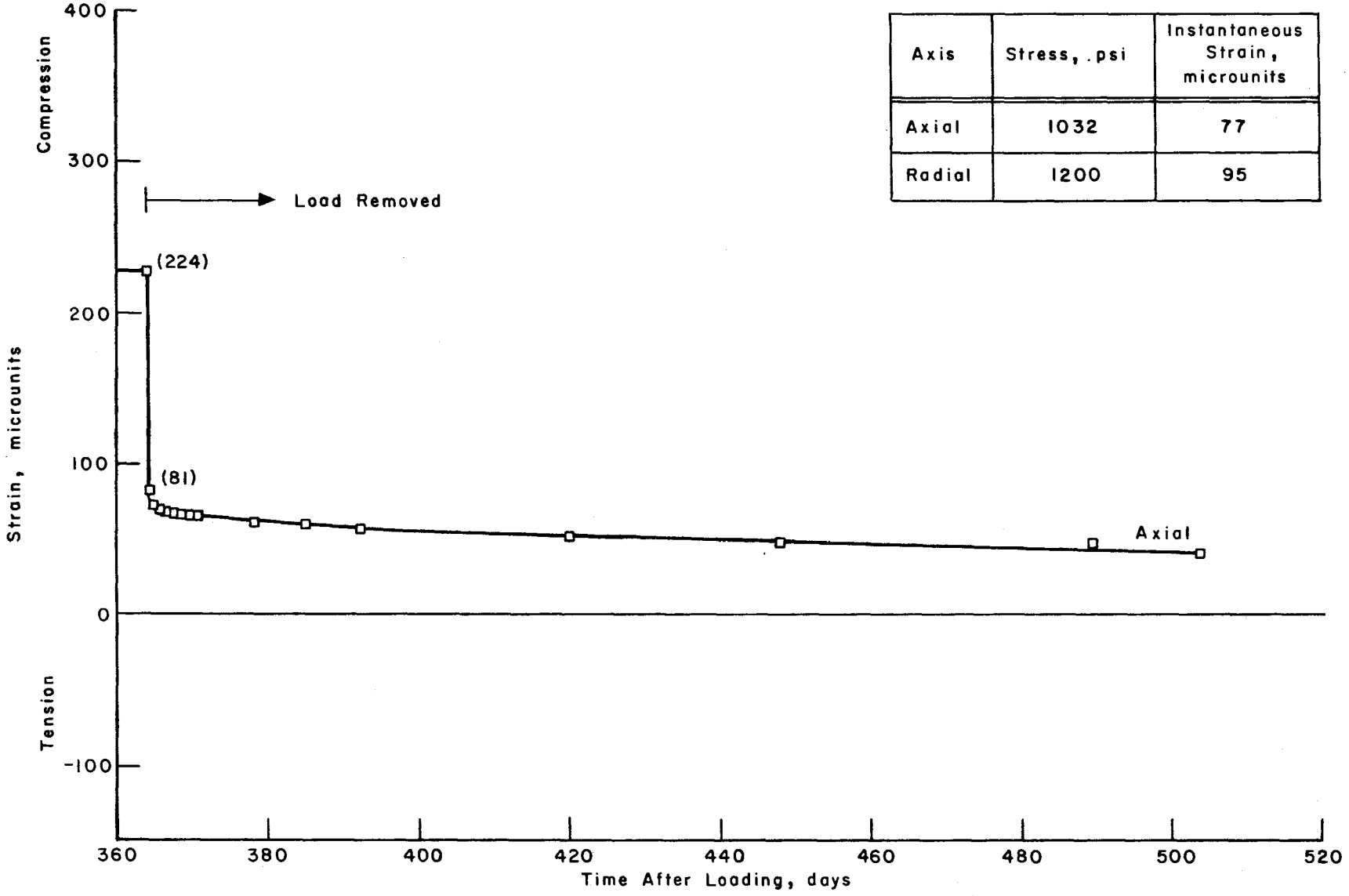

Axis	Stress, psi	Instantaneous Strain, microunits
Axial	1032	77
Radial	1200	95

Fig D.5. Total strain less shrinkage strain after unloading for specimen C-12.

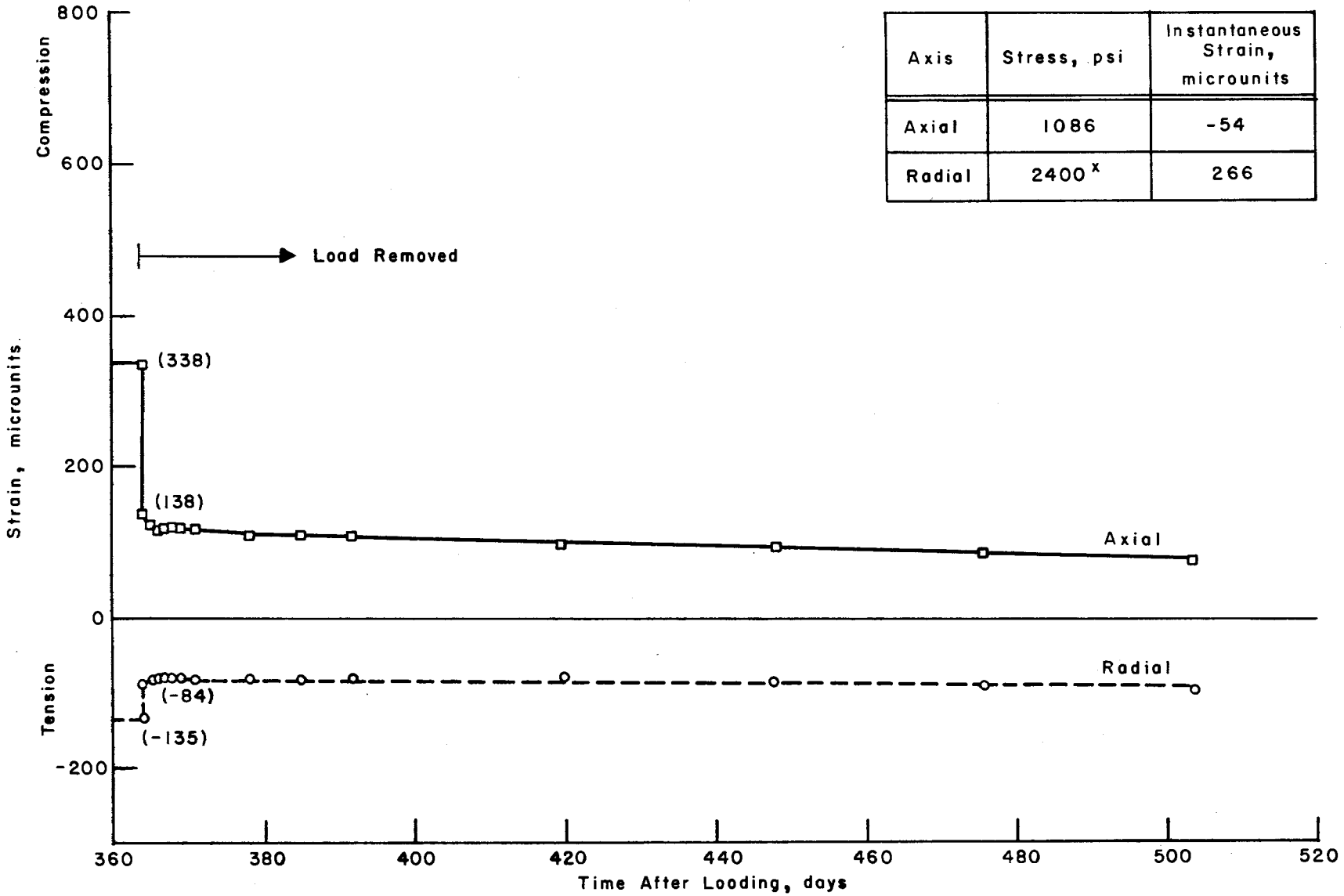

Axis	Stress, psi	Instantaneous Strain, microunits
Axial	1086	-54
Radial	2400 x	266

Fig D.6. Total strain less shrinkage strain after unloading for specimen D-2.

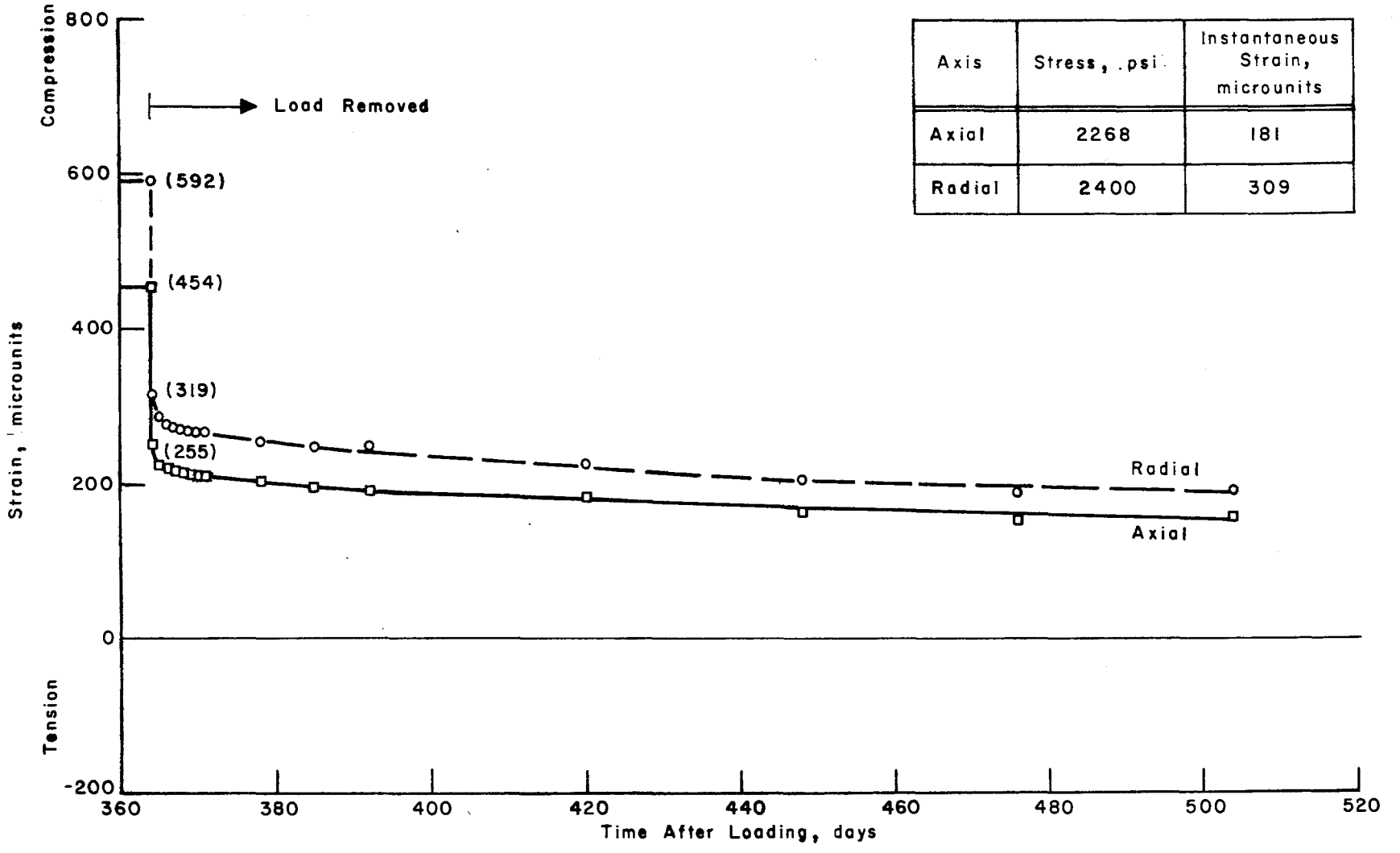

Axis	Stress, psi	Instantaneous Strain, microunits
Axial	2268	181
Radial	2400	309

Fig D.7. Total strain less shrinkage strain after unloading for specimen G-9.

APPENDIX E

TOTAL STRAIN LESS SHRINKAGE STRAIN CURVES AFTER UNLOADING FOR AIR-DRIED SPECIMENS AT 150° F

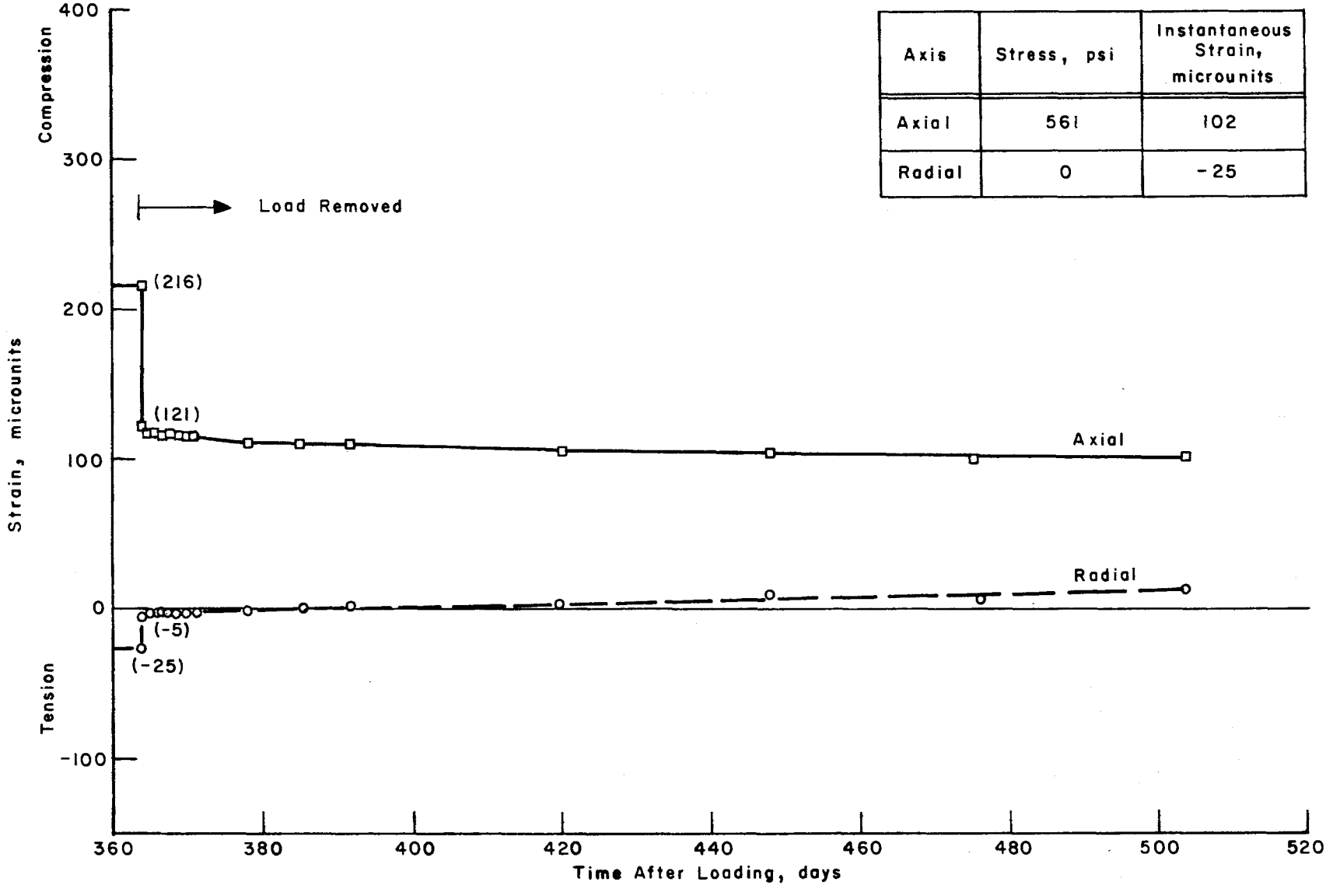

Axis	Stress, psi	Instantaneous Strain, microunits
Axial	561	102
Radial	0	-25

Fig E.1. Total strain less shrinkage strain after unloading for specimen B-1.

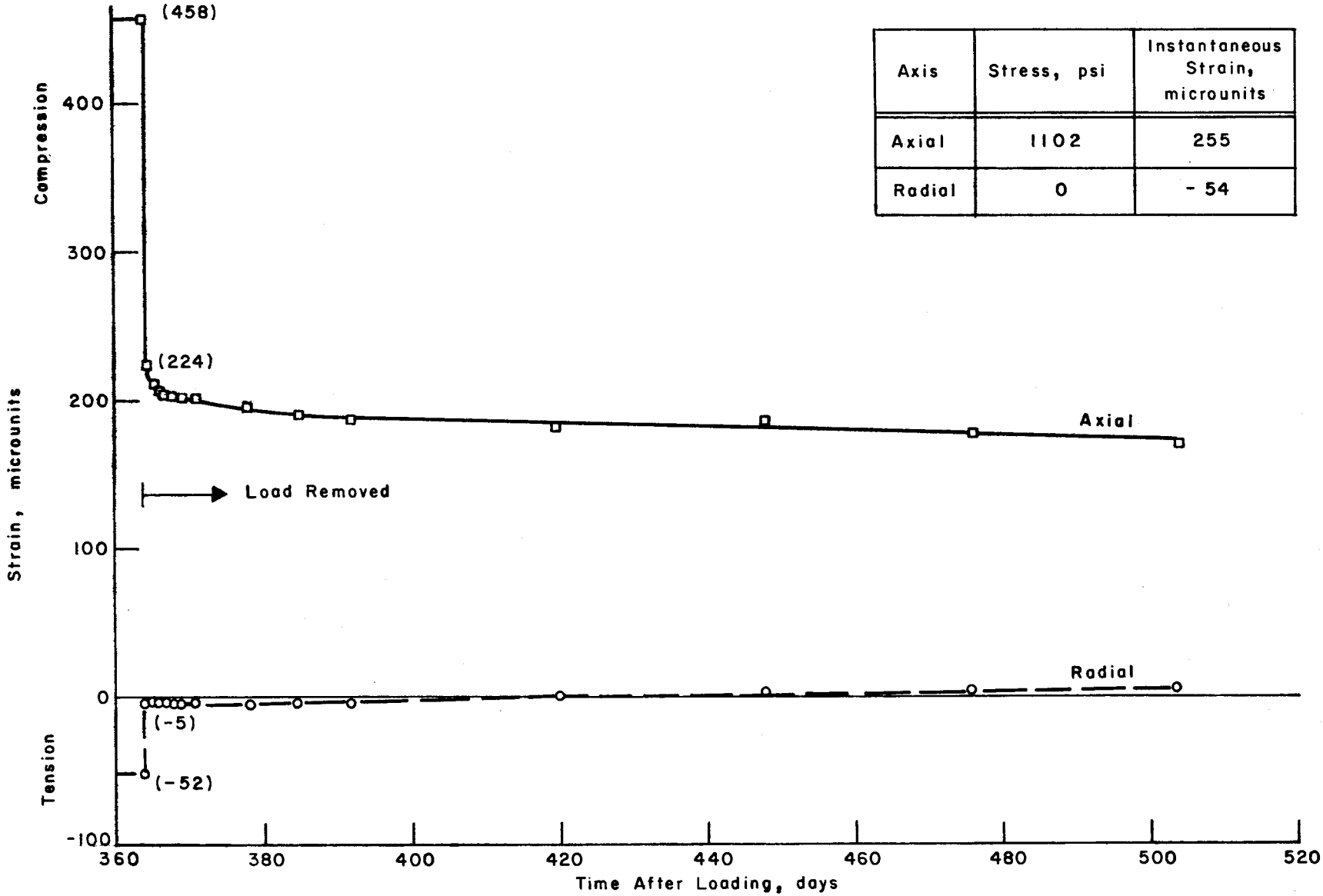

Axis	Stress, psi	Instantaneous Strain, microunits
Axial	1102	255
Radial	0	- 54

Fig E.2. Total strain less shrinkage strain after unloading for specimen D-22.

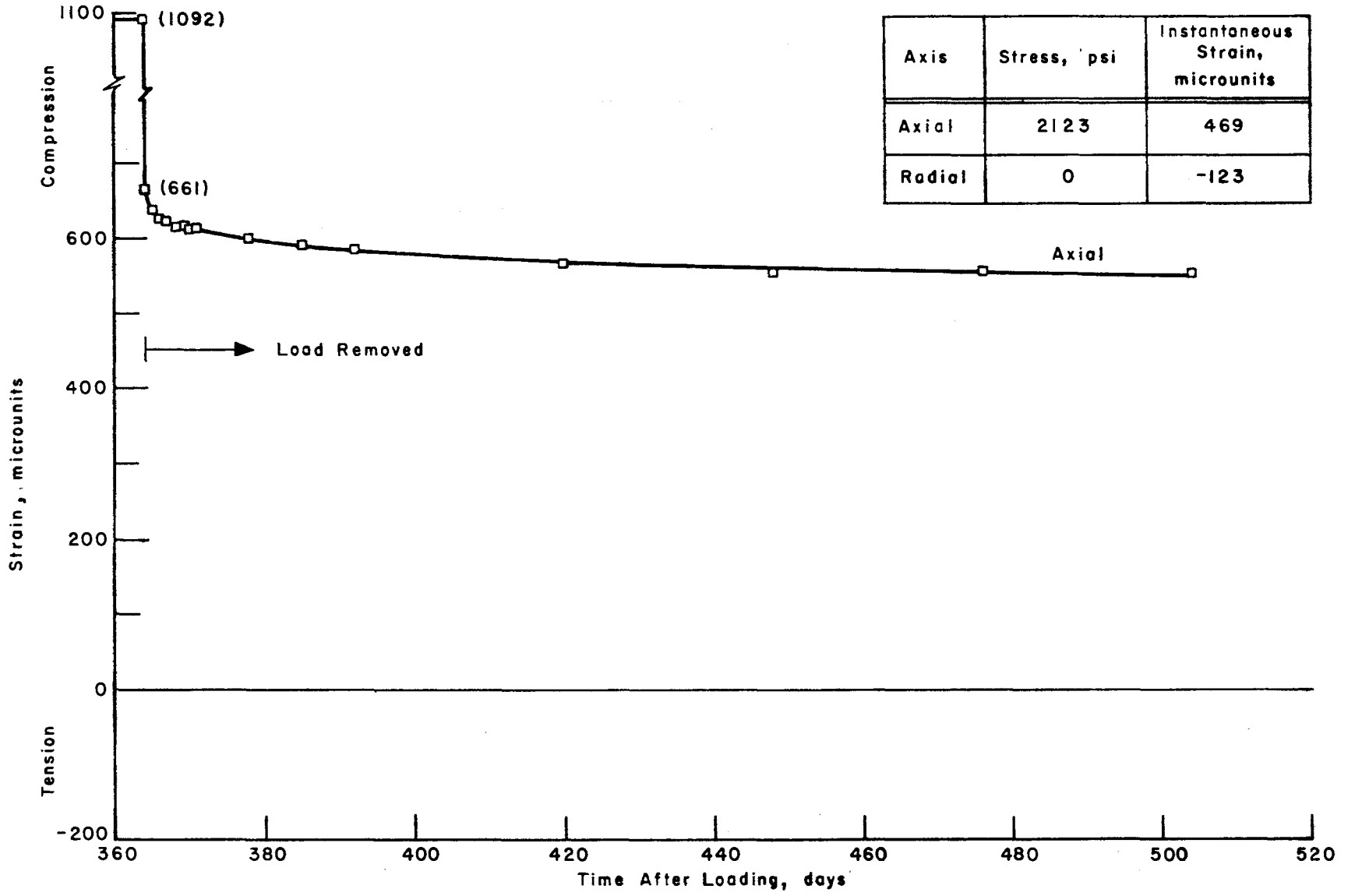

Axis	Stress, psi	Instantaneous Strain, microunits
Axial	2123	469
Radial	0	-123

Fig E.3. Total strain less shrinkage strain after unloading for specimen F-34.

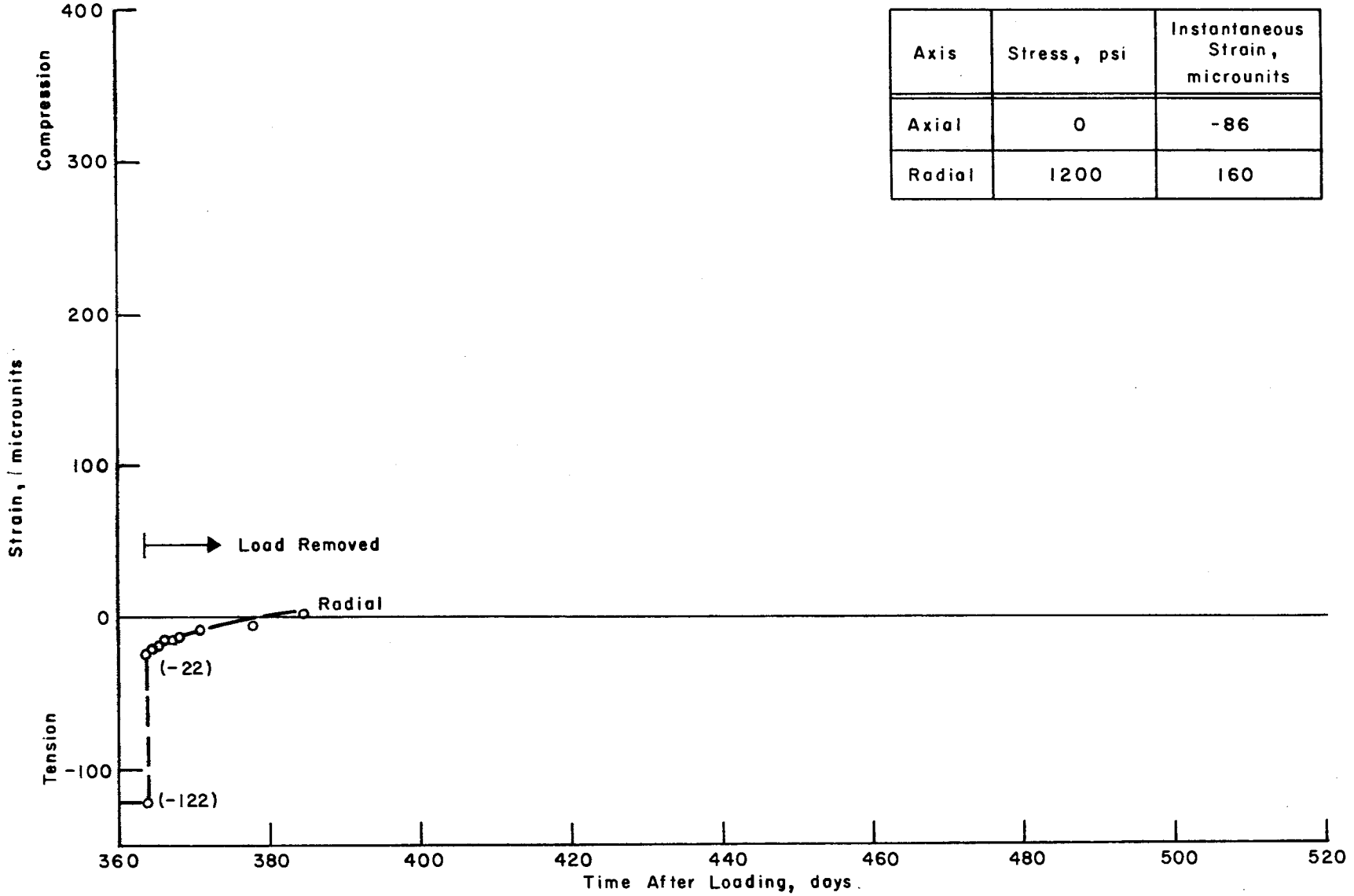

Fig E.4. Total strain less shrinkage strain after unloading for specimen D-3.

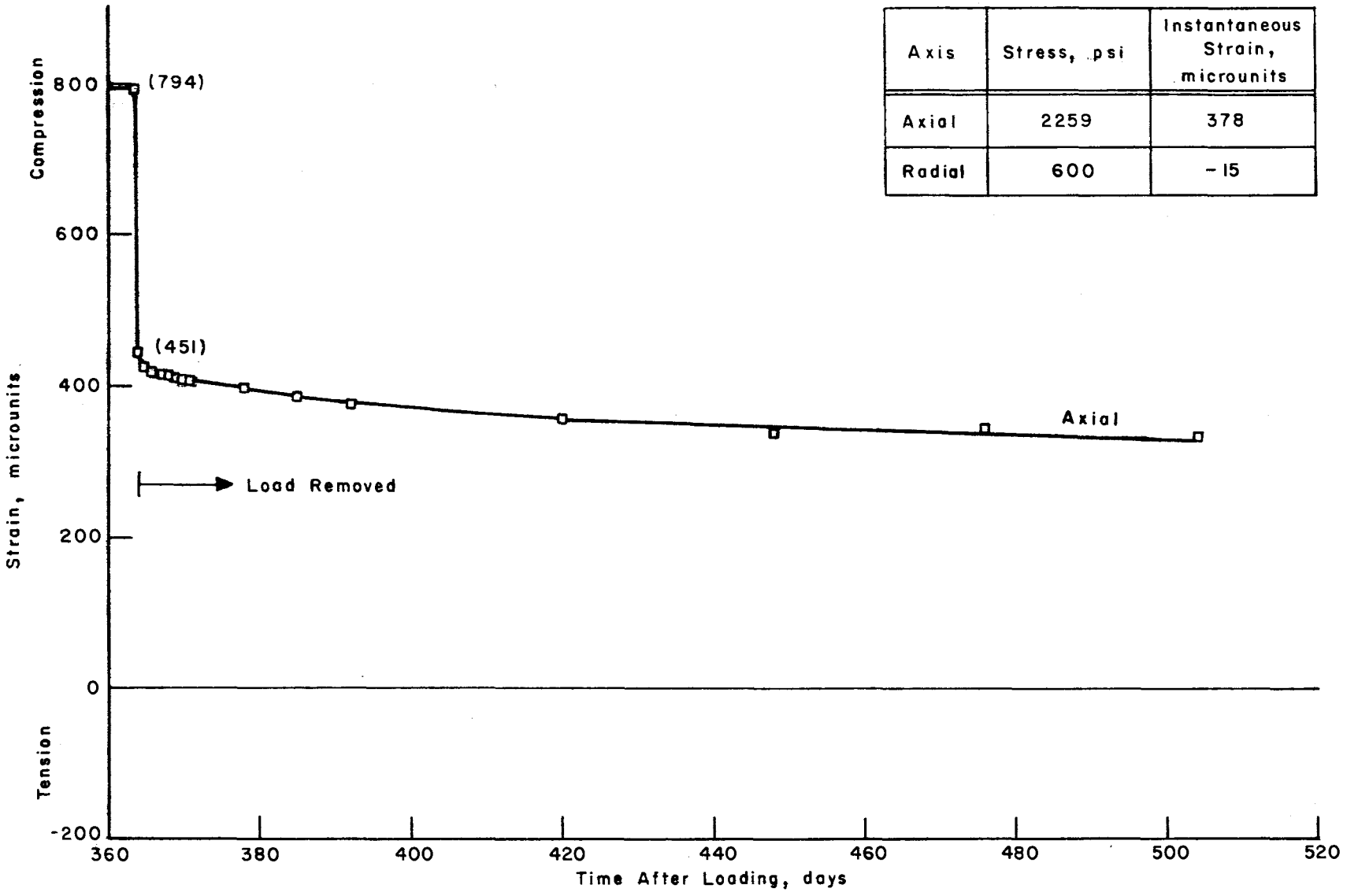

Axis	Stress, psi	Instantaneous Strain, microunits
Axial	2259	378
Radial	600	-15

Fig E.5. Total strain less shrinkage strain after unloading for specimen E-4.

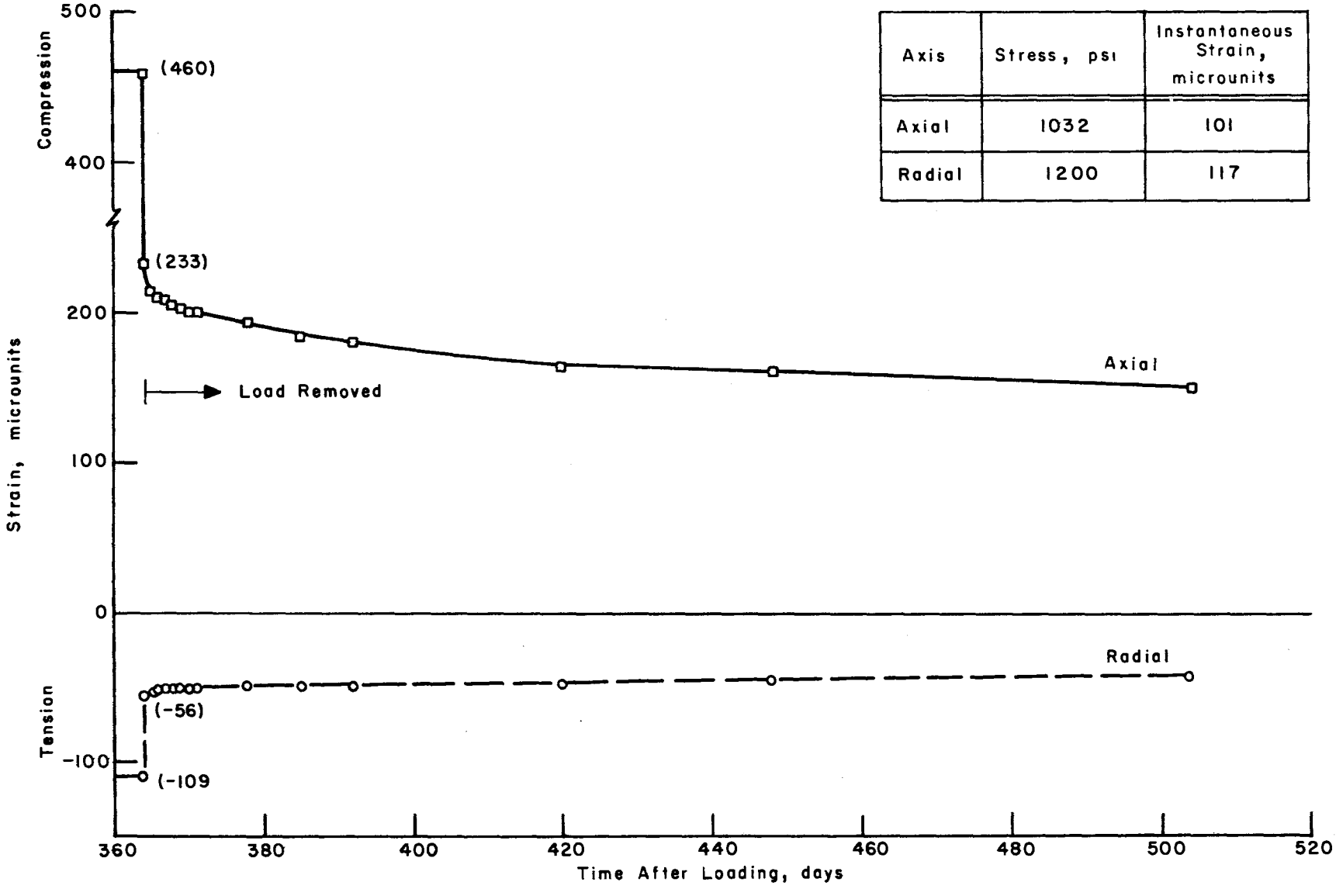

Fig E.6. Total strain less shrinkage strain after unloading for specimen C-46.

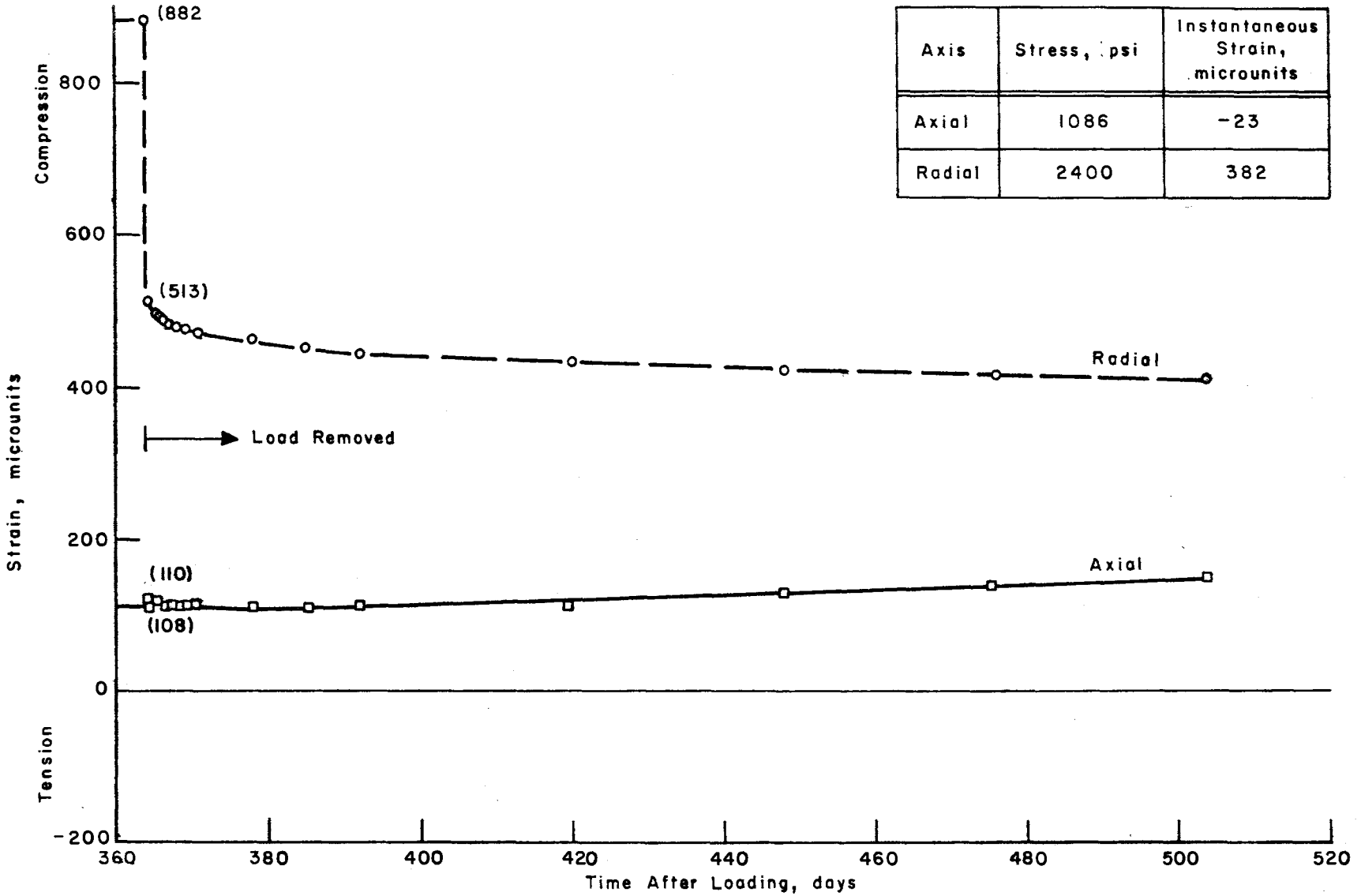

Axis	Stress, psi	Instantaneous Strain, microunits
Axial	1086	-23
Radial	2400	382

Fig E.7. Total strain less shrinkage strain after unloading for specimen D-41.

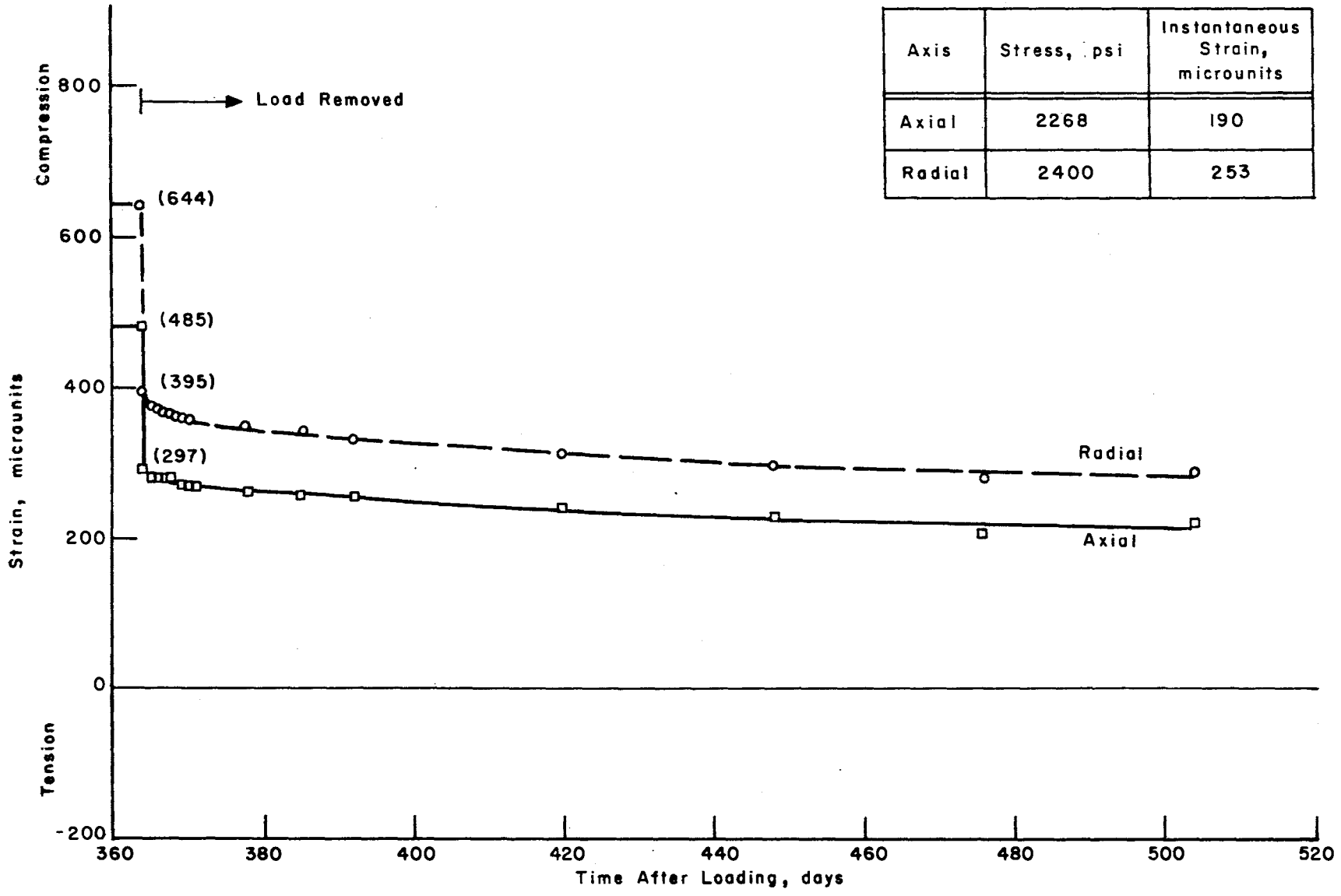

Axis	Stress, psi	Instantaneous Strain, microunits
Axial	2268	190
Radial	2400	253

Fig E.8. Total strain less shrinkage strain after unloading for specimen G-19.

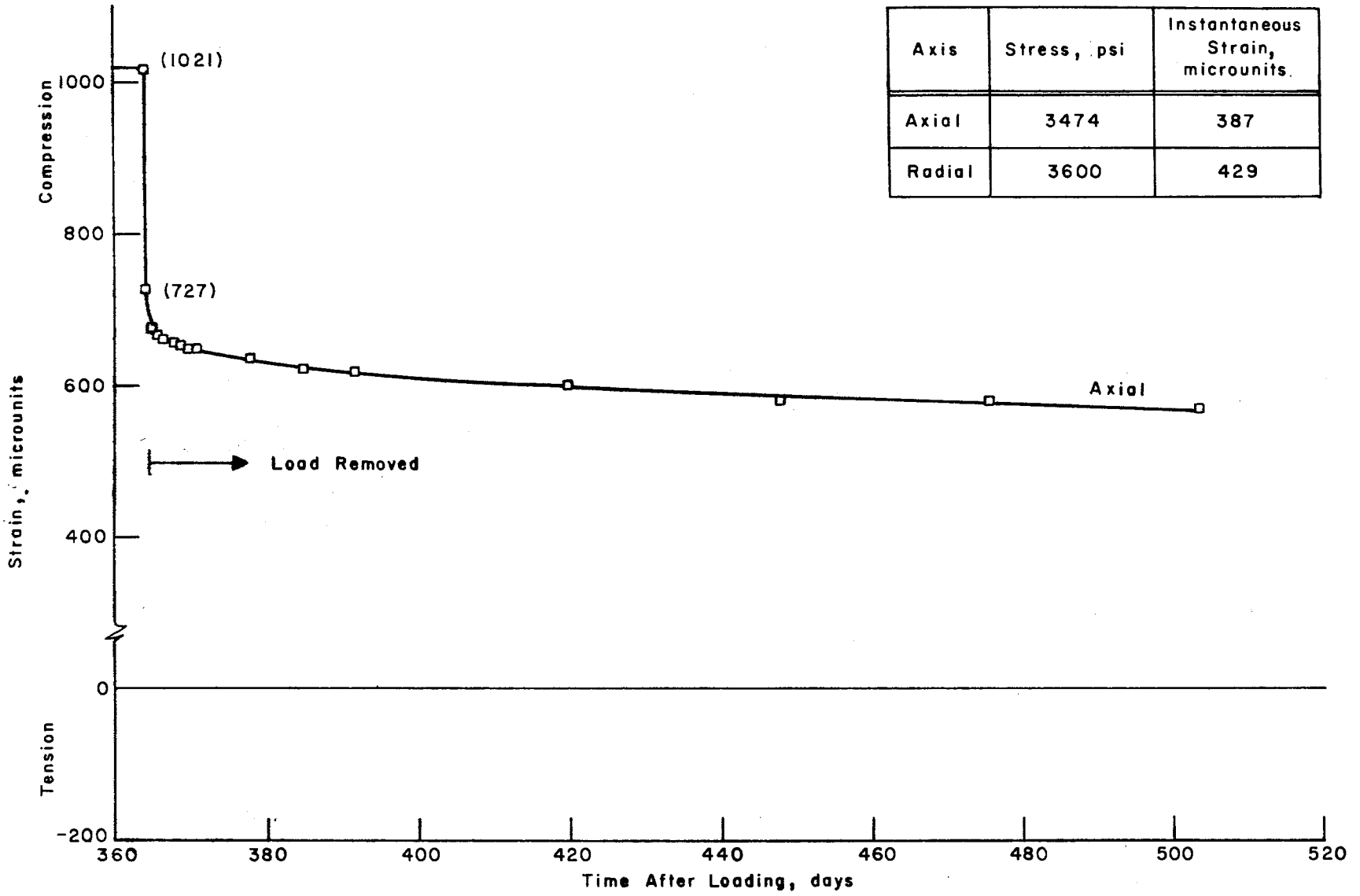

Axis	Stress, psi	Instantaneous Strain, microunits
Axial	3474	387
Radial	3600	429

Fig E.9. Total strain less shrinkage strain after unloading for specimen F-6.